INTERPLAY OF PROTEIN KINASE C, THE MARCKS PROTEIN, AND PHOSPHOINOSITIDES IN REGULATING MAST CELL SIGNALING

A Dissertation

Presented to the Faculty of the Graduate School

of Cornell University

In Partial Fulfillment of the Requirements for the Degree of

Doctor of Philosophy

by

Deepti Gadi

January 2012

INTERPLAY OF PROTEIN KINASE C, THE MARCKS PROTEIN, AND PHOSPHOINOSITIDES IN REGULATING MAST CELL SIGNALING

Deepti Gadi, Ph.D.

Cornell University 2012

Stimulation of immunoglobulin E (IgE)-sensitized mast cells by multivalent antigen triggers a cascade of intracellular signaling events that results in granule exocytosis as a principal outcome. Granule exocytosis results in the release of histamine and other inflammatory mediators of the allergic response, and this process is mediated by Ca^{2+}mobilization and activation of protein kinase C (PKC). MARCKS, a major PKC substrate, has been implicated in granule exocytosis. MARCKS has a polybasic effector domain (ED) that associates strongly with phosphatidylinositol 4,5-bisphosphate (PIP_2) and other phosphoinositides at the inner leaflet of the plasma membrane. Using real-time fluorescence imaging, we observed antigen-stimulated oscillatory recruitment of EGFP-tagged PKCβI to the plasma membrane in a process that is synchronous with the oscillatory displacement of mRFP-MARCKS-ED.

To investigate the role of PKC-mediated MARCKS phosphorylation in granule exocytosis, we created a MARCKS-ED mutant that cannot be phosphorylated. We observed that MARCKS-EDSA4 delays the onset of Ca^{2+} mobilization that is dependent on PIP_2 hydrolysis to produce IP_3 in response to antigen, but it does not inhibit store-operated Ca^{2+} entry (SOCE) activated by the SERCA pump inhibitor thapsigargin. Under these conditions, we found that granule exocytosis stimulated by

antigen as well as by thapsigargin is substantially inhibited. Our results provide strong evidence that phosphoinositides participate in the terminal steps of granule exocytosis, and they support the hypothesis that PKC normally regulates access of PIP_2 to multiple proteins in both Ca^{2+} mobilization and granule exocytosis.

We also investigated the role of endogenous MARCKS and found that its knockdown resulted in reduced Ca^{2+} and degranulation responses to antigen, suggesting a positive regulatory role for endogenous MARCKS in these processes. These results contrast with the inhibition by MARCKS-ED SA4 in these processes, and they suggest that full length, endogenous MARCKS may be regulating multiple pathways. We hypothesize that endogenous MARCKS positively regulates antigen-stimulated store-operated Ca^{2+} entry and granule exocytosis due to its association with Ca^{2+} bound calmodulin under stimulated conditions. These findings provide useful mechanistic insights into the roles of PKC, MARCKS and PIP_2 in the intricate regulation of Ca^{2+} mobilization and granule exocytosis in stimulated mast cell signaling.

BIOGRAPHICAL SKETCH

Deepti Gadi was born to Dr. Satish K. Gadi and Mrs. Anita Gadi on May 7, 1984 in Delhi, India. She started appreciating science in her early school days at Presentation Convent School, a catholic school run by Irish nuns. She was instilled with a drive to contribute towards the betterment of society and imbibed high moral standards at her alma mater. She excelled in Chemistry at high school which encouraged her to pursue this subject at the undergraduate level at St. Stephen's College, Delhi University. She was adjudged to be the most proficient in laboratory work in the entire chemistry department in her final year at St. Stephen's College, which motivated her to consider research as a career. She further went on to get a Master's degree in Chemistry at Indian Institute of Technology, Delhi, where she worked in a Biochemistry laboratory for her Master's project. She instantly loved doing experiments in Biology with the hope that they can contribute in some small way to solve the currently existing medical challenges. Determined to delve deeper into Biology, she decided to come to Cornell University for her Ph.D. studies in the Chemistry and Chemical Biology department. At Cornell, she chose to perform her graduate research in Baird-Holowka laboratory, where she focused on understanding the mechanism of the signaling pathway leading to allergy. After the completion of her Ph.D. degree, she plans to move to New York to pursue her career as a post-doctoral scientist.

This dissertation is dedicated to my family and friends for their unconditional support.

ACKNOWLEDGMENTS

I am extremely thankful to Barbara Baird and David Holowka for giving me an opportunity to be a part of their research group and for being wonderful mentors throughout my graduate career. Their constant guidance, encouragement and confidence in me have been a major driving force behind my transition from Chemistry to Cell Biology. I am thankful to my committee members Rick Cerione and Brian Crane for their insightful thoughts and comments. I also had the opportunity to collaborate with Dr. Ishrat Khan at Clark Atlanta University and I am grateful to him and Barbara for constantly getting funds for this research.

I would like to thank all my colleagues in Baird-Holowka lab for creating a great research environment in the lab: Alice for patiently teaching me molecular biology techniques in the lab and for her delightful company and support, Alexis for helping me get started in the lab and for his excellent ideas and comments, calcium subgroup members – Roy, Nat, Kate and Marcela for their valuable discussions and suggestions for my research, Norah for always answering my questions and for her extremely helpful nature, Kirsten and Josh for a congenial environment in the lab office. All past and current lab members -- Dwaipayan, Lavanya, Stephanie, Ethan, Amit, Jinmin, Kari, Sarah, Devin, Fatima, Olga, John, Tristan -- have contributed in making my experience in this lab a very memorable one. A special thanks to Carol Bayles, in charge of microscopy facility at Cornell University, for her willingness to always help with technical problems.

I am especially thankful to my parents, grandparents and my brother for their constant love and encouragement, for supporting all my decisions and for believing in

me all the way. I am immensely grateful to them for helping me develop into the person that I am today.

I had the good fortune of having an excellent set of friends in Ithaca who were like my family away from home in States. I had a wonderful time with Lekha, Debamita, Kalyan, Abhinav and Jaya – who were two years senior to me at Cornell and always pampered me and listened to my constant complaining and frustration of failed experiments, coursework and grading. They were always there in my times of happiness and despair and I have enjoyed countless hours of chatting, dinners, movies, shopping, dancing, excursions to state parks, waterfalls, lakes and many other places with them. I especially enjoyed having coffee and bubble tea with Lekha and Debamita while enjoying the view from Libe slope and having long philosophical discussions as well as gossiping! Apart from them, I also had the joy of making many other amazing friends in Ithaca – Trina, Debashree, Rachna, Aritro, Anand, Siddarth, Parag, Swapna, Snad, Soumya, Debashree, Shridhar, Abhishek, Nabanita, Garima, Anupam, Ushati, Anandaroop, Amrita, Pavithra, Gaganpreet, Kasturi and many more. I had a very fun-filled, exciting time in Ithaca due to their presence and I will always be glad that I got an opportunity to make so many close friends.

My graduate life at Cornell University was a wonderful journey filled with many memorable moments and I am thankful to God for all His blessings.

TABLE OF CONTENTS

LIST OF FIGURES

LIST OF TABLES

LIST OF ABBREVIATIONS

A23187	Calcium Ionophore
A488-IgE	Alexa-488 Immunoglobulin E
Ag	Antigen
BSA	Bovine Serum Albumin
BSS	Buffered Salt Solution
Ca^{2+}	Calcium
CaM	Calmodulin
Cyto-D	Cytochalasin D
DAG	Diacyl Glycerol
DCT	Dinitrophenyl Caproic Tyrosine
DGK	Diacyl Glycerol Kinase
DNP-BSA	Dinitrophenyl-Bovine Serum Albumin
EC	Extracellular
EDTA	Ethylenediamide Tetraacetic Acid
EGFP	Enhanced Green Fluorescent Protein
ER	Endoplasmic Reticulum
FBS	Fetal Bovine Serum
FcεRI	High affinity receptor for immunoglobulin E
FITC	Fluorescein Isothiocyanate
IgE	Immunoglobulin E
IgG	Immunoglobulin G
IL-6	Interleukin-6
IP	Immunoprecipitated Product
IP_3	Inositol-(1,4,5)-trisphosphate
LAT	Linker for Activation of T-cells
MARCKS	Myristoylated Alanine-Rich C-Kinase Substrate
MARCKS-ED	Myristoylated Alanine-Rich C-Kinase Substrate's Effector Domain
MEM	Minimal Essential Medium
mRFP	Monomeric Red Fluorescent Protein
NSF	N-ethylmaleimide Sensitive Fusion Protein
PIP_2	Phosphatidylinositol-(4,5)-bisphosphate
PIP_3	Phosphatidylinositol 3,4,5-trisphosphate
PIPs	Phosphatidylinositol Phosphates
PKC	Protein Kinase C
PKCβI	Protein Kinase C Beta I isoform
PLC	Phospholipase C
PM	Plasma Membrane
PMA	Phorbol Myristoyl Acetate
RBL	Rat Basophilic Leukemia
SDS-PAGE	Sodium Dodecyl Sulfate Polyacrylamide Gel Electrophoresis
SNARE	Soluble NSF Attachment Receptor Protein
STIM1	Stromal Interaction Molecule 1
SERCA	Sarcoplasmic-Endoplasmic Reticulum Ca^{2+} ATPase
siRNA	Short interfering Ribonucleic Acids
SOCE	Store Operated Ca^{2+} Entry

Tx-100	TritonX-100
VAMP	Vesicle Associated Membrane Protein

CHAPTER 1

INTRODUCTION

1.1 Mast cells: A brief overview

Mast cells were discovered in the late 1800's by Paul Ehrlich due to their strikingly characteristic staining of dense cytoplasmic granules containing vasoactive mediators including histamine (Prussin and Metcalfe, 2003). Mast cells are key players in allergy and asthma and are found underneath the epithelial layer, primarily lining the gut and the respiratory tract, and hence they form the first line of defense in the body. First exposure of the mucosal lining to any allergen/antigen results in production of IgE immunoglobulin from plasma cells (differentiated B cells) specific for that antigen. IgE binds to its high-affinity receptor FcεRI expressed on mast cells, and these mast cells are termed as being "sensitized" towards that antigen. Secondary exposure to antigen causes cross-linking of IgE-bound to its receptor on mast cells which releases allergic mediators in tissues and in the blood stream, causing smooth muscle contraction, vasodilation and increased vascular permeability (Metcalfe et al., 1997). This elicits the symptoms of allergy such as sneezing, itching etc. in an immediate response, followed by de novo synthesis and release of cytokines after several hours (Qiao et al., 2006).

Rat basophilic leukemia cells (RBL-2H3 cells) are a cultured, mucosal mast cell line, often used as a model system for investigating IgE-mediated signaling cascade (Barsumian et al., 1981). Stimulation of anti-DNP (2,4-dinitrophenyl) IgE-sensitized cells with DNP conjugated to

bovine serum albumin (DNP-BSA) occurs as the result of cross linking of IgE leading to clustering of FcεRI. As depicted in Figure 1.1, receptor aggregation results in tyrosine phosphorylation of the receptor by the Src family kinase, Lyn, which leads to the recruitment of Syk kinase from the cytosol causing phosphorylation of downstream targets. A key signaling event is activation of phospholipase Cγ (PLCγ), which hydrolyzes membrane phospholipid phosphatidylinositol 4,5-bisphosphate (PIP_2) to produce two important second messengers: inositol 1,4,5-trisphosphate (IP_3) and diacyl 2,3-glyecrol (DAG). IP_3 binds to its receptors in the endoplasmic reticulum causing release of Ca^{2+} from the ER stores. DAG together with Ca^{2+} causes activation of multiple isoforms of protein kinase C (PKC). Elevation of cytosolic Ca^{2+} and PKC activation synergistically stimulate granule exocytosis (also referred to as degranulation) in mast cells, causing the release of preformed allergic mediators and also causing cell ruffling and spreading (Blott and Griffiths, 2002; Sagi-Eisenberg and Pecht, 1984). Release of histamines and serotonin causes minor allergy symptoms, however, in some extreme cases, these symptoms can escalate to more serious medical conditions like anaphylaxis and asthma. Currently available drugs are only partially effective in the treatment of these life threatening conditions. Understanding the intricate regulatory mechanisms of exocytosis in mast cells will provide useful insight for the development of novel therapeutics.

1.2 Ca^{2+}: Critical requirement for granule exocytosis

Cytosolic Ca^{2+} elevation is a universal requirement for many cellular mechanisms in both excitable and non-excitable cells. A primary requirement for exocytosis in mast cells is elevated

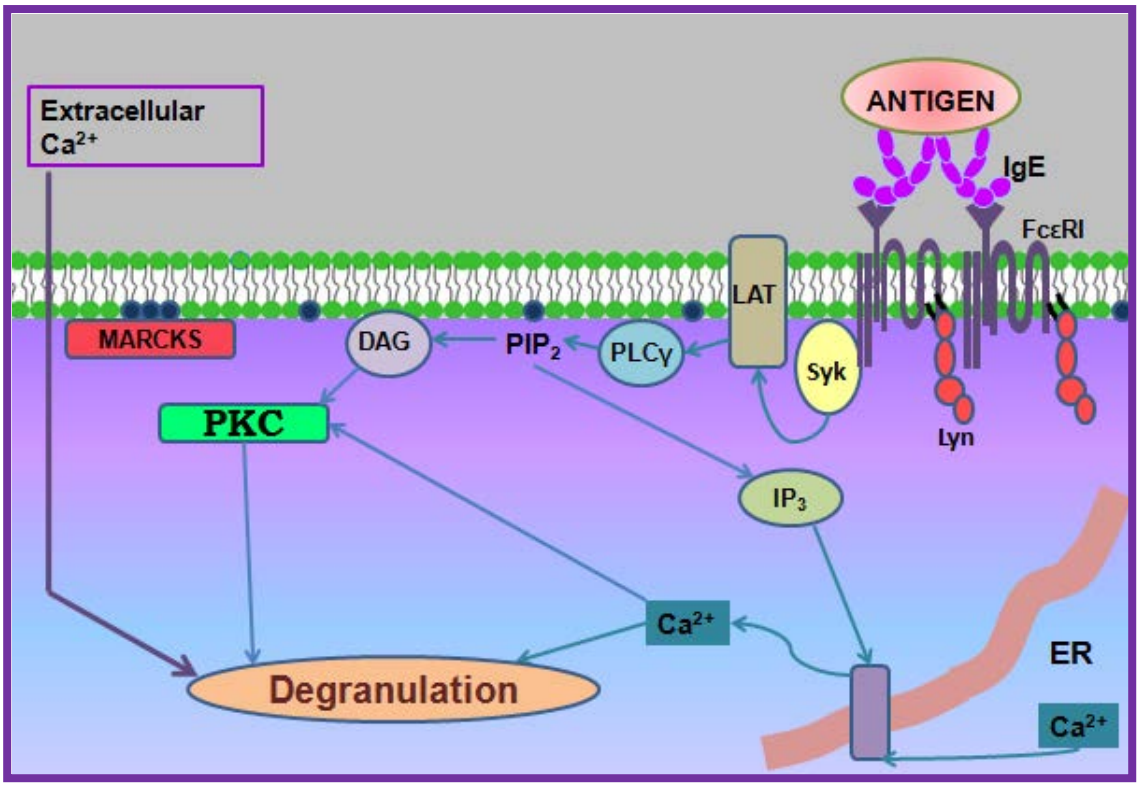

Figure 1.1: IgE-mediated signaling cascade within an antigen-stimulated mast cell resulting in degranulation.

cytosolic Ca^{2+}, which facilitates the fusion of secretory vesicles with the plasma membrane (Berridge, 2004; Clapham, 2007). Receptor stimulation causes Ca^{2+} elevation in the form of puffs (localized increase), waves or oscillations (Berridge, 2006). Ca^{2+} elevation in mammalian cells is a biphasic process: IP_3-mediated Ca^{2+} release from endoplasmic reticulum (ER) stores causes the initial rise in cytosolic Ca^{2+} concentration; this is followed by sustained transient elevations (oscillations) dependent on extracellular Ca^{2+} (Narenjkar et al., 1999; Putney and Bird, 1993). Stromal interaction molecule 1 (STIM1), an EF-hand domain transmembrane protein present in the ER senses depletion of Ca^{2+} from the ER and redistributes to junctions with the plasma membrane where it couples with the Ca^{2+} channel protein, Orai1, leading to influx of extracellular Ca^{2+} into the cytosol (Feske et al., 2006; Liou et al., 2005; Zhang and McCloskey, 1995).

The amplitude and frequency of Ca^{2+} oscillations varies from cell to cell, and it remains intriguing why Ca^{2+} elevation follows such a rhythmic pattern. One of the most widely accepted speculations in the literature is that oscillatory elevation of Ca^{2+} is required to selectively regulate a variety of downstream effectors, and each oscillatory peak encodes signals for different signaling pathways (Dolmetsch et al., 1998).

Previous studies have indicated a temporal correlation between the peaks of stimulated Ca^{2+} oscillations with the fusion of secretory granules with the plasma membrane in RBL cells (Kim et al., 1997). However, it should be noted that thapsigargin, a pharmacologic agent which prevents the re-uptake of Ca^{2+} into the ER causes a sustained, non-oscillatory elevation of Ca^{2+}

in the cytosol and also induces significant granule exocytosis in adherent mast cells (Wolfe et al., 1996). The mechanism by which Ca^{2+} participates in exocytosis is still unclear. Ca^{2+} binding to PIPs has been shown to be involved in facilitating the insertion of synaptotagmins bound to secretory vesicles into the plasma membrane prior to fusion (Bai et al., 2004).

1.3 Protein Kinase C: Regulator of degranulation in mast cells

Protein Kinase C was discovered in late 1970's by Nishizuka and colleagues as a target for phorbol esters, which brought PKC to the forefront of cancer research (Nishizuka et al., 1978; Takai et al., 1979). Phorbol esters are structural analogs of diacylglycerol (DAG), which is a physiological activator of PKC. DAG is readily metabolized in cells resulting in transient PKC activation, however, phorbol esters cannot be metabolized by the cells, causing sustained PKC activation and resulting in tumor promotion due to increased proliferative activity of cells. In mast cells, previous studies have shown evidence for the involvement of PKC in granule exocytosis due to the synergistic action of phorbol myristoyl acetate (PMA) and Ca^{2+} ionophore to cause stimulated degranulation (Sagi-Eisenber and Pecht, 1984).

PKC is a family of Ser/Thr kinases, all of which contain a regulatory region at the N-terminus and a catalytic kinase core at the C-terminus (Steinberg, 2008). The regulatory region is composed of a Cys-rich C1 domain and/or a C2 domain which is known to bind Ca^{2+} ions in conjunction with negatively charged phospholipids. It has also been reported recently that conventional PKCs bind directly to PIP_2 through their C2 domain (Corbalan-Garcia et al., 2007). The kinase core has an auto inhibitory motif occupying the active site in the inactive state of

PKC, and, upon PKC activation, conformational changes cause release of this auto inhibitory motif, thus exposing the active site of PKC as shown in Figure 1.2.

All PKC isoforms have been subdivided into three categories based on their activation requirements. The conventional class of PKCs (α, β and γ) has C1 and C2 domains which bind DAG and Ca^{2+}, respectively, for activation. The PKCβ isoform has two splice variants, βI and βII, which are generated by alternative splicing of C-terminal exons (V5 domain) (Ono et al., 1987). The novel class of PKCs (δ, ε, η and θ) requires only DAG for activation as they lack a C2 domain for Ca^{2+} binding. The atypical PKC class (ζ and λ) does not require either DAG or Ca^{2+} for their activity, but instead it is activated by ceramides by an unknown mechanism. Although binding of Ca^{2+} enhances the capacity of conventional PKC isoforms to translocate to the membrane and bind to DAG, this is not essential, as shown by the capacity of phorbol esters to cause translocation of conventional PKC isoforms independently of Ca^{2+} elevation (Oancea and Meyer, 1998).

Apart from Ca^{2+} binding, conventional PKC isoforms also require sustained DAG production for their translocation to the plasma membrane. DAG, a product of PIP_2 metabolism, shows sustained elevation in stimulated mast cells (Kennerly et al., 1979). Mast cells also express various isoforms of DAG kinases (DGK) which phosphorylate DAG, resulting in phosphatidic acid production. Koretzky and colleagues have demonstrated that DGKζ$^-$ deficient bone marrow-derived mast cells exhibit significantly decreased degranulation, Ca^{2+} response, PLCγ activity, as well as decreased PKCβII membrane recruitement (Olenchock et al., 2006). Based on their results, one can speculate that DGKs play a significant role in the dissociation of PKC from the membrane or that phosphatidic acid is important for PLCγ activation. RBL-2H3

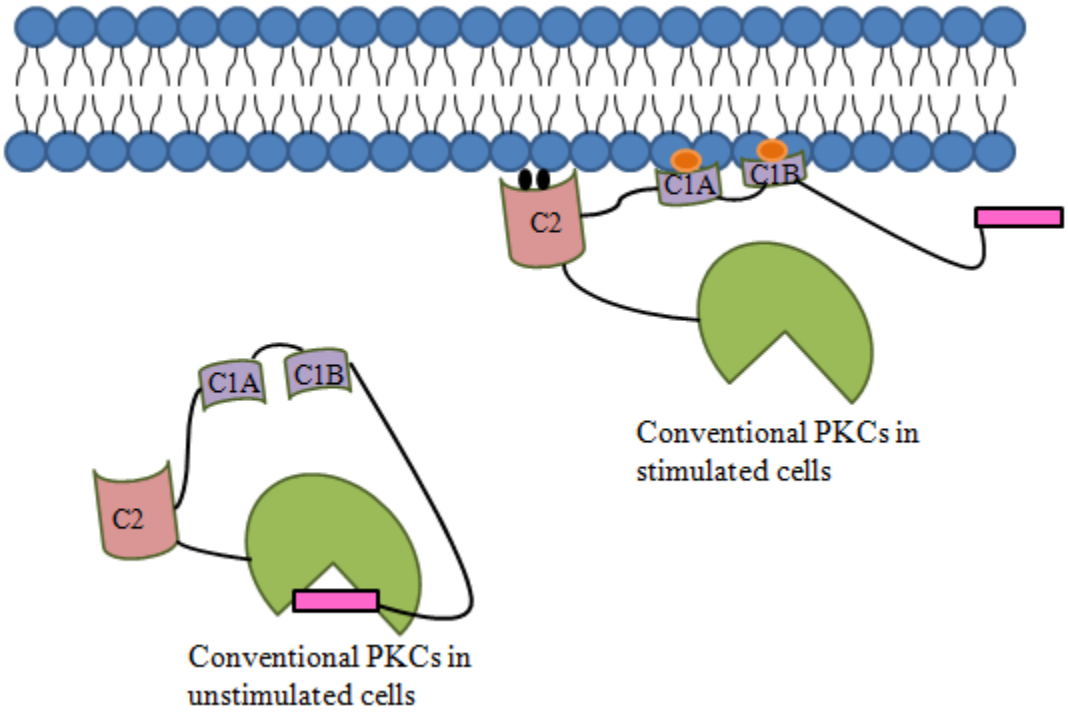

Figure 1.2: Schematic diagram showing conventional PKC isoforms in their inactive (left) and active (right) states. In the resting state of cells, the active site of PKC is sequestered by an auto inhibitory sequence (pink). Upon Ca^{2+} (black) binding, PKC translocates to the plasma membrane, where it binds to DAG (orange) via its C1A and C1B domains, resulting in the exposure of the active site of PKC in the kinase domain (green).

cells express both conventional and novel isoforms (α,β,δ,ε and ζ), and studies have shown that their over expression results in increased proliferative response and enhancement or inhibition of the production of certain cytokines (Chang et al., 1997). Previous studies have shown that over expression of the PKCβ isoform significantly increases secretion, phospholipase A2 activation, and production of IL-6. Reconstitution studies with PKC isoforms (Ozawa et al., 1993a; Ozawa et al., 1993b), together with genetic knockout have established a positive regulatory role of the PKCβ isoform in mast cell stimulation-secretion coupling (Nechushtan et al., 2000). Interestingly, knockout of PKCδ results in an enhancement in mast cells degranulation, suggesting that this isoform plays a negative regulatory role in granule exocytosis (Leitges et al., 2002). However, the mechanism by which these isoforms participate in regulating the exocytotic machinery is not well understood. However, it is well established that PKC regulates exocytosis at a terminal step, as demonstrated by the capacity of PKC inhibitors to inhibit degranulation in mast cells with equal effectiveness when stimulated by antigen or Ca^{2+} ionophore (Wolfe et al., 1996).

Recent studies with GFP-tagged PKCs have demonstrated the spatio-temporal dynamics of PKC translocation in single, living cells upon stimulation. Meyer and colleagues have shown transient oscillatory translocation of PKCγ isoform in RBL cells upon receptor stimulation (Oancea and Meyer, 1998).

1.4 MARCKS and its interaction with phosphoinositides

Myristoylated alanine-rich C-kinase substrate (MARCKS) is a major, ubiquitous substrate of PKC. It was discovered in brain synaptosomes in 1982 (Wu et al., 1982) and plays

multiple roles in regulating cellular signaling processes such as membrane ruffling and cell spreading. Interestingly, MARCKS expression levels have been found to be significantly reduced in cancerous cells and over-expression of MARCKS can suppress cancer cell proliferation (Manenti et al., 1998). Studies have shown that knockout of MARCKS results in abnormal brain development and is embryonically lethal in mice (Stumpo et al., 1995). It has also been reported in the literature that PKC-dependent phosphorylation of MARCKS is important for brain and retina development in mice. Blackshear and colleagues reported that the phosphomimetic mutant of MARCKS can rescue these defects, but these mice did not survive after few hours (Scarlett and Blackshear, 2003). The capacity of a 24 amino acid peptide identical to the N-terminus of MARCKS (MANS peptide) to inhibit mucin secretion from human airway epithelial cells in-vitro and in mice has made it an attractive target in therapeutics (Singer et al., 2004). PKC-dependent MARCKS phosphorylation has also been shown to be important in regulating granule exocytosis in chromaffin cells (Elzagallaai et al., 2000), however, the mechanism is still not understood.

MARCKS is 309 amino acids long and has a myristoyl moiety at the N-terminus, as shown in Figure 1.3. Many of the functional interactions of MARCKS, including PKC phosphorylation, phospholipid binding, F-actin cross-linking, and calmodulin binding are due to the presence of a highly polybasic 25 amino acid long sequence of charge +13 referred to as effector domain (MARCKS-ED) (McLaughlin and Murray, 2005). This effector domain has four Ser residues, three of which are phosphorylated by PKC, the phosphorylation of fourth Ser residue is controversial. In resting cells, MARCKS is strongly localized to the membrane due to myristoylation as well as to electrostatic interactions of its effector domain with anionic

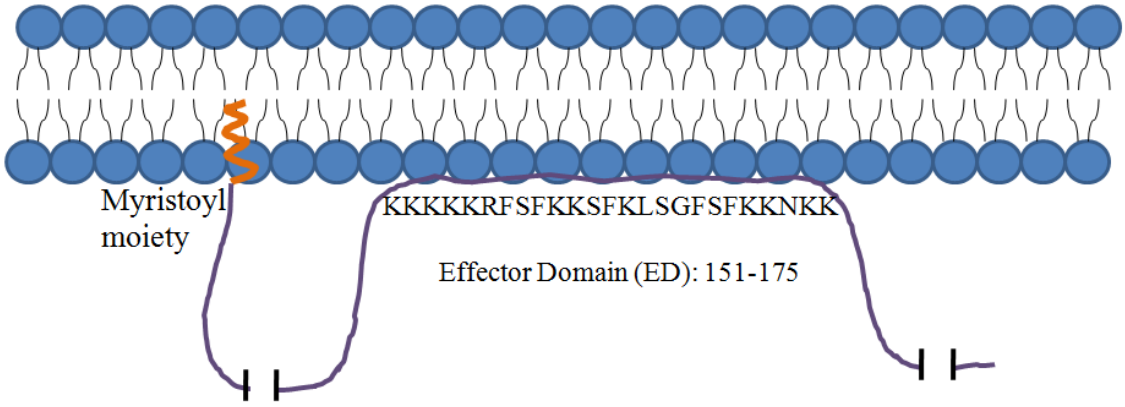

Figure 1.3: Schematic diagram depicting the association of MARCKS with the plasma membrane through anchorage of its myristoyl moiety and through electrostatic interactions of the effector domain with negatively charged phospholipids.

phospholipids (Swierczynski and Blackshear, 1996). As depicted in Figure 1.4, PKC activation in stimulated cells results in phosphorylation of Ser residues in the MARCKS effector domain, thereby disrupting its electrostatic interaction with the membrane and causing its translocation to the cytosol. MARCKS is dephosphorylated by protein phosphatase I, protein phosphatase 2A or calcineurin, casuing it to reassociate with the plasma membrane (Seki et al., 1995).

There is growing evidence in the literature that negatively charged phosphatidylinositol lipids, specifically, PIP_2 and PIP_3, are sequestered in the plasma membrane by proteins that have clusters of positively charged amino acids. Even though PIP_2 comprises only 1% of the total phospholipid content in the plasma membrane, it plays multiple, critical roles in signaling pathways such as endocytosis, exocytosis, phagocytosis and membrane ruffling (Di Paolo and De Camilli, 2006). McLaughlin and colleagues have demonstrated that MARCKS-ED shows tight binding to lipid bilayers that incorporate PIPs (Wang et al., 2001). Dissociation of MARCKS from the plasma membrane due to PIP_2 hydrolysis and inhibition of PIP synthesis has demonstrated that PIPs are primarily responsible for the association of MARCKS with the plasma membrane, as shown by Meyer and colleagues (Heo et al., 2006). As PIP_2 has a net charge of -4 at neutral pH (McLaughlin et al., 2002), a single MARCKS-ED can electrostatically sequester three molecules of PIP_2. The capacity of MARCKS to regulate the availability of phosphoinositides reversibly under physiological conditions makes it a suitable candidate for regulating PIP-dependent processes upon receptor stimulation.

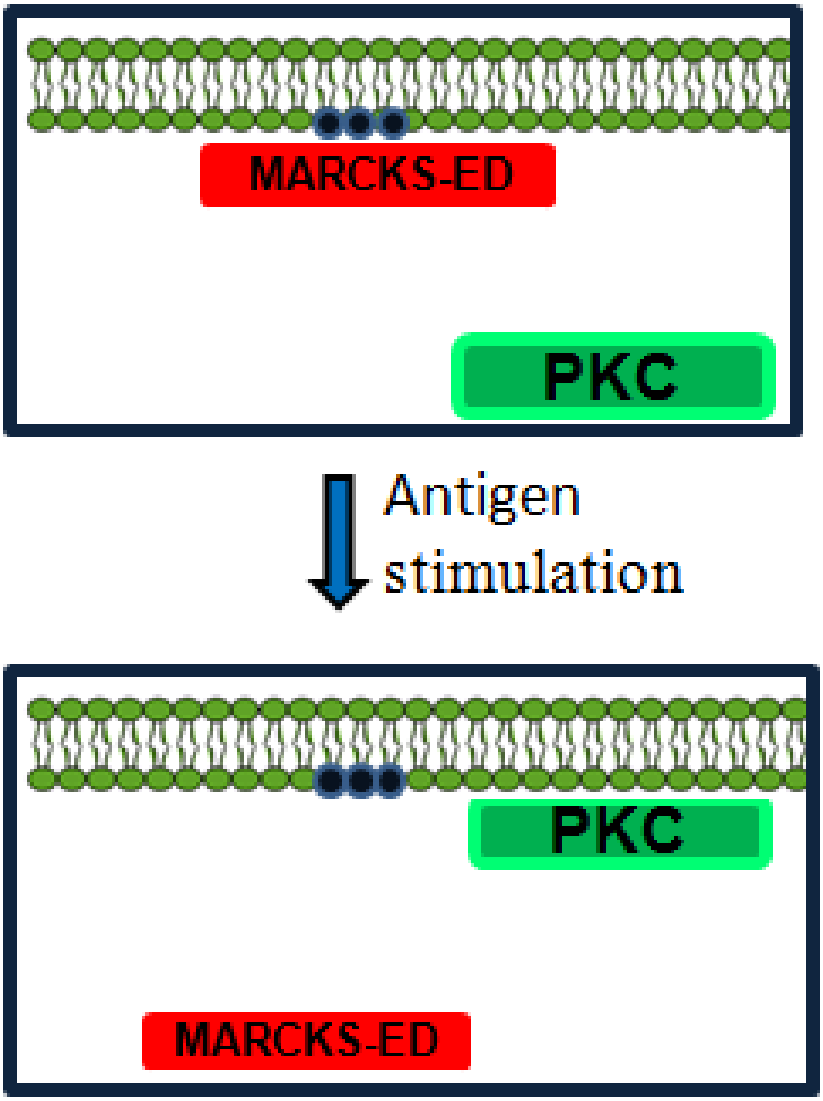

Figure 1.4: Stimulation of cells results in translocation and activation of PKC, causing phosphorylation of MARCKS-ED and consequent dissociation from the plasma membrane.

1.5 Granule exocytosis in mast cells

Mast cell secretory granules store pre-formed allergic mediators including histamine and serotonin as well as certain enzymes such as β-hexosaminidase, all of which are secreted upon stimulation of these cells. The terminal steps resulting in granule exocytosis in mast cells are a complex, well-coordinated process which is still not fully understood. This involves translocation of secretory vesicles to the plasma membrane, docking of secretory vesicles, followed by fusion and release of secretory content into the extracellular environment (Martin, 2003).

Mast cells express the essential components of exocytotic machinery, namely, synaptotagmins and soluble N-ethylmaleimide sensitive fusion (NSF) attachment receptor proteins (SNAREs) which tightly regulate the exocytosis process with the help of adaptor proteins and Ca^{2+}. Similar to synaptic vesicle exocytosis (Rizo and Rosenmund, 2008), mast cell exocytosis also has a critical requirement for an interaction between vesicle or v-SNAREs and target or t-SNAREs to form a trans-SNARE complex resulting in membrane fusion prior to release of chemical mediators. A variety of SNARE proteins are expressed in RBL cells, including syntaxin 4, SNAP 23 (non-neuronal isoform of SNAP 25), VAMP-7 and VAMP-8 that have been shown to be essential for mast cell degranulation (Paumet et al., 2000; Sander et al., 2008). Due to the sensitivity of granule exocytosis to PKC inhibitors, a lot of work has been done to understand the roles of PKC substrates in the fusion process including SNARES as shown by in-vitro studies. A survey of literature indicates that other PKC substrates may also

play critical roles in degranulation. Munc18-1, a prominent PKC substrate, has turned out to be a very promising candidate due to its capacity to bind to syntaxin-1, which is a t-SNARE and possesses a juxtamembrane stretch of basic amino acids capable of interacting with acidic phospholipids (Burgoyne and Morgan, 2003). Interestingly, disruption of the Munc 18-1 - syntaxin-1 interaction can cause inhibition and delay of granule fusion events in PC12 cells (Barclay, 2008).

Recent advances in imaging and electrochemical methods such as patch-clamp capacitance measurements have enabled significant mechanistic insights into granule exocytosis at a single cell level. The ability to fluorescently label secretory lysosomes has made it possible to visualize individual secretory vesicles. One of the recently developed approaches to monitor exocytosis events at high spatial and temporal resolution utilizes fluorescein isothiocyanate-conjugated dextran (FITC-dextran), which is taken up by fluid phase pinocytosis into secretory lysosomes. Mast cell granules, which originate from secretory lysosomes (Dragonetti et al., 2000), have acidic pH due to which FITC fluorescence remains quenched, however, upon fusion with the plasma membrane, FITC fluorescence can be visually monitored due to fluorescence dequenching upon neutralization. Single cell techniques employed simultaneously with other exocytosis quantification methodologies will certainly help gain more clear mechanistic insights into the intricate regulation of exocytotic machinery.

1.6 Current studies

This dissertation describes the dynamics of PKCβ, MARCKS and phosphoinositides in

regulating stimulated granule exocytosis in mast cells. The data presented in Chapter 2 shows the dynamic interaction of PKCβI-EGFP with the plasma membrane upon antigen stimulation, which correlates with oscillatory elevations of Ca^{2+} in the cytoplasm. Furthermore, we show that mRFP-MARCKS-ED association with the plasma membrane oscillates in synchrony with the association of PKC with the plasma membrane, which in turn is synchronized to Ca^{2+} oscillations. To investigate the role of PKC-dependent exposure of PIPs under stimulated conditions, we created a mutant of mRFP-MARCKS-ED (SA4) which cannot be phosphorylated by PKC. The capacity of this probe to alter IP_3-dependent Ca^{2+} release from stores provides strong evidence for its capacity to sequester phosphoinositides. To investigate the role of PKC and PIPs in granule exocytosis, we compared the effect of mRFP-MARCKS-ED and mRFP-MARCKS-ED SA4 on stimulated granule exocytosis. We observe substantial inhibition of both antigen and thapsigargin-stimulated granule exocytosis by the latter but not the former construct, suggesting that events downstream of Ca^{2+} mobilization in granule exocytosis depend on sequestration of PIPs in a non-reversible manner.

In Chapter 3, we perform knockdown of full length endogenous MARCKS in RBL cells and characterize the effects of this perturbation on stimulated Ca^{2+} mobilization and degranulation. Our results indicate that full length, endogenous MARCKS positively regulates these processes, and we hypothesize that its association with Ca^{2+}/calmodulin under stimulated conditions inhibits the interaction of Ca^{2+}/calmodulin with STIM1, hence positively regulating SOCE and granule exocytosis.

In Appendix 1, we characterize a broad series of bifunctional sulfonated DNP-poly(2-methoxystyrene) polymers and a biodegradable polymer for their potential to serve as leads for

allergy therapeutics.

REFERENCES

Bai, J., Tucker, W.C., and Chapman, E.R. (2004). PIP2 increases the speed of response of synaptotagmin and steers its membrane-penetration activity toward the plasma membrane. Nat Struct Mol Biol *11*, 36-44.

Barclay, J.W. (2008). Munc-18-1 regulates the initial release rate of exocytosis. Biophys J *94*, 1084-1093.

Barsumian, E.L., Isersky, C., Petrino, M.G., and Siraganian, R.P. (1981). IgE-induced histamine release from rat basophilic leukemia cell lines: isolation of releasing and nonreleasing clones. Eur J Immunol *11*, 317-323.

Berridge, M.J. (2004). Calcium signal transduction and cellular control mechanisms. Biochim Biophys Acta *1742*, 3-7.

Berridge, M.J. (2006). Calcium microdomains: organization and function. Cell Calcium *40*, 405-412.

Blott, E.J., and Griffiths, G.M. (2002). Secretory lysosomes. Nat Rev Mol Cell Biol *3*, 122-131.

Burgoyne, R.D., and Morgan, A. (2003). Secretory granule exocytosis. Physiol Rev *83*, 581-632.

Chang, E.Y., Szallasi, Z., Acs, P., Raizada, V., Wolfe, P.C., Fewtrell, C., Blumberg, P.M., and Rivera, J. (1997). Functional effects of overexpression of protein kinase C-alpha, -beta, -delta, -epsilon, and -eta in the mast cell line RBL-2H3. J Immunol *159*, 2624-2632.

Clapham, D.E. (2007). Calcium signaling. Cell *131*, 1047-1058.

Corbalan-Garcia, S., Guerrero-Valero, M., Marin-Vicente, C., and Gomez-Fernandez, J.C. (2007). The C2 domains of classical/conventional PKCs are specific PtdIns(4,5)P(2)-sensing domains. Biochem Soc Trans *35*, 1046-1048.

Di Paolo, G., and De Camilli, P. (2006). Phosphoinositides in cell regulation and membrane dynamics. Nature *443*, 651-657.

Dolmetsch, R.E., Xu, K., and Lewis, R.S. (1998). Calcium oscillations increase the efficiency and specificity of gene expression. Nature *392*, 933-936.

Dragonetti, A., Baldassarre, M., Castino, R., Demoz, M., Luini, A., Buccione, R., and Isidoro, C. (2000). The lysosomal protease cathepsin D is efficiently sorted to and secreted from regulated secretory compartments in the rat basophilic/mast cell line RBL. J Cell Sci *113 (Pt 18)*, 3289-3298.

Elzagallaai, A., Rose, S.D., and Trifaro, J.M. (2000). Platelet secretion induced by phorbol esters stimulation is mediated through phosphorylation of MARCKS: a MARCKS-derived peptide

blocks MARCKS phosphorylation and serotonin release without affecting pleckstrin phosphorylation. Blood *95*, 894-902.

Feske, S., Gwack, Y., Prakriya, M., Srikanth, S., Puppel, S.H., Tanasa, B., Hogan, P.G., Lewis, R.S., Daly, M., and Rao, A. (2006). A mutation in Orai1 causes immune deficiency by abrogating CRAC channel function. Nature *441*, 179-185.

Heo, W.D., Inoue, T., Park, W.S., Kim, M.L., Park, B.O., Wandless, T.J., and Meyer, T. (2006). PI(3,4,5)P3 and PI(4,5)P2 lipids target proteins with polybasic clusters to the plasma membrane. Science *314*, 1458-1461.

Kennerly, D.A., Sullivan, T.J., Sylwester, P., and Parker, C.W. (1979). Diacylglycerol metabolism in mast cells: a potential role in membrane fusion and arachidonic acid release. J Exp Med *150*, 1039-1044.

Kim, T.D., Eddlestone, G.T., Mahmoud, S.F., Kuchtey, J., and Fewtrell, C. (1997). Correlating Ca2+ responses and secretion in individual RBL-2H3 mucosal mast cells. J Biol Chem *272*, 31225-31229.

Leitges, M., Gimborn, K., Elis, W., Kalesnikoff, J., Hughes, M.R., Krystal, G., and Huber, M. (2002). Protein kinase C-delta is a negative regulator of antigen-induced mast cell degranulation. Mol Cell Biol *22*, 3970-3980.

Liou, J., Kim, M.L., Heo, W.D., Jones, J.T., Myers, J.W., Ferrell, J.E., Jr., and Meyer, T. (2005). STIM is a Ca2+ sensor essential for Ca2+-store-depletion-triggered Ca2+ influx. Curr Biol *15*, 1235-1241.

Manenti, S., Malecaze, F., Chap, H., and Darbon, J.M. (1998). Overexpression of the myristoylated alanine-rich C kinase substrate in human choroidal melanoma cells affects cell proliferation. Cancer Res *58*, 1429-1434.

Martin, T.F. (2003). Tuning exocytosis for speed: fast and slow modes. Biochim Biophys Acta *1641*, 157-165.

McLaughlin, S., and Murray, D. (2005). Plasma membrane phosphoinositide organization by protein electrostatics. Nature *438*, 605-611.

McLaughlin, S., Wang, J., Gambhir, A., and Murray, D. (2002). PIP(2) and proteins: interactions, organization, and information flow. Annu Rev Biophys Biomol Struct *31*, 151-175.

Metcalfe, D.D., Baram, D., and Mekori, Y.A. (1997). Mast cells. Physiol Rev *77*, 1033-1079.

Narenjkar, J., Marsh, S.J., and Assem, E.S. (1999). The characterization and quantification of antigen-induced Ca2+ oscillations in a rat basophilic leukaemia cell line (RBL-2H3). Cell Calcium *26*, 261-269.

Nechushtan, H., Leitges, M., Cohen, C., Kay, G., and Razin, E. (2000). Inhibition of

degranulation and interleukin-6 production in mast cells derived from mice deficient in protein kinase Cbeta. Blood *95*, 1752-1757.

Nishizuka, Y., Takai, Y., Kishimoto, A., Hashimoto, E., Inoue, M., Yamamoto, M., Criss, W.E., and Kuroda, Y. (1978). A role of calcium in the activation of a new protein kinase system. Adv Cyclic Nucleotide Res *9*, 209-220.

Oancea, E., and Meyer, T. (1998). Protein kinase C as a molecular machine for decoding calcium and diacylglycerol signals. Cell *95*, 307-318.

Olenchock, B.A., Guo, R., Silverman, M.A., Wu, J.N., Carpenter, J.H., Koretzky, G.A., and Zhong, X.P. (2006). Impaired degranulation but enhanced cytokine production after Fc epsilonRI stimulation of diacylglycerol kinase zeta-deficient mast cells. J Exp Med *203*, 1471-1480.

Ono, Y., Kikkawa, U., Ogita, K., Fujii, T., Kurokawa, T., Asaoka, Y., Sekiguchi, K., Ase, K., Igarashi, K., and Nishizuka, Y. (1987). Expression and properties of two types of protein kinase C: alternative splicing from a single gene. Science *236*, 1116-1120.

Ozawa, K., Szallasi, Z., Kazanietz, M.G., Blumberg, P.M., Mischak, H., Mushinski, J.F., and Beaven, M.A. (1993a). Ca(2+)-dependent and Ca(2+)-independent isozymes of protein kinase C mediate exocytosis in antigen-stimulated rat basophilic RBL-2H3 cells. Reconstitution of secretory responses with Ca2+ and purified isozymes in washed permeabilized cells. J Biol Chem *268*, 1749-1756.

Ozawa, K., Yamada, K., Kazanietz, M.G., Blumberg, P.M., and Beaven, M.A. (1993b). Different isozymes of protein kinase C mediate feedback inhibition of phospholipase C and stimulatory signals for exocytosis in rat RBL-2H3 cells. J Biol Chem *268*, 2280-2283.

Paumet, F., Le Mao, J., Martin, S., Galli, T., David, B., Blank, U., and Roa, M. (2000). Soluble NSF attachment protein receptors (SNAREs) in RBL-2H3 mast cells: functional role of syntaxin 4 in exocytosis and identification of a vesicle-associated membrane protein 8-containing secretory compartment. J Immunol *164*, 5850-5857.

Prussin, C., and Metcalfe, D.D. (2003). 4. IgE, mast cells, basophils, and eosinophils. J Allergy Clin Immunol *111*, S486-494.

Putney, J.W., Jr., and Bird, G.S. (1993). The inositol phosphate-calcium signaling system in nonexcitable cells. Endocr Rev *14*, 610-631.

Qiao, H., Andrade, M.V., Lisboa, F.A., Morgan, K., and Beaven, M.A. (2006). FcepsilonR1 and toll-like receptors mediate synergistic signals to markedly augment production of inflammatory cytokines in murine mast cells. Blood *107*, 610-618.

Rizo, J., and Rosenmund, C. (2008). Synaptic vesicle fusion. Nat Struct Mol Biol *15*, 665-674.

Sagi-Eisenberg, R., and Pecht, I. (1984). Protein kinase C, a coupling element between stimulus and secretion of basophils. Immunol Lett *8*, 237-241.

Sander, L.E., Frank, S.P., Bolat, S., Blank, U., Galli, T., Bigalke, H., Bischoff, S.C., and Lorentz, A. (2008). Vesicle associated membrane protein (VAMP)-7 and VAMP-8, but not VAMP-2 or VAMP-3, are required for activation-induced degranulation of mature human mast cells. Eur J Immunol *38*, 855-863.

Scarlett, C.O., and Blackshear, P.J. (2003). Neuroanatomical development in the absence of PKC phosphorylation of the myristoylated alanine-rich C-kinase substrate (MARCKS) protein. Brain Res Dev Brain Res *144*, 25-42.

Seki, K., Chen, H.C., and Huang, K.P. (1995). Dephosphorylation of protein kinase C substrates, neurogranin, neuromodulin, and MARCKS, by calcineurin and protein phosphatases 1 and 2A. Arch Biochem Biophys *316*, 673-679.

Singer, M., Martin, L.D., Vargaftig, B.B., Park, J., Gruber, A.D., Li, Y., and Adler, K.B. (2004). A MARCKS-related peptide blocks mucus hypersecretion in a mouse model of asthma. Nat Med *10*, 193-196.

Steinberg, S.F. (2008). Structural basis of protein kinase C isoform function. Physiol Rev *88*, 1341-1378.

Stumpo, D.J., Bock, C.B., Tuttle, J.S., and Blackshear, P.J. (1995). MARCKS deficiency in mice leads to abnormal brain development and perinatal death. Proc Natl Acad Sci U S A *92*, 944-948.

Swierczynski, S.L., and Blackshear, P.J. (1996). Myristoylation-dependent and electrostatic interactions exert independent effects on the membrane association of the myristoylated alanine-rich protein kinase C substrate protein in intact cells. J Biol Chem *271*, 23424-23430.

Takai, Y., Kishimoto, A., Iwasa, Y., Kawahara, Y., Mori, T., and Nishizuka, Y. (1979). Calcium-dependent activation of a multifunctional protein kinase by membrane phospholipids. J Biol Chem *254*, 3692-3695.

Wang, J., Arbuzova, A., Hangyas-Mihalyne, G., and McLaughlin, S. (2001). The effector domain of myristoylated alanine-rich C kinase substrate binds strongly to phosphatidylinositol 4,5-bisphosphate. J Biol Chem *276*, 5012-5019.

Wolfe, P.C., Chang, E.Y., Rivera, J., and Fewtrell, C. (1996). Differential effects of the protein kinase C activator phorbol 12-myristate 13-acetate on calcium responses and secretion in adherent and suspended RBL-2H3 mucosal mast cells. J Biol Chem *271*, 6658-6665.

Wu, W.C., Walaas, S.I., Nairn, A.C., and Greengard, P. (1982). Calcium/phospholipid regulates phosphorylation of a Mr "87k" substrate protein in brain synaptosomes. Proc Natl Acad Sci U S A *79*, 5249-5253.

Zhang, L., and McCloskey, M.A. (1995). Immunoglobulin E receptor-activated calcium conductance in rat mast cells. J Physiol *483 (Pt 1)*, 59-66.

CHAPTER 2

SEQUESTRATION OF PHOSPHOINOSITIDES BY MUTATED MARCKS EFFECTOR DOMAIN INHIBITS STIMULATED CA^{2+} MOBILIZATION AND DEGRANULATION IN MAST CELLS

2.1 Abstract

Protein kinase C β (PKCβ) participates in antigen-stimulated mast cell degranulation mediated by the high affinity receptor for IgE, FcεRI, but the molecular basis is unclear. We investigated the hypothesis that the polybasic effector domain (ED) of the abundant intracellular substrate for PKC known as MARCKS sequesters phosphoinositides at the inner leaflet of the plasma membrane until MARCKS dissociates after phosphorylation by activated PKC. Real time fluorescence imaging confirms synchronization between stimulated oscillations of intracellular Ca^{2+} concentrations and oscillatory association of PKCβ-EGFP with the plasma membrane. Similarly, MARCKS-ED tagged with mRFP undergoes antigen-stimulated oscillatory dissociation and rebinding to the plasma membrane with a time course that is synchronized with reversible plasma membrane association of PKCβ. We find that MARCKS-ED dissociation is prevented by mutation of four serine residues that are potential sites of phosphorylation by PKC. Cells expressing this mutated MARCKS-ED S4A show delayed onset of antigen-stimulated Ca^{2+} mobilization and substantial inhibition of granule exocytosis. Stimulation of degranulation by thapsigargin, which bypasses inositol 1,4,5-trisphosphate production, is also substantially reduced in the presence of MARCKS-ED S4A, but store-operated Ca^{2+} entry is not inhibited. These results show the capacity of MARCKS-ED to regulate granule exocytosis in a PKC-dependent manner, consistent with regulated sequestration of phosphoinositides that mediate

granule fusion at the plasma membrane.

2.2 Introduction

Granule exocytosis in mast cells is stimulated by antigen-mediated crosslinking of IgE bound to high affinity receptors (FcεRI), and much is known about this physiologically important process in allergic and inflammatory responses (Blank and Rivera, 2004; Gilfillan and Tkaczyk, 2006). As for many other receptor-activated exocytotic responses in other cell types, critical roles for Ca^{2+} mobilization and PKC activation are well established (Ma and Beaven, 2009; Nechushtan et al., 2000). Mast cells do not exhibit voltage-gated Ca^{2+} influx, but it is known that store operated Ca^{2+} entry participates in IgE receptor-stimulated degranulation. Previous studies revealed contributions both from CRAC channels, Orai1/CRACM1 (Vig et al., 2008) and from TRPC channels (Ma et al., 2008; Suzuki et al., 2010). As for exocytosis in other cell types, mast cell granules, which are secretory lysosomes (Dragonetti et al., 2000; Xu et al., 1998), depend on elevated intracellular [Ca^{2+}] for fusion with the plasma membrane, and this requirement has been suggested to be due to triggering of SNARE-mediated fusion by granule-associated Ca^{2+}/synaptotagmin complexes bound to polyphosphoinositides at the inner leaflet of the plasma membrane (Dai et al., 2007; Paddock et al., 2008). The involvement of phosphatidylinositol 4,5- bisphosphate (PIP_2) in facilitating the membrane fusion triggered by synaptotagmin implicates this phospholipid as a key player in Ca^{2+}-dependent exocytosis (Bai et al., 2004).

The mechanism of PKC participation in mast cell granule exocytosis is less clear. PKC comprises a family of at least 10 different Ser/Thr kinases that play multiple roles in cell

signaling (Newton, 2010; Nishizuka, 1995). These isoforms of PKC have been classified into three categories based on structural and activation requirements: conventional and novel subfamilies are activated by diacylglycerol binding to a C1 domain, and conventional isoforms also require Ca^{2+} binding to a C2 domain. These subfamilies are activated by phorbol esters, which are structural mimics of diacylglycerol, providing early evidence for participation of PKC activity in mast cell degranulation (Sagi-Eisenberg et al., 1985). Reconstitution studies with PKC isoforms in permeabilized RBL mast cells yielded the first direct evidence for positive roles for PKCβ and δ in IgE receptor-stimulated degranulation (Ozawa et al., 1993a). Genetic knockout of PKCβI revealed that this isotype is important in mast cell degranulation (Nechushtan et al., 2000). Despite these advances, the mechanism for PKC activity in this and other exocytotic cell processes is not well understood.

A prominent substrate for PKC isoforms is the myristoylated alanine-rich C-kinase substrate commonly called MARCKS (Aderem, 1992; Blackshear, 1993). MARCKS binds tightly to membranes containing negatively charged phospholipids via a 25 amino acid sequence that contains 13 basic amino acids and is known as its effector domain (ED) (Wang et al., 2001). Meyer and colleagues showed that this sequence could be displaced from the plasma membrane by depletion of polyphosphoinositides, providing evidence that these negatively charged phospholipids are the principal means by which this protein anchors to the plasma membrane (Heo et al., 2006). This ED sequence contains four serine residues, three of which are phosphorylated by activated PKC to cause its dissociation from the plasma membrane (Graff et al., 1989a; Graff et al., 1989b). MARCKS has been shown to participate in granule exocytosis in platelets and chromaffin cells (Trifaro et al., 2008), but the mechanism is unknown.

Although PIP_2 constitutes only ~1% of the phospholipids in the plasma membrane, it plays a key role in regulating a large number of cellular processes, including clathrin-mediated endocytosis, activation of ion channels, actin polymerization, phagocytosis, and synaptic vesicle exocytosis (Di Paolo and De Camilli, 2006). In mast cells, antigen-stimulated activation of phospholipase Cγ (PLCγ) results in hydrolysis of PIP_2 to form inositol 1,4,5-trisphosphate (IP_3) and diacylglycerol; thus, PIP_2 is an important participant in Ca^{2+} mobilization and activation of PKCs. However, the lack of specific inhibitors of PIP_2 synthesis has made it difficult to probe the mechanisms by which PIP_2 regulates multiple, diverse functions in mammalian cells. We hypothesize that one of the key roles of PIP_2 -- wherein it interacts with synaptotagmins to facilitate granule exocytosis -- is controlled by PKC activity: PKC regulates the availability of PIP_2 because PKC phosphorylation causes MARCKS dissociation, thereby exposing PIP_2 to interact with other proteins. In the present study, we utilize the high avidity of the MARCKS-ED peptide and introduce mutations to prevent its dissociation from the plasma membrane by activated PKC. We demonstrate that expression of this mutated protein (MARCKS-ED S4A) effectively delays antigen-stimulated Ca^{2+} mobilization that is dependent on PIP_2-mediated IP_3 production. Furthermore, MARCKS-ED S4A inhibits granule exocytosis by antigen as well as by thapsigargin, which bypasses the need for IP_3 production in this process. These results provide strong evidence that this mutated MARCKS-ED construct is an effective inhibitor of PIP_2-dependent processes, and thereby it serves as a useful tool for investigating these processes.

2.3 Experimental

cDNA plasmids

PKCβI-EGFP was from Clontech (Palo Alto, CA). mRFP-MARCKS-ED was made from YFP-MARCKS-ED by exchanging YFP for mRFP by using the Nhe I and Hind III restriction sites. To generate mRFP-MARCKS-ED SA4, mutation of serines 159, 163, 167 and 170 (MARCKS full-length sequence numbers (Stumpo et al., 1989)) to alanines were performed by using QuickChange Site-Directed Mutagenesis Kit from Stratagene (La Jolla, CA) as previously described (Smith et al., 2010). Mutations were confirmed by DNA sequence analysis. MARCKS-ED and MARCKS-ED SA4 were generated by removing mRFP from the respective fluorescent constructs. The PM-EGFP construct was prepared as previously described (Pyenta et al., 2001)

Cell Culture and Transient/Stable Transfection

RBL-2H3 cells were maintained as monolayers in minimal essential medium (MEM) containing 20% fetal bovine serum and 10μg/mL gentamicin sulfate. Cells were harvested using trypsin-EDTA (Invitrogen) and transiently transfected using electroporation as previously described (Cohen et al., 2009). Electroporated cells were plated into MatTek coverslip wells (Dover, MA) in full medium and sensitized with mouse monoclonal anti-DNP IgE (0.5 μg/ml;(Posner et al., 1992)) during overnight culture. All experiments were done 20-24 h post transfection. For the generation of stable RBL cell lines expressing mRFP-MARCKS-ED SA4, transfected cells were selected in MEM containing 600 μg/ml G418 (Gibco, Invitrogen Corp., Carlsbad, CA). Cells positive for mRFP-MARCKS-ED SA4 were identified by mRFP fluorescence. Clones of cells expressing mRFP-MARCKS-ED SA4 were picked using calcium alginate fiber tipped wood applicator swabs (Fisher HealthCare, TX). One mutant clone with a

relatively low expression level and two mutant clones expressing relatively high levels of mRFP-MARCKS-ED SA4 were produced and characterized.

Live cell imaging and analysis

Prior to imaging, cells were rinsed with buffered saline solution (BSS: 20 mM HEPES, 135 mM NaCl, 1.8 mM $CaCl_2$, 1 mM $MgCl_2$, 5mM KCl, 5.6 mM glucose, 1 mg/ml BSA, pH 7.4), then imaged using a Leica TCS SP2 upright confocal microscope with an APO 63x dipping objective. Images were collected every 4 s for 1-2 min before stimulation, followed by 5-10 min of image acquisition post-stimulation using DNP-BSA (0.2 μg/ml – 1 μg/ml) or thapsigargin (0.15 μM). All live cell imaging was carried out between 25-37˚C as specified. For image analysis, a small cytoplasmic region of interest was chosen in each cell to monitor the fractional cytoplasmic fluorescence intensity changes with time using ImageJ (NIH).

Intracellular [Ca^{2+}] measurement of adherent cells

Overnight-plated and IgE-sensitized cells in MatTek dishes were loaded with Fluo-4 AM (Invitrogen) or Fura Red AM (Invitrogen) at 1 μg/mL in BSS buffer containing 0.5 mM sulfinpyrazone (Sigma) for 10 min at 37˚C. Cells were then washed 3 times in BSS/sulfinpyrazone. Fields of cells were selected to contain both transfected and untransfected cells and monitored as previously described (Calloway et al., 2009). For measurement of Ca^{2+} release from endoplasmic reticulum stores alone, BSS without Ca^{2+} was used while imaging, and 2 mM $CaCl_2$ was added subsequently to observe store-operated Ca^{2+} entry.

Intracellular [Ca^{2+}] measurements of suspended cells

Cells suspended in BSS were sensitized with anti-DNP IgE and loaded with indo-1 AM (Invitrogen). Time-based acquisition of cytoplasmic [Ca^{2+}] was monitored in an SLM 8100C fluorimeter, and cells were stimulated with 0.2 μg/ml DNP-BSA or 0.15 μM thapsigargin. Stimulated [Ca^{2+}] responses were normalized by dividing by (the total indo-1 fluorescence following cell lysis by addition of 0.1% Triton X-100) minus (the fluorescence in the presence of excess EDTA) (Vasudevan et al., 2009).

Granule exocytosis monitored by FITC-dextran release

Cells were transfected with mRFP-MARCKS-ED SA4 and cultured as described above. They were further loaded overnight with 1 mg/ml FITC-dextran (10,000 MW from Sigma-Aldrich) and 0.2 mM 5-hydroxytryptamine (Sigma-Aldrich) as described in Cohen et al. (submitted). Cells were washed 3 times with BSS, and live cell imaging was performed at 37˚C on a Zeiss 710 confocal microscope with maximum pinhole size to visualize degranulation events throughout the entire cell depth. Cells were stimulated with 0.4 μg/ml DNP-BSA, and detection of degranulation events as fluorescence bursts were recorded from movies similar to that in Supplemental Movie M2.4. Time of onset of degranulation was determined as the average time for the first five exocytosis events.

Granule exocytosis monitored by anti-CD63 labeling

Cells were co-transfected with unlabeled MARCKS-ED SA4 and palmitoylated,

myristoylated EGFP (PM-EGFP) or transfected with PM-EGFP alone (control) by electroporation, then cultured in full media as described above. Cells were sensitized with anti-DNP IgE (0.5 μg/ml) overnight and then stimulated with 0.4 μg/ml of DNP-BSA or 1 μM thapsigargin in the presence of 1 μM cytochalasin D (Sigma-Aldrich) for 10 minutes at 37˚ C, then fixed with 4% paraformaldehyde and 0.1% glutaraldehyde for 15 minutes at room temperature. Fixed cells were labeled with 5 μg/ml anti-CD63 mouse antibody (AD1; PharMingen) for 1 h at room temperature, followed by 10 μg/ml fluorescent secondary antibody (Alexa-555 goat anti-mouse IgGγ1; Invitrogen) for 1 h at room temperature. Imaging of fixed samples was carried out at the equatorial plane of the cells using a Leica confocal TCS SP2 microscope as described above. Analysis of images was done by first generating a plasma membrane mask by thresh holding the PM-EGFP image in Matlab (Mathworks; (Calloway et al., 2009)). Fluorescence of Alexa-555 goat anti-mouse IgGγ1 was determined by integrating the fluorescence intensity of all pixels in the plasma membrane mask for each cell. Control labeling was performed using non-specific primary mouse IgG antibody under the same conditions as for AD1 labeling.

2.4 Results

To characterize the spatial and temporal changes of PKCβI in antigen-stimulated RBL-2H3 cells, we performed real time fluorescence imaging of PKCβI-EGFP in transiently transfected cells. In unstimulated cells, PKCβI-EGFP is distributed homogeneously in the cytoplasm. Upon antigen stimulation, we observe a rapid translocation of PKCβI-EGFP to the plasma membrane in 70-80% of transfected cells with variable onset times, and this is followed by periodic dissociation and re-association with the plasma membrane. Figure 2.1 and the

supplemental movie M2.1 show this for PKCβI-EGFP at 37^{o}C; the accompanying plot quantifies changes in cytoplasmic fluorescence for a single representative cell. Antigen stimulation of RBL cells at 25^{o}C also causes PKCβI-EGFP association and dissociation with the plasma membrane as shown in Figure 2.2A. The periodicity of these oscillations in multiple cells is in the range of 40-60 s, similar to that at 37°C. The average lag time for the onset of this response at 37^{o}C is 50 s (SEM = $\pm$ 4.2 s; n = 28), and this lag time is 10 s longer at 25^{o}C (40 $\pm$ 3.3 s; n=43). Thapsigargin, an inhibitor of the sarcoplasmic/endoplasmic reticulum ATPase, also activates PKCβI-EGFP recruitment to the plasma membrane, but this occurs more slowly and without the oscillatory association and dissociation that is seen with antigen (Figure 2.2B). This recruitment may be due to diacylglycerol production stimulated by thapsigargin in a pathway that utilizes activation of phospholipase D (Peng and Beaven, 2005).

We compared the time course of antigen-stimulated oscillations in Ca^{2+} concentrations to the periodic translocation of PKCβI-EGFP to the plasma membrane by simultaneously imaging PKCβI-EGFP and [Ca^{2+}] using the indicator Fura Red, which exhibits a decrease in fluorescence when [Ca^{2+}] is elevated. As represented in Figure 1D, we observe a strong temporal correlation between the time course of [Ca^{2+}] oscillatory increases in the cytoplasm and that for PKCβI-EGFP oscillatory translocation to the plasma membrane. Recruitment of PKCβI-EGFP to the plasma membrane follows the onset of the cytoplasmic [Ca^{2+}] increase by several seconds for each of the [Ca^{2+}] oscillations, and this is evident in Figure 2.3 as a delay in the depletion of cytoplasmic PKCβI-EGFP relative to the increase in cytoplasmic [Ca^{2+}] at each oscillation.

To monitor the activity of PKC at the plasma membrane, we co-expressed MARCKS-ED

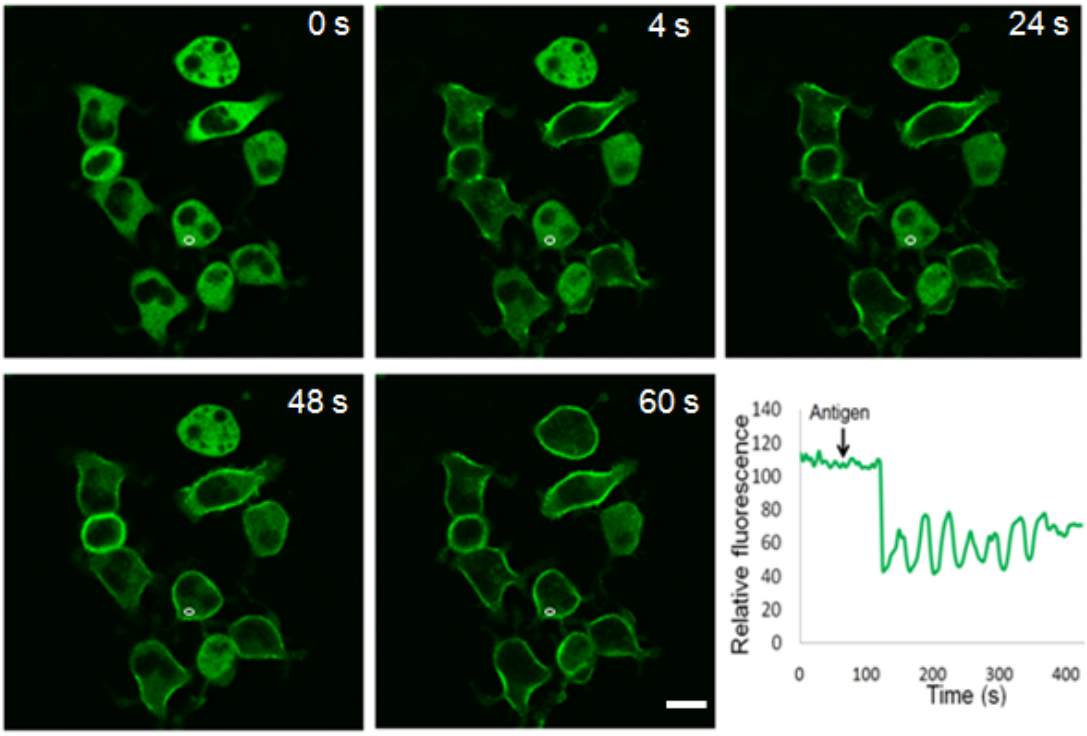

Figure 2.1: Dynamics of stimulated PKCβI-EGFP redistributions in IgE-sensitized RBL cells. Time course of PKCβI-EGFP redistributions (green) in cells upon stimulation with antigen at 37^{o}C (still frames from Supplemental Movie M2.1). Times in images indicate intervals after antigen addition. Plot shows relative cytoplasmic fluorescence in the region of interest marked in a representative individual cell. Bars, 10 μm.

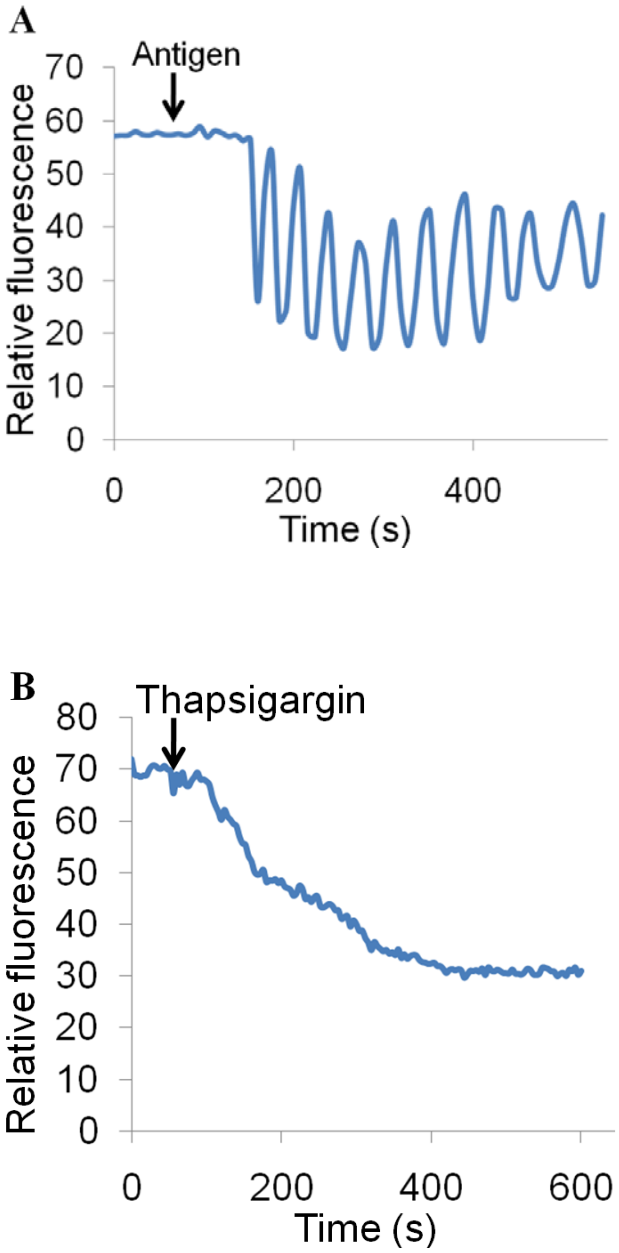

Figure 2.2: (A) Time course of PKCβI-EGFP recruitment to the plasma membrane upon antigen stimulation at 25^{o}C monitored as depletion of cytoplasmic fluorescence in a single representative cell. (B) Time course of PKCβI-EGFP recruitment to the plasma membrane upon stimulation with thapsigargin at 37^{o}C monitored as depletion of cytoplasmic fluorescence for an average of 6 cells.

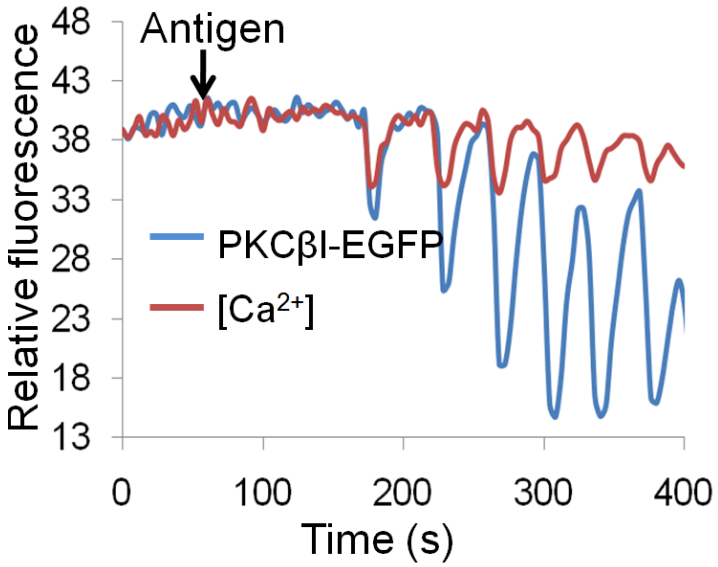

Figure 2.3: Time courses of PKCβI-EGFP recruitment to the plasma membrane monitored as depletion of cytoplasmic fluorescence (blue) and cytoplasmic [Ca^{2+}] changes monitored by Fura Red (red) in a single representative cell stimulated with antigen at 37^{o}C.

labeled with mRFP. In unstimulated RBL cells, mRFP-MARCKS-ED is concentrated at the plasma membrane as shown in Figure 2.4, upper panel. Upon stimulation with antigen, dissociation of mRFP-MARCKS-ED from the plasma membrane correlates with recruitment of PKCβI-EGFP (Figure 2.4, lower panel; in Supplemental Movies M2.2a and M2.2b). As shown in Figure 2.5, there is a strong temporal correlation between the association of PKCβI-EGFP and the dissociation of mRFP-MARCKS-ED from the plasma membrane, suggesting that stimulated PKC recruitment and activation results in periodic phosphorylation and dissociation of MARCKS-ED. We observed similar temporal correlation between MARCKS-ED PKCβI oscillations in 81% of cells co-expressing these two constructs (n = 21).

To evaluate the roles of phosphoinositides in stimulated Ca^{2+} mobilization and degranulation, we developed a probe to inhibit their accessibility under conditions where they are normally available. (Heo et al., 2006) showed that recruitment of inositol 5'-phosphatase to the plasma membrane to hydrolyze PIP_2, together with pharmacologic inhibition of PI3-and PI4-kinases, causes MARCKS-ED to dissociate from the plasma membrane. We reasoned that if we eliminated the capacity of PKC to displace MARCKS-ED from the plasma membrane under stimulating conditions, tight binding of MARCKS-ED to phosphoinositides would prevent access of proteins that utilize PIP_2 for their function, including phospholipase C and synaptotagmins (Chapman, 2002; Rhee and Choi, 1992). Toward this end we mutated the four serine residues to alanine in MARCKS-ED, and we found that this prevented the periodic dissociation and rebinding of MARCKS-ED to phosphoinositides at the plasma membrane. As shown in Figure 2.6, RBL cells were transfected with mRFP-MARCKS-ED SA4 and labeled with Ca^{2+} indicator Fluo-4, which increases in fluorescence with increase in Ca^{2+} concentration. Both Ca^{2+} mobilization (upper panel) and mRFP-MARCKS-ED SA4 in the cytoplasm (lower

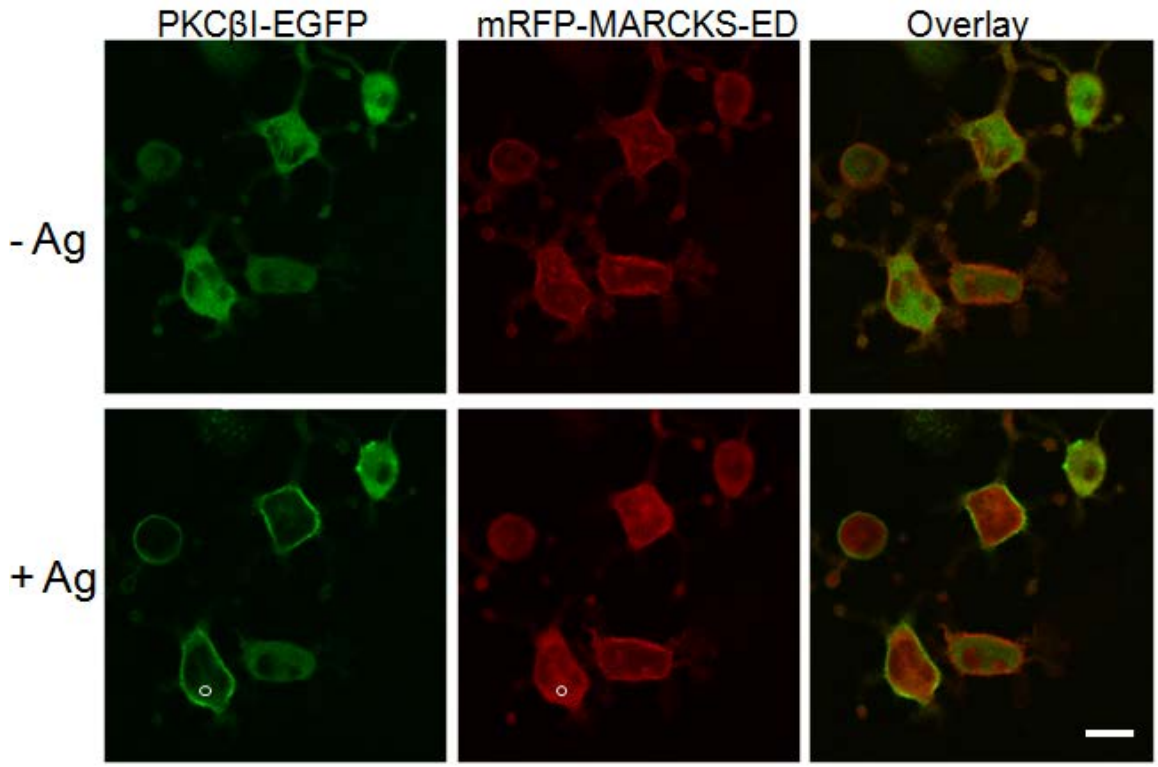

Figure 2.4: Live cell imaging of antigen-stimulated mRFP-MARCKS-ED and PKCβI-EGFP oscillations. Representative images showing the distributions of PKCβI-EGFP (green) and mRFP-MARCKS-ED (red) before (top panel) and 100 sec after antigen addition at 25^{o}C (bottom panel) (still frames from Supplemental Movies M2.2a and M2.2b). Bars, 10 μm.

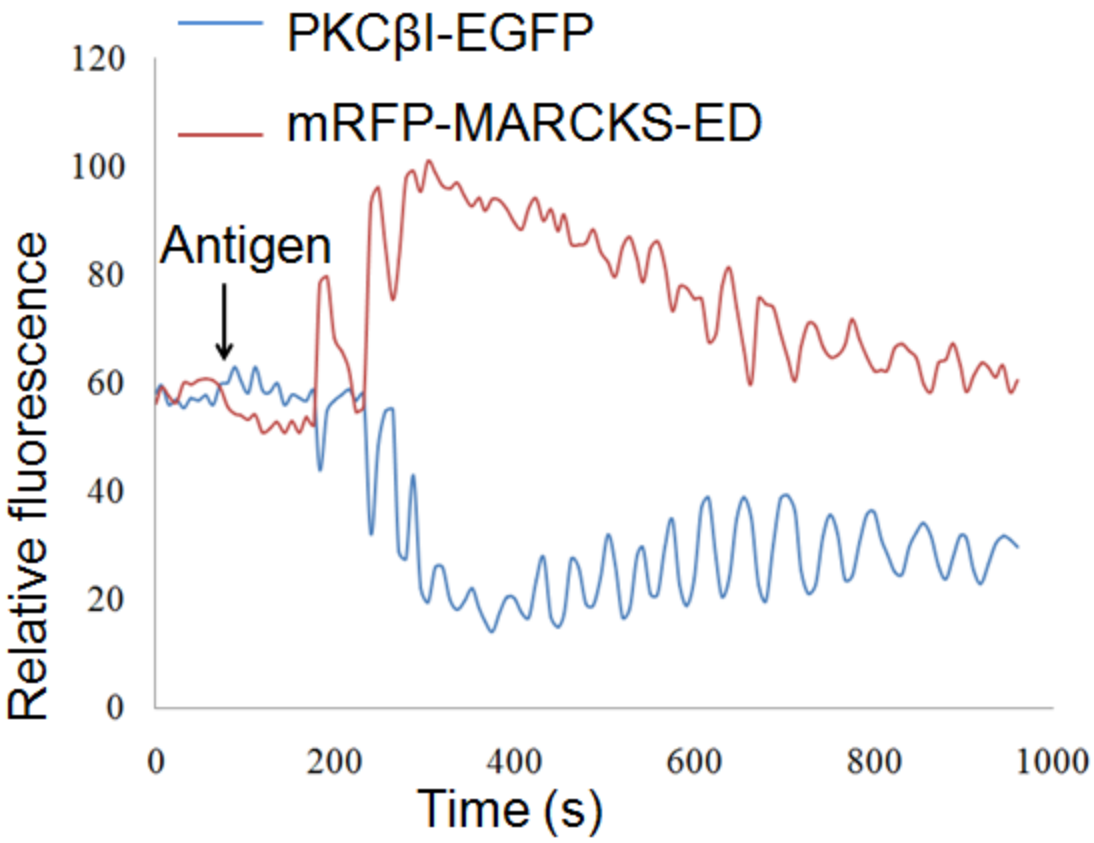

Figure 2.5: Time courses of cytoplasmic changes of PKCβI-EGFP (blue) and mRFP-MARCKS-ED (red) in a region of interest indicated in representative RBL cell in Figure 2.4.

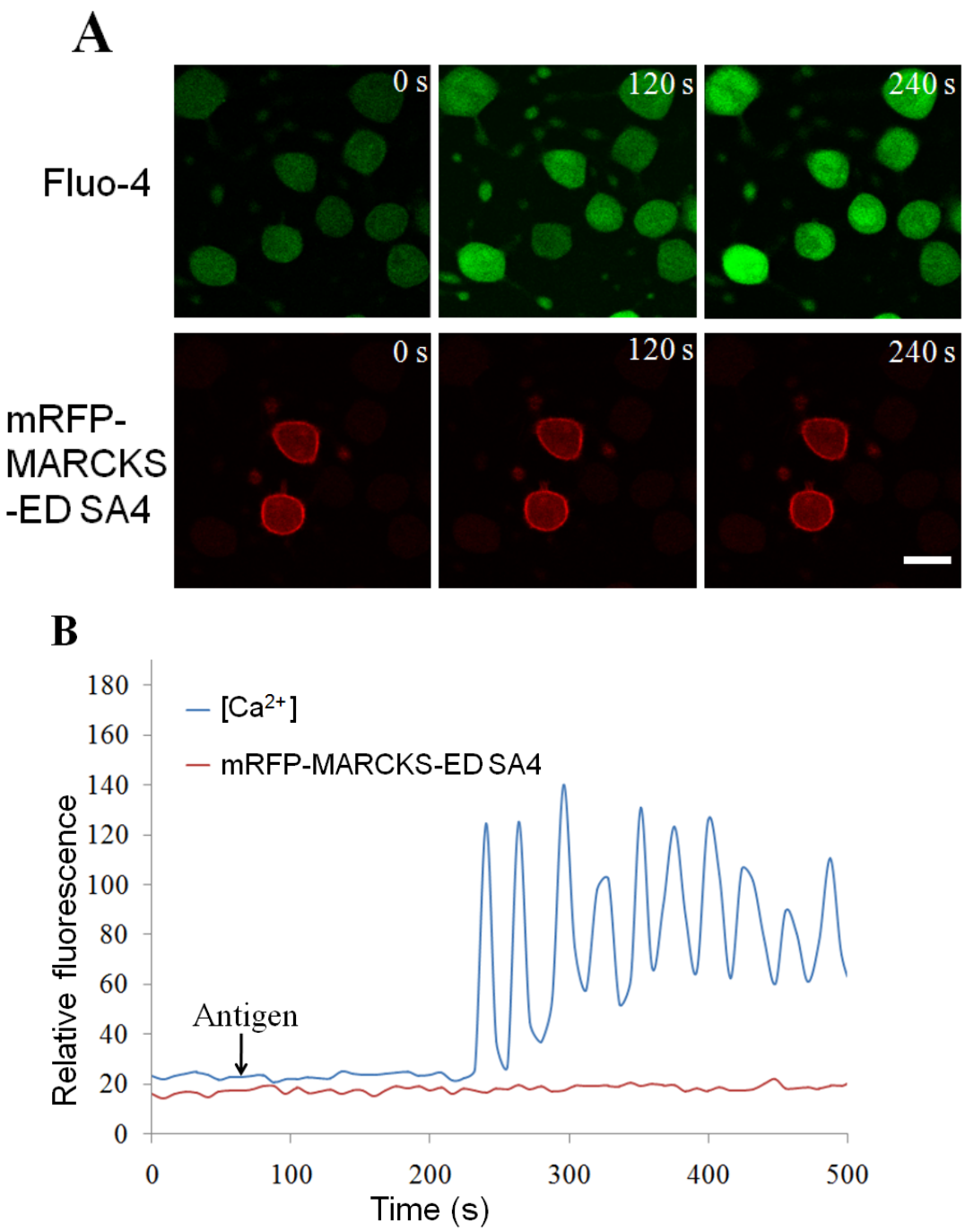

Figure 2.6: Association of mRFP-MARCKS-ED SA4 with the plasma membrane during stimulation by antigen. (A) Images of RBL cells transiently transfected with mutant mRFP-MARCKS-ED (red) and labeled with the [Ca^{2+}] indicator Fluo-4 (green) at various times of stimulation by antigen at 25^{o}C. Images show distributions of labels at time points before and after addition of antigen. Bars, 10 μm. (B) Fluorescence intensities from a cytoplasmic region of interest in arepresentative cell show that mRFP-MARCKS-ED SA4 (red) remains concentrated at the plasma membrane while stimulated [Ca^{2+}] oscillations are observed.

panel) were monitored during antigen stimulation. In contrast to results with unmutated MARCKS-ED, the SA4 mutant stays associated with the plasma membrane during stimulated Ca^{2+} responses (Figures 2.6A and 2.6B). As illustrated in Figure 2.7 and Supplemental Movie M2.3, the onset of Ca^{2+} responses to antigen in cells expressing mRFP-MARCKS-ED SA4 is delayed relative to that for cells not expressing this construct. The average time to onset of the Ca^{2+} response is 162 s (SEM = $\pm$ 20 s; n = 51) in the presence of this mutated construct, and it is 67 s (SEM = $\pm$ 15 s; n = 63) for cells expressing unmutated mRFP-MARCKS-ED. To investigate further the effect of MARCKS-ED SA4 expression on Ca^{2+} mobilization, we compared the Ca^{2+} response to antigen in the absence of extracellular Ca^{2+}, conditions under which the response is restricted to IP_3-mediated Ca^{2+} release from ER stores (Lee et al., 2005). As shown for a representative cell in Figure 2.8, the transient Ca^{2+} response in the absence of extracellular Ca^{2+} is delayed for cells expressing mRFP-MARCKS-ED SA4 cells as compared to control cells not expressing this mutant. We observed an average delay in the onset of Ca^{2+} release from stores in MARCKS-ED SA4-expressing cells of 200 s (SEM = $\pm$ 22 s; n = 18) compared to that for untransfected control cells.

To further characterize the effects of MARCKS-ED SA4 on functional responses, RBL-2H3 cells were stably transfected with mRFP-MARCKS-ED SA4, and Ca^{2+} mobilization was monitored with indo-1 in a fluorimetry-based assay of suspended cells. As shown in Figure 2.9, mRFP-MARCKS-ED SA4-expressing cells exhibit a slower Ca^{2+} response to antigen when compared to the control cells, although the maximal response attained is similar for both. In the absence of extracellular Ca^{2+}, control RBL cells show transient Ca^{2+} release from stores after antigen stimulation, returning to the baseline after several hundred seconds (Figure 2.10). This response is delayed for RBL cells stably expressing MARCKS-ED SA4. In both cases, addition of extracellular Ca^{2+} results in a rapid increase in intracellular Ca^{2+} to similar levels, indicating

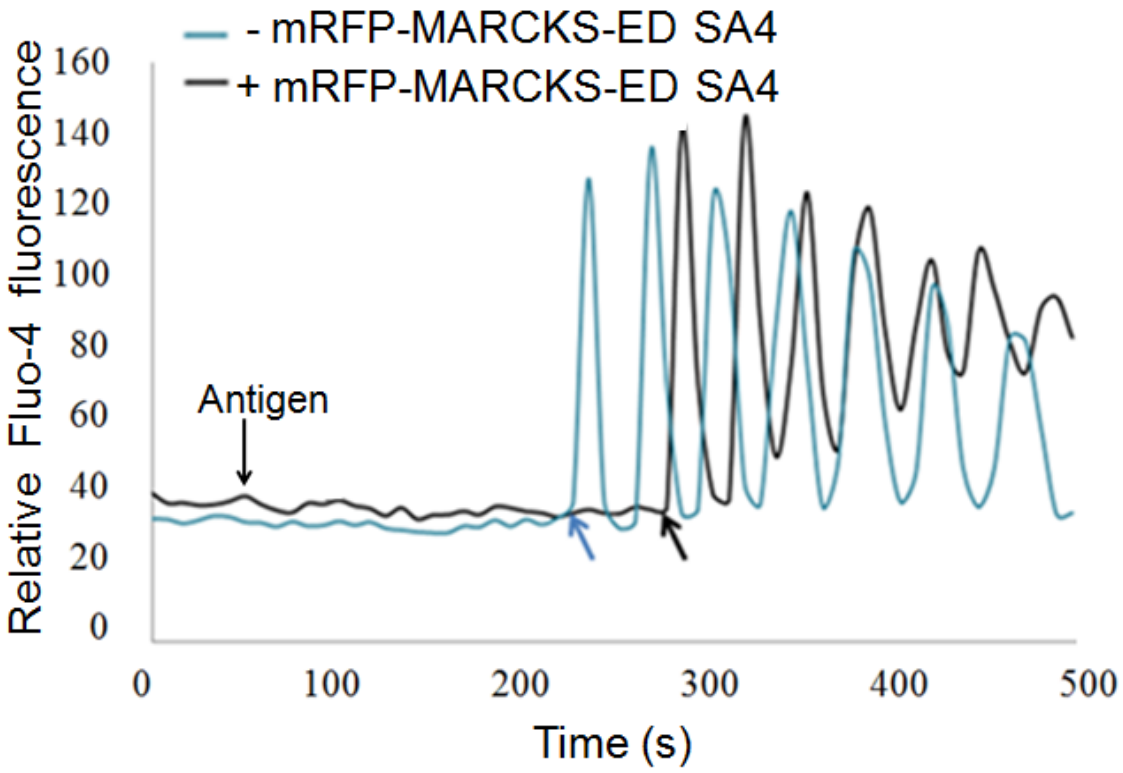

Figure 2.7: Ca^{2+} mobilization in response to Ag at 25°C is delayed in a cell expressing mutant mRFP-MARCKS-ED (black) compared with an untransfected cell (blue); cells shown in Supplemental Movie M2.3.

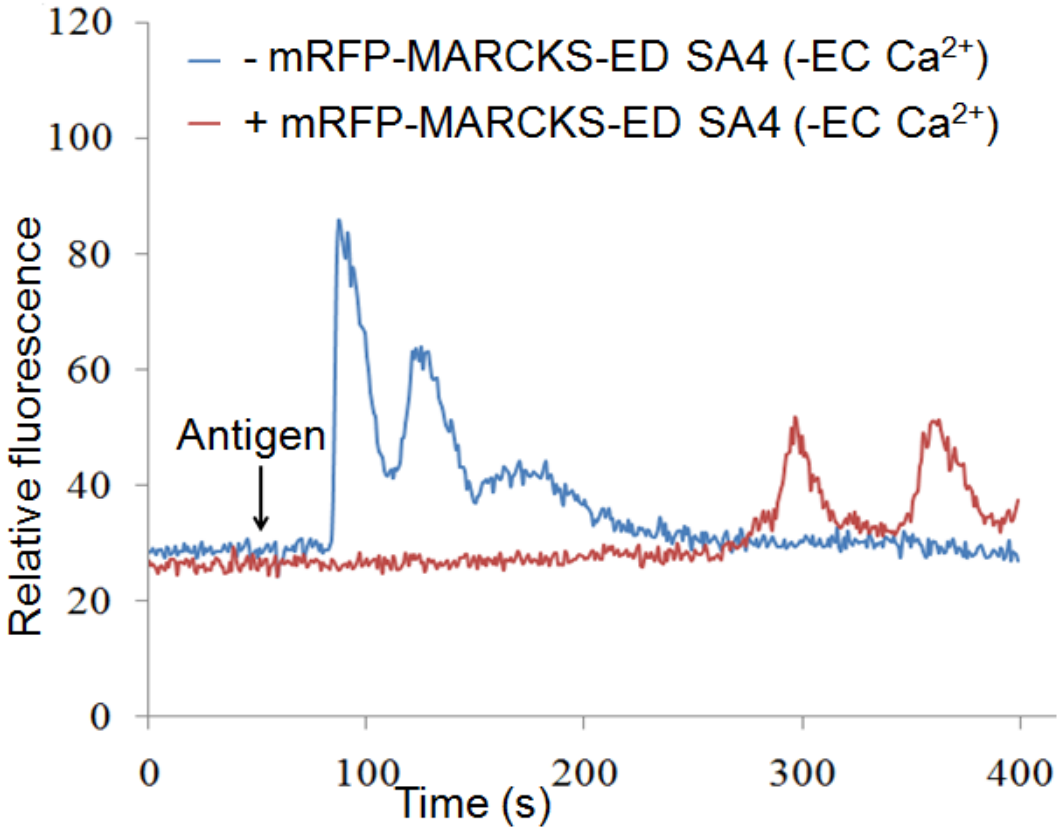

Figure 2.8: Ca^{2+} response to antigen in the absence of extracellular Ca^{2+} is substantially delayed in a cell transiently expressing mutant mRFP-MARCKS-ED (red) compared with the response in an untransfected cell (blue) in the same sample.

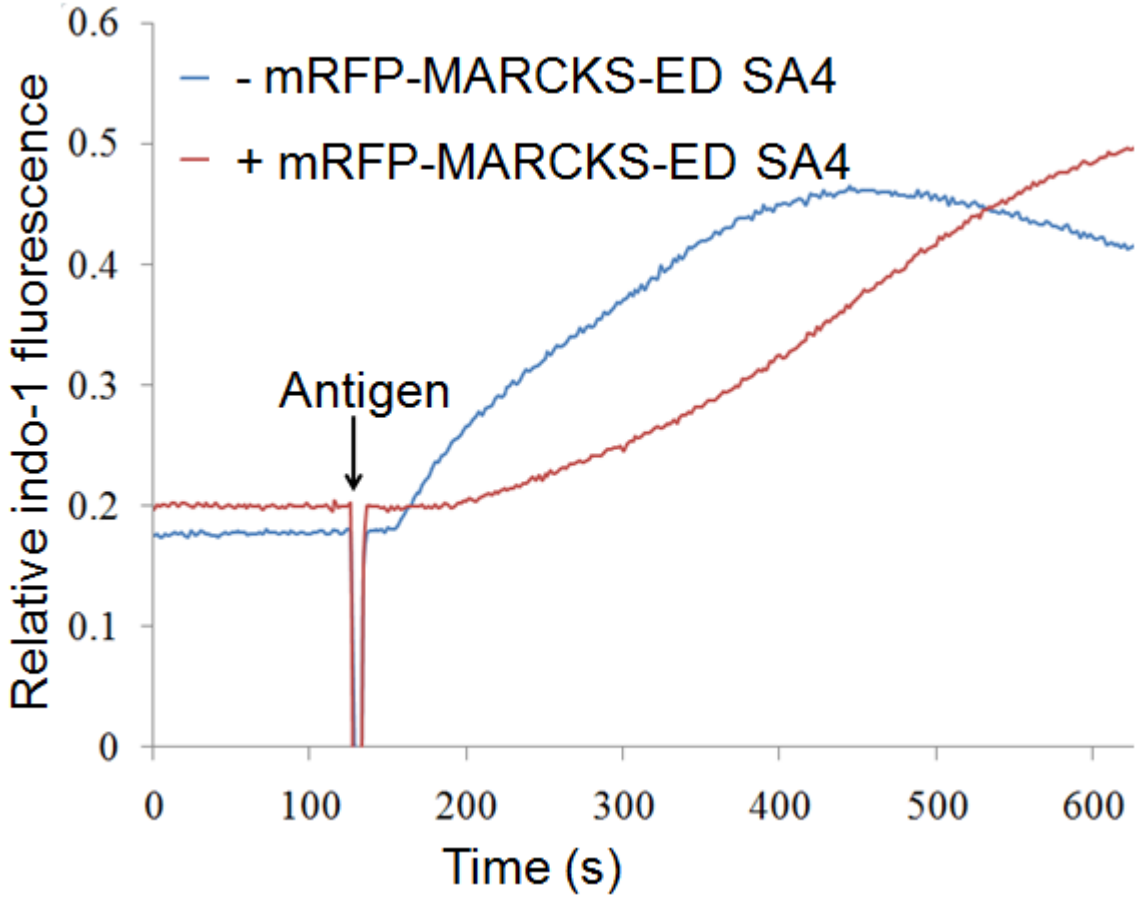

Figure 2.9: Antigen-stimulated Ca^{2+} mobilization is delayed in cells stably expressing mRFP-MARCKS-ED SA4. Steady state fluorimetry responses to antigen in control RBL cells (blue) and cells stably expressing mRFP-MARCKS-ED SA4 (red).

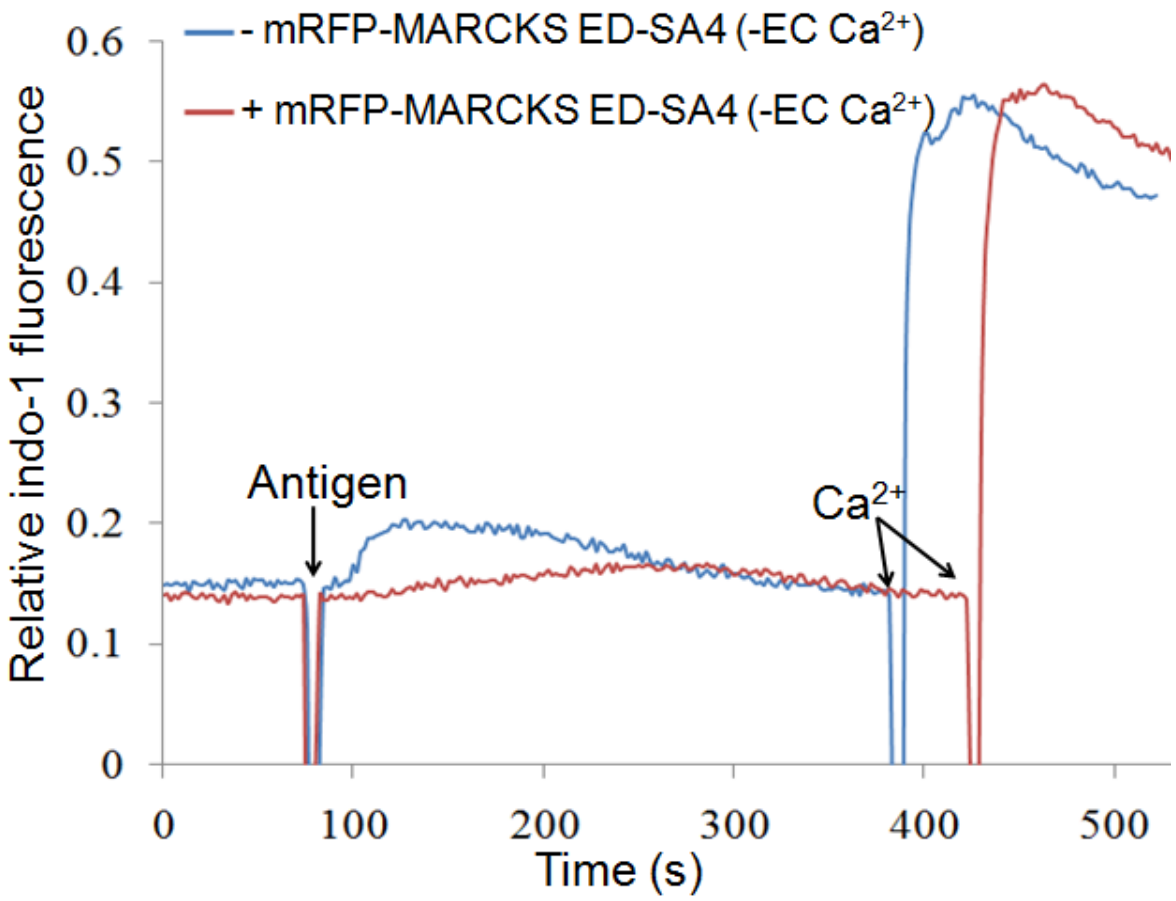

Figure 2.10: Ca^{2+} response to antigen in the absence of extracellular Ca^{2+} is substantially delayed in RBL cells stably expressing mutant mRFP-MARCKS-ED (red) compared with the response in untransfected cells (blue). Subsequent addition of 1.8 mM [Ca^{2+}] results in similar Ca^{2+} entry for each.

similar activation of store-operated Ca^{2+} entry. To determine the effect of expression of MARCKS-ED SA4 on store-operated Ca^{2+} entry, independent of PLCγ-mediated release from stores, cells were stimulated with thapsigargin. As shown in Figure 2.11, thapsigargin causes a rapid increase in cytosolic Ca^{2+} levels due to leakage of Ca^{2+} from ER, and this is followed by a more sustained phase due to store-operated Ca^{2+} entry. Cells stably expressing MARCKS-ED SA4 showed a similar rapid increase in store-operated Ca^{2+} influx and a sustained level of store-operated Ca^{2+} entry that is somewhat larger than in control cells. These results show that the delay in the antigen-stimulated Ca^{2+} response due to MARCKS-ED SA4 expression is not observed for stimulation with thapsigargin, consistent with selective inhibition of antigen-stimulated PIP_2 hydrolysis by MARCKS-ED SA4 and consequent inhibition of IP_3-dependent Ca^{2+} release from stores.

Because of known roles for PKC as well as for Ca^{2+} mobilization in granule exocytosis, we evaluated the effect of MARCKS-ED SA4 expression on degranulation by two different methods. In one approach, we loaded granules, which are known to be secretory lysosomes in these cells (Dragonetti et al., 2000; Xu et al., 1998), with FITC-dextran by fluid phase pinocytosis (Cohen, et al., submitted for publication). Live cell imaging showed transient, single granule fusion events as monitored by bursts of FITC fluorescence, which increases when exposed to extracellular pH upon antigen stimulation. As represented in Supplemental Movie M2.4, we observe that cells transfected with mRFP-MARCKS-ED have delayed onset of degranulation events and also a reduced frequency of these fusion events. As illustrated in Figure 2.12, still movie frames at different time-points show degranulation events starting 1.9 min (SEM = $\pm$ 0.1 min; n = 22) after antigen addition to cells not expressing MARCKS-ED SA4. In contrast, we observe that the onset of granule fusion upon antigen stimulation occurs after 5.8

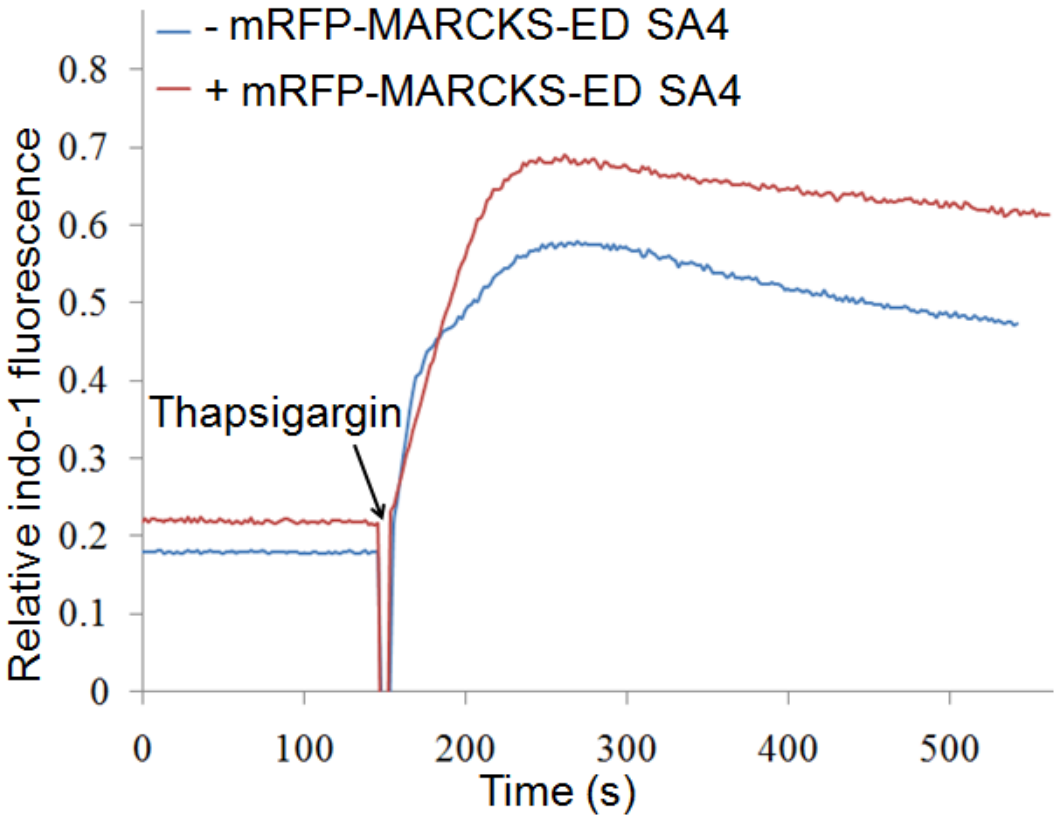

Figure 2.11: Ca^{2+} mobilization in response to thapsigargin in RBL cells stably expressing mRFP-MARCKS-ED SA4 (red) is similar compared with the response in untransfected RBL cells (blue).

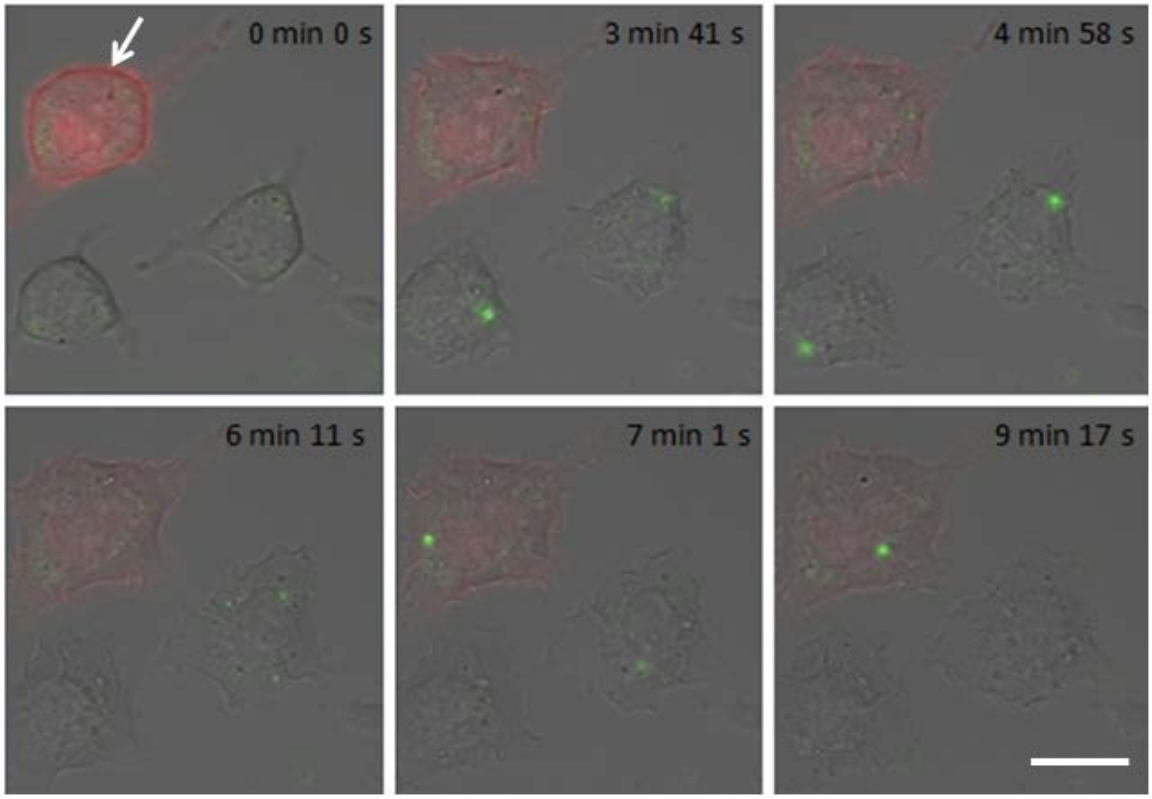

Figure 2.12: MARCKS-ED SA4 inhibits antigen-stimulated degranulation monitored by real time imaging. Degranulation monitored as FITC-dextran bursts from antigen-stimulated RBL cells shows delayed and reduced responses in cells expressing mRFP-MARCKS-ED SA4. Times in images indicate intervals after antigen addition; white arrow identifies a cell expressing mRFP-MARCKS-ED SA4. Bars,10 μm. See Supplemental Movie M2.4.

min (SEM = ± 0.2 min; n = 22) in cells that express mRFP-MARCKS-ED SA4. Quantification of exocytosis events occurring within 10 min of antigen stimulation reveals reduced exocytosis in cells transfected with mRFP-MARCKS-ED SA4 (14.6 ± 1.4 average number of fusion events per cell; n = 22) compared to untransfected cells in the same sample (46.1 ± 4.0 average number of fusion events per cell; n = 22). For thapsigargin stimulation, we did not observe any significant delay in the onset of fusion events in untransfected cells (6.6 ± 0.8 min; n = 7) as compared to cells expressing mRFP-MARCKS-ED SA4 in the same sample (7.1 ± 0.6 min; n = 7). Under these conditions, we observed reduced exocytosis events in cells expressing mRFP-MARCKS-ED SA4 (8.4 ± 1.3 average number of fusion events per cell; n = 7) compared to cells not expressing this mutant construct in the same sample (15.4 ± 2.4 average number of fusion events per cell; n = 7). (data not shown).

Because it is difficult to quantify differences in degranulation responses by this real-time imaging method, we also utilized a second method in which cells are fixed after stimulation and then labeled with anti-CD63 mAb followed by a fluorescent secondary antibody. CD63, also known as LAMP2 (Metzelaar et al., 1991), is localized primarily to secretory lysosomes, but a small amount is present at the plasma membrane in unstimulated cells. In these experiments, unlabeled MARCKS-ED SA4 was co-transfected with the plasma membrane marker PM-EGFP that we used to identify transfected cells and also to define the plasma membrane for image quantification of localized Alexa555-labeled anti-CD63. As shown in Figure 2.13, labeling of CD63 increases at the plasma membrane upon antigen stimulation of RBL cells, and this is clearly stronger in non-transfected cells in the same sample. Figure 2.14 quantifies this analysis for multiple cells. Some CD63 is evident at the plasma membrane in unstimulated cells, and this is similar with and without expression of MARCKS-ED SA4. For antigen-stimulated cells

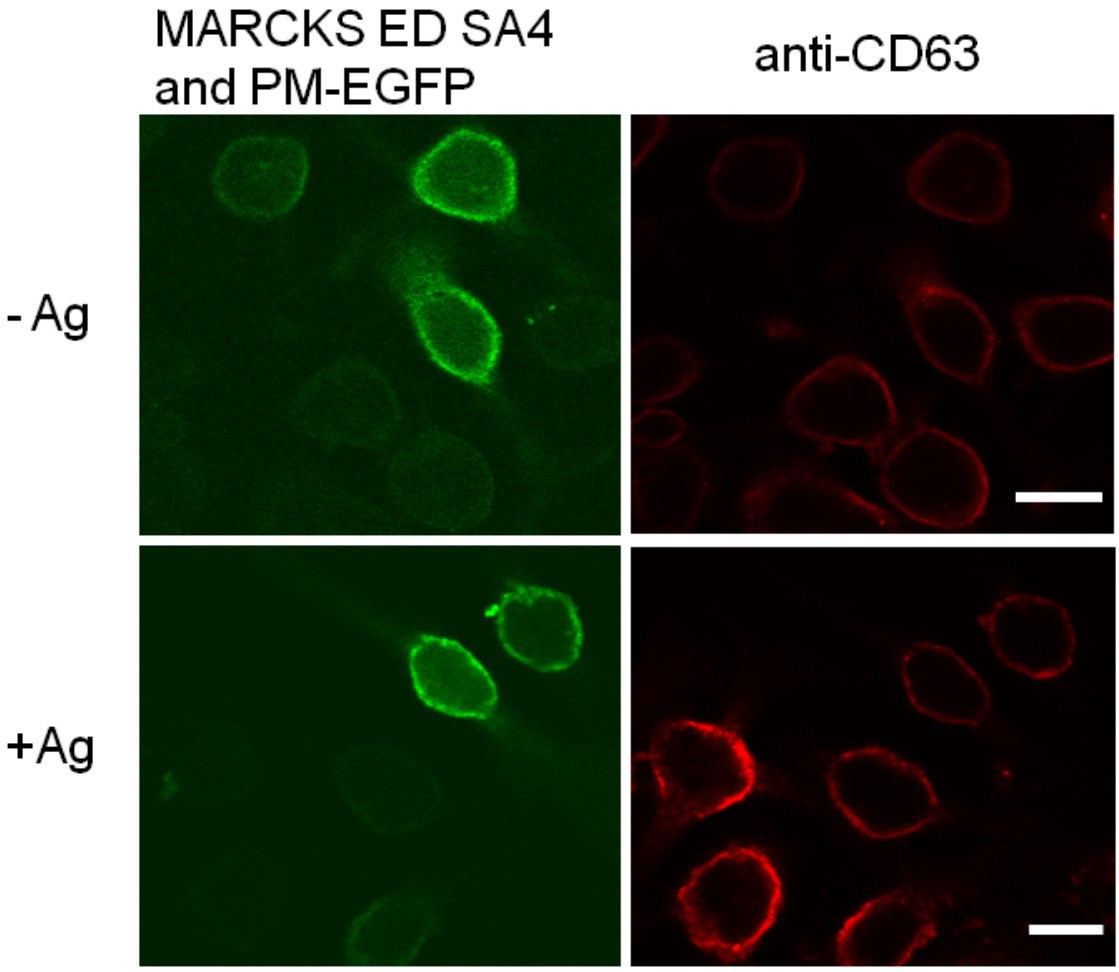

Figure 2.13: Inhibition of degranulation due to expression of MARCKS-ED SA4 as monitored by CD63 appearance at the plasma membrane. Representative images showing reduced plasma membrane labeling by anti-CD63 due to antigen stimulation in cells expressing mutated MARCKS-ED expression. Bars, 10 μm.

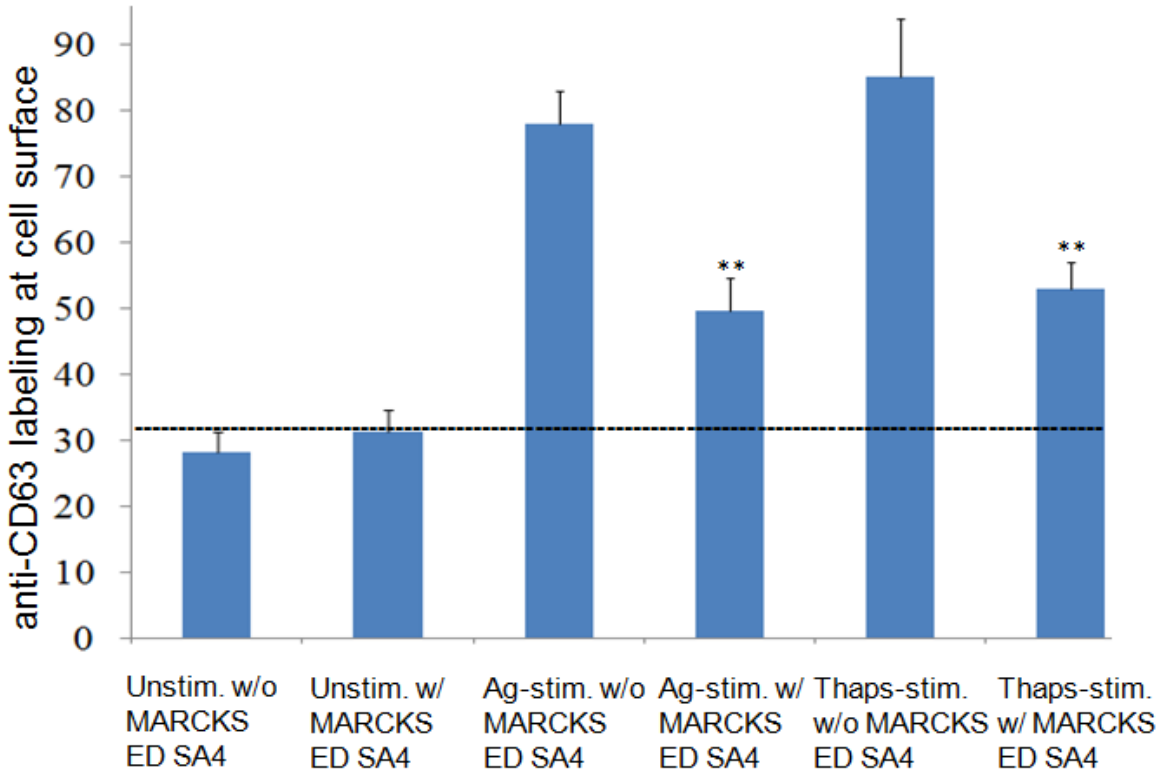

Figure 2.14: Quantification of anti-CD63 labeling at the plasma membrane for unstimulated, antigen-stimulated and thapsigargin-stimulated cells with and without expression of MARCKS-ED SA4. Error bars show SEM for 90-100 cells for each condition from n=6 experiments. P-values from Student's t-test show **P<0.01 for stimulated cells expressing MARCKS-ED SA4 compared to stimulated control cells.

transfected with PM-EGFP without MARCKS-ED SA4 (control cells), the plasma membrane level of CD63 increases by >2.5-fold. By comparison, antigen-stimulated cells expressing MARCKS-ED SA4 show a substantially smaller stimulated increase in CD63 at the plasma membrane: This stimulated increase was inhibited by ~60% due to expression of MARCKS-ED SA4 (n=90-100 for each condition).

We also determined whether MARCKS-ED SA4 inhibits granule exocytosis stimulated by thapsigargin, which bypasses PIP_2 hydrolysis and IP_3-dependent Ca^{2+} mobilization. In a separate set of experiments, we again found no significant effect of MARCKS-ED SA4 on basal levels of CD63 at the plasma membrane in unstimulated cells. We observed almost a 3-fold increase in CD63 at the plasma membrane due to stimulation by an optimal dose of thapsigargin, and this was inhibited by 65% in cells expressing MARCKS-ED SA4 compared to cells expressing PM-EGFP alone. Together, these results provide strong evidence that MARCKS-ED SA4 exerts a direct inhibitory effect on granule exocytosis. Because MARCKS-ED SA4 has been shown to bind tightly to phosphoinositides at the plasma membrane, our results suggest that the sequestration of these lipids provides a significant barrier to granule exocytosis.

2.5 Discussion

Antigen activation of IgE receptors on mast cells results in stimulated granule exocytosis, which utilizes Ca^{2+}-triggered membrane fusion and also depends on the activation of PKC. As shown by our results, the strong temporal synchronizations of antigen-stimulated oscillations of cytoplasmic [Ca^{2+}], PKCβI, and MARCKS-ED (Figures 2.1 – 2.5) are consistent with the involvement of [Ca^{2+}]-controlled PKCβI activation resulting in phosphorylation of MARCKS as

a pathway involved in the regulation of exocytosis. These results are reminiscent of IgE receptor-stimulated, periodic recruitment of PKCγ-EGFP to the plasma membrane previously characterized by Oancea and Meyer (Oancea and Meyer, 1998). The temporal correlation of PKCβI-EGFP oscillations that are stimulated by antigen with [Ca^{2+}] oscillations in the cytoplasm suggests that [Ca^{2+}] elevation is involved in activation of this PKC isoform. Consistent with this, activation of PKC□I-EGFP recruitment by antigen is transient in the absence of extracellular Ca^{2+}, corresponding to a transient elevation in cytoplasmic [Ca^{2+}] under these conditions (Supplementary Figure S2.1). Bypassing IP_3-dependent Ca^{2+} mobilization with thapsigargin results in slower, non-oscillatory translocation of PKCβI-EGFP to the plasma membrane (Figure 2.2B), and this is consistent with slower activation of diacylglycerol production via phospholipase D under these conditions (Peng and Beaven, 2005). Stimulated dissociation of mRFP-MARCKS-ED from and rebinding to the plasma membrane correspond to the dynamics of PKCβI-EGFP oscillatory association with the plasma membrane and are consistent with a role for PKC activation in this process.

We find that stimulated dissociation of mRFP-MARCKS-ED is prevented by our SA4 mutation of the serine residues that are phosphorylated by activated PKC (Figure 2.6), consistent with previous studies with MARCKS-ED (Kim et al., 1994). Heo et al. (2006) showed previously that decreased phosphoinositide levels at the plasma membrane cause dissociation of MARCKS-ED, and we obtained similar results with our mutant MARCKS-ED SA4 (Smith et al., 2010). Thus, the strong temporal synchronizations of oscillations of cytoplasmic [Ca^{2+}], PKCβI, and MARCKS-ED under conditions of antigen stimulation are consistent with a role for PKCβI in regulating access of PIPs by endogenous MARCKS. The positively charged, polybasic peptide sequence MARCKS-ED S4A retains its capacity to bind tightly to highly negatively

charged phosphoinositides at the plasma membrane and, importantly, does not dissociate in response to activation of PKC. As monitored with both transient and stable expression of this construct, we observed a delay in antigen-stimulated Ca^{2+} mobilization due to this expression, consistent with reduced accessibility of PIP_2 for hydrolysis by PLCγ (Figures 2.6 – 2.11). Despite this delay, the levels of sustained Ca^{2+} response to antigen are similar in the presence and absence of MARCKS-ED S4A. In contrast, stimulation by thapsigargin results in store-operated Ca^{2+} entry that is similar in magnitude and kinetics in the presence and absence of MARCKS-ED S4A.

The inhibitory effect of MARCKS-ED S4A on the kinetics of antigen-stimulated Ca^{2+} mobilization indicates that the isolated MARCKS-ED segment functions differently in this process than when it is part of intact, endogenous MARCKS. This inhibition is due primarily to the serine to alanine mutations, because unmutated MARCKS-ED does not inhibit granule exocytosis (Figure S2.4). However, inhibitors of PKC activity, such as bisindolylmaleimide I, do not inhibit antigen-stimulated Ca^{2+} mobilization in RBL mast cells (Wolfe et. al., 1996; our data not shown), implying that PKC-dependent dissociation of endogenous MARCKS is not necessary for PLCγ mediated hydrolysis of PIP_2 in these cells. Activation of PKC by phorbol esters can negatively regulate antigen-stimulated Ca^{2+} mobilization, in part by inhibition of PLCγ (Ozawa et al., 1993b), but PKC activation by antigen does not normally alter Ca^{2+} mobilization as described above. These differences may reflect the degree of activation of PKC by phorbol ester vs. antigen, but they also suggest some difference in the pools of PIP_2 bound by endogenous MARCKS and by MARCKS-ED SA4.

We find that MARCKS-ED S4A effectively delays and inhibits granule exocytosis using

two different approaches. Real time monitoring of individual granule exocytosis events using FITC-dextran (Cohen et al., submitted) permits us to visualize the rate of this process (Figure 2.12 and Supplemental Movie M2.4). These results clearly reveal a delay in granule exocytosis in response to antigen that is predicted by the delay in antigen-stimulated Ca^{2+} mobilization we observe due to transient expression of MARCKS-ED S4A (Figure 2.7). Measurement of the stimulated increase in the granule marker CD63 at the plasma membrane permits quantification of granule exocytosis following fixation of activated cells. Inhibition of thapsigargin-stimulated degranulation to a similar extent as that for antigen demonstrates that MARCKS-ED S4A inhibits a step in granule exocytosis that is downstream of Ca^{2+} mobilization. This step is apparently dependent on PKC activation, because expression of the non-mutated MARCKS-ED sequence does not inhibit degranulation in similar experiments (Supplemental Figure S2.4).

What is the mechanism of this inhibition? The previous finding by Heo et al., 2006, which showed that MARCKS-ED binds to the plasma membrane primarily through its association with phosphoinositides, together with our previous results with MARCKS-ED S4A (Smith et al., 2010), make it likely that the functional effects we observe in the present study are due to phosphoinositide binding by MARCKS-ED S4A. Certainly, the delay of antigen-stimulated Ca^{2+} mobilization, both in the presence and absence of extracellular Ca^{2+}, is readily accounted for by the capacity of MARCKS-ED S4A to tie up the pool of PIP_2 that is normally hydrolyzed by activated PLCγ. Although this electrostatic binding is tight, it is not specific in the usual sense of a binding site, and it is possible that PLC or other proteins have limited access to PIP_2 under these conditions (Gambhir et al., 2004).

The mechanism by which MARCKS-ED S4A interferes with granule exocytosis is also

likely to depend on its capacity to bind tightly to phosphoinositides, but the specific interactions that are prevented by this association are not yet clear. Synaptotagmins are a family of [Ca^{2+}]sensor proteins that participate in multiple exocytotic processes, including mast cell degranulation (Sagi-Eisenberg, 2007), and synaptotagmin-2 is the principal isoform that mediates granule exocytosis in mast cells (Melicoff et al., 2009). Two C2 domains in synaptotagmins bind to Ca^{2+} and PIP_2 to trigger the SNARE-mediated fusion of secretory vesicles to the plasma membrane (Li et al., 2006; Schwarz, 2004). A plausible mechanism for the inhibitory effects of mutant MARCKS-ED involves its interference with this PIP_2-dependent process. A variety of SNARE proteins are expressed in RBL cells, including syntaxin 4, SNAP 23, VAMP-7 and VAMP-8 (Paumet et al., 2000; Sander et al., 2008), and studies in other cell types have provided evidence for a role for PIP_2 in regulating syntaxin-1 and VAMP-2-mediated membrane fusion (Daily et al., 2010). Thus it is possible that MARCKS-ED S4A affects PIP_2 binding to several different proteins in this process.

It is also possible that other PKC substrates participate in the terminal steps of mast cell degranulation. Munc18-1 is a prominent PKC substrate, and disruption of Munc 18-1 association with syntaxin-1 inhibits granule fusion events in PC12 cells (Barclay, 2008). In addition to phosphorylation by PKC, binding of Ca^{2+}-activated calmodulin to MARCKS causes translocation of MARCKS from the plasma membrane and thereby releases sequestered PIP_2, as reviewed elsewhere (McLaughlin and Murray, 2005). This mechanism of MARCKS-ED displacement, which is independent of phosphorylation by PKC, may account for the incomplete inhibition of degranulation by MARCKS-ED SA4 that we observe. Overall, our results highlight a possible role for PKC in the regulation of PIP_2 accessibility, and they establish the utility of MARCKS-ED S4A as an effective inhibitor of phosphoinositide-dependent processes. Ligand-

dependent recruitment of PI 5'-phosphatases can cause acute reduction of plasma membrane PIP_2 (Stauffer et al., 1998; Varnai and Balla, 1998), but this alternative approach requires co-expression of multiple constructs that can be difficult to achieve at sufficiently high levels for effective interference in some cell types.

In summary, our results provide mechanistic insights into the regulation of granule exocytosis by PKC and phosphoinositides. We have shown that MARCKS-ED S4A stably associates with the plasma membrane, delays the onset of antigen-stimulated Ca^{2+} mobilization and degranulation responses, and inhibits both antigen and thapsigargin-stimulated granule exocytosis. These effects can be accounted for by tight association of MARCKS-ED SA4 with phosphoinositides, although contributions from interactions with other binding partners may also contribute to these functional outcomes. PIP_2 has been shown to enhance the Ca^{2+} affinity of synaptotagmins, and it may thereby facilitate triggering of secretory granule fusion with the plasma membrane. Thus, we propose that PKC is a key to regulating the access of PIP_2, such that PKC activation during stimulation results in exposure of PIP_2 necessary for granule fusion.

2.6 Supplemental Material

Supplementary Figures:

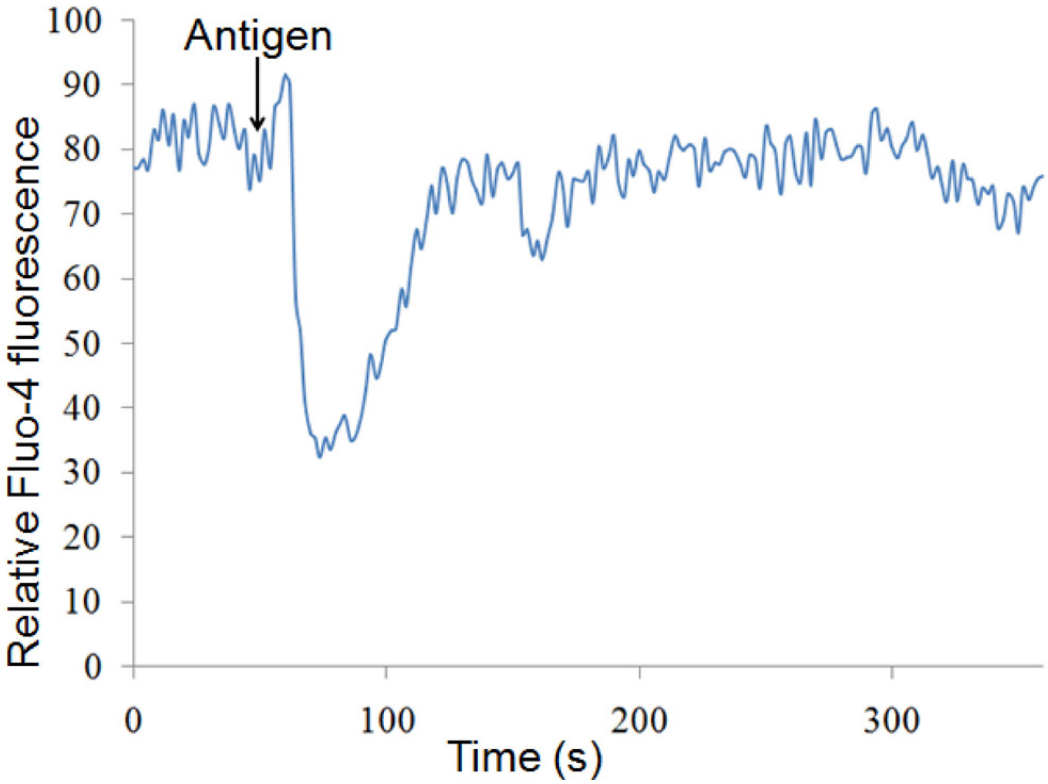

Figure S2.1: Stimulation by antigen in the absence of extracellular Ca^{2+} results in transient translocation of PKC to the plasma membrane at 37°C, monitored as transient depletion from a region of interest in the cytoplasm of a representative cell.

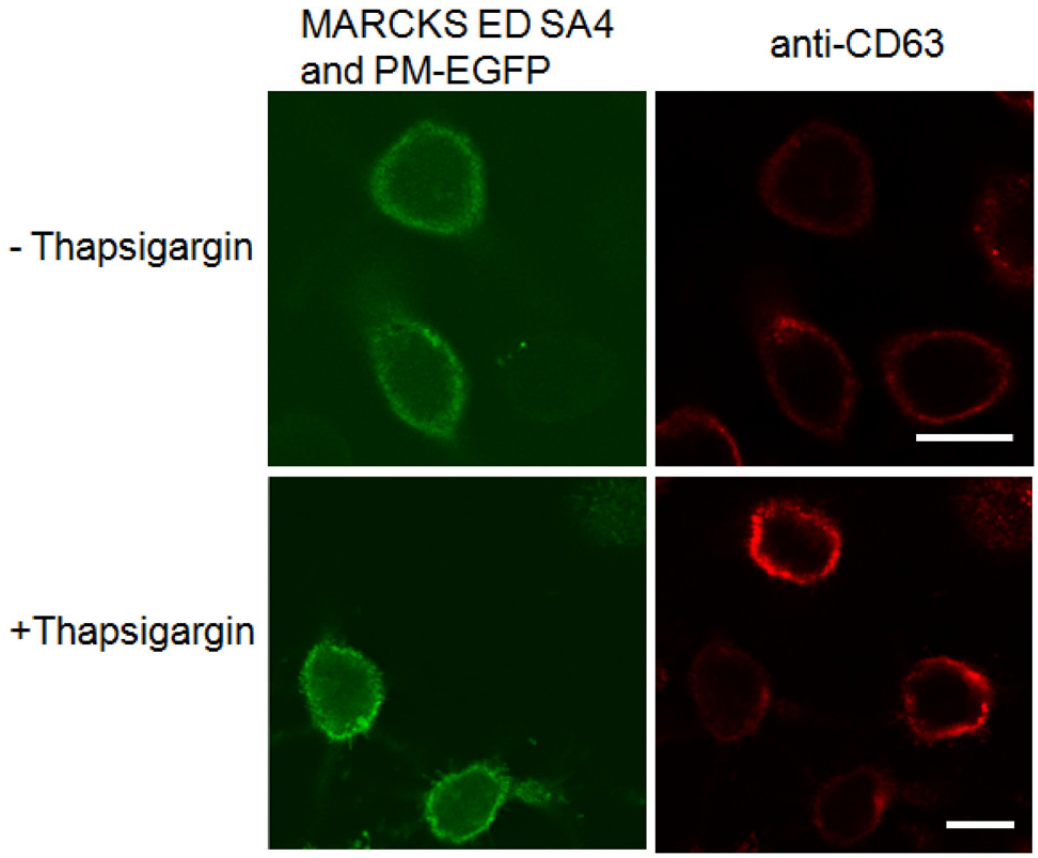

Figure S2.2:. Representative images showing less intense anti-CD63 labeling of thapsigargin-stimulated cells expressing MARCKS-ED SA4 as compared to cells not expressing this mutant. Bars,10 μm.

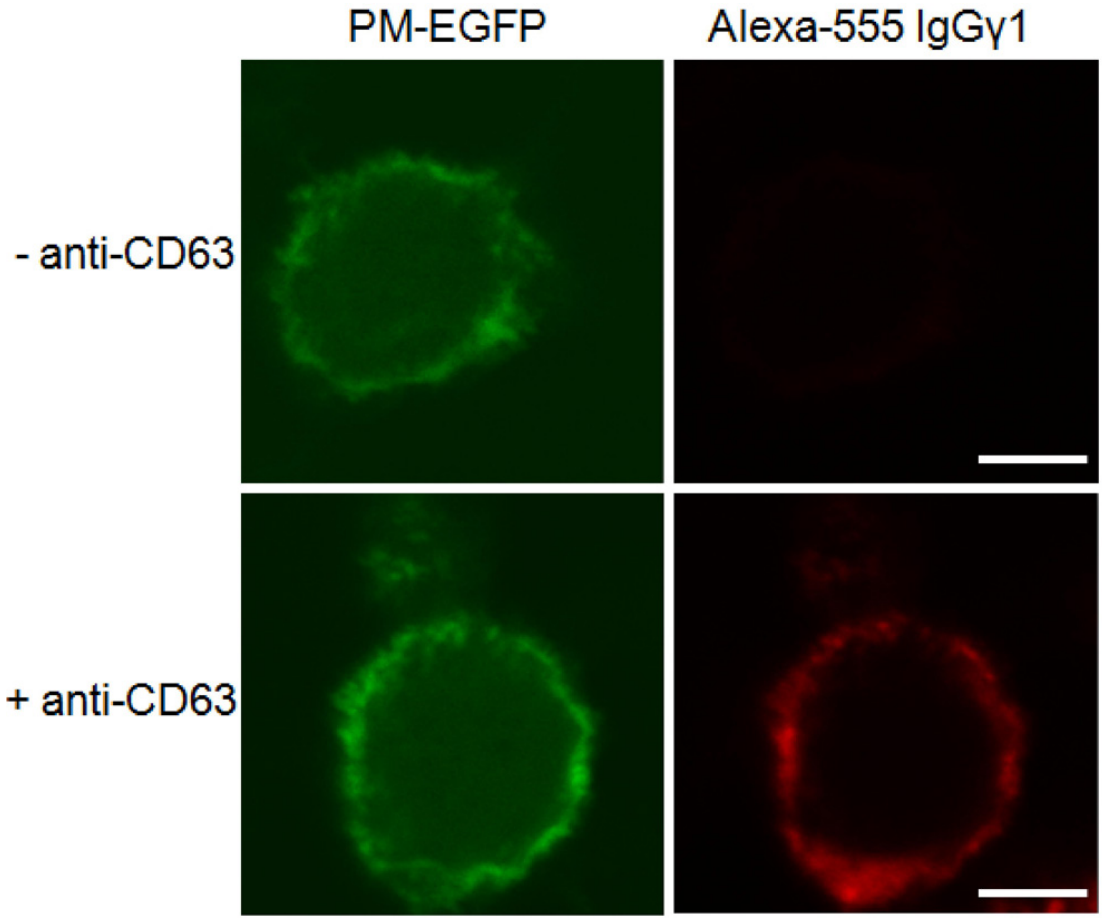

Figure S2.3: Alexa-555-anti-mIgGγ1 does not label RBL cells in the absence of anti-CD63 antibody, demonstrating specificity of secondary antibody for the primary antibody in CD63 quantification. Bars, 5 μm.

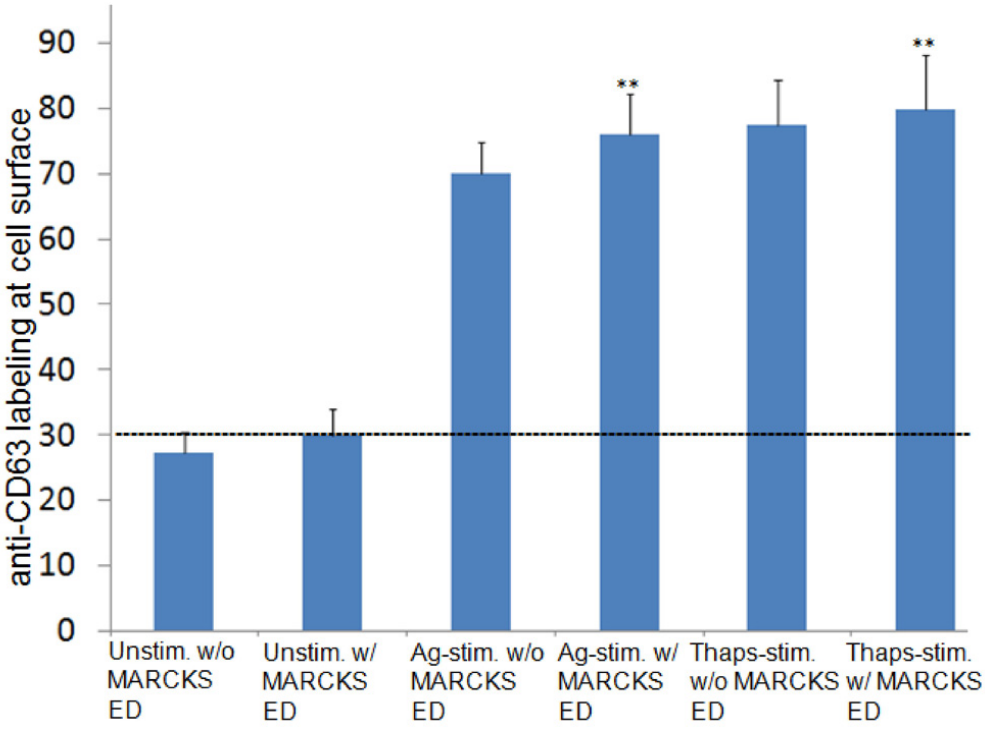

Figure S2.4: Quantification of anti-CD63 labeling at the plasma membrane for unstimulated, antigen-stimulated and thapsigargin-stimulated cells with and without expression of MARCKS-ED. Error bars show SEM for 25-30 cells for each condition. **P<0.01 for antigen-stimulated and thapsigargin-stimulated cells expressing MARCKS-ED compared to stimulated cells not expressing MARCKS-ED.

Supplementary movies can be accessed online at: http://www.molbiolcell.org/content/early/2011/10/16/mbc.E11-07-0614/suppl/DC1

REFERENCES

Aderem, A. (1992). The MARCKS brothers: a family of protein kinase C substrates. Cell *71*, 713-716.

Bai, J., Tucker, W.C., and Chapman, E.R. (2004). PIP2 increases the speed of response of synaptotagmin and steers its membrane-penetration activity toward the plasma membrane. Nat Struct Mol Biol *11*, 36-44.

Barclay, J.W. (2008). Munc-18-1 regulates the initial release rate of exocytosis. Biophys J *94*, 1084-1093.

Blackshear, P.J. (1993). The MARCKS family of cellular protein kinase C substrates. J Biol Chem *268*, 1501-1504.

Blank, U., and Rivera, J. (2004). The ins and outs of IgE-dependent mast-cell exocytosis. Trends Immunol *25*, 266-273.

Calloway, N., Vig, M., Kinet, J.P., Holowka, D., and Baird, B. (2009). Molecular clustering of STIM1 with Orai1/CRACM1 at the plasma membrane depends dynamically on depletion of Ca2+ stores and on electrostatic interactions. Mol Biol Cell *20*, 389-399.

Chapman, E.R. (2002). Synaptotagmin: a Ca(2+) sensor that triggers exocytosis? Nat Rev Mol Cell Biol *3*, 498-508.

Cohen, R., Corwith, K., Holowka, D. and Baird, B. Spatiotemporal resolution of mast cell granule exocytosis reveals enhanced degranulation from extended protrusions in response to limiting doses of antigen, submitted for publication.

Cohen, R., Torres, A., Ma, H.T., Holowka, D., and Baird, B. (2009). Ca2+ waves initiate antigen-stimulated Ca2+ responses in mast cells. J Immunol *183*, 6478-6488.

Dai, H., Shen, N., Arac, D., and Rizo, J. (2007). A quaternary SNARE-synaptotagmin-Ca2+-phospholipid complex in neurotransmitter release. J Mol Biol *367*, 848-863.

Daily, N.J., Boswell, K.L., James, D.J., and Martin, T.F. (2010). Novel interactions of CAPS (Ca2+-dependent activator protein for secretion) with the three neuronal SNARE proteins required for vesicle fusion. J Biol Chem *285*, 35320-35329.

Di Paolo, G., and De Camilli, P. (2006). Phosphoinositides in cell regulation and membrane dynamics. Nature *443*, 651-657.

Dragonetti, A., Baldassarre, M., Castino, R., Demoz, M., Luini, A., Buccione, R., and Isidoro, C.

(2000). The lysosomal protease cathepsin D is efficiently sorted to and secreted from regulated secretory compartments in the rat basophilic/mast cell line RBL. J Cell Sci *113 (Pt 18)*, 3289-3298.

Gambhir, A., Hangyas-Mihalyne, G., Zaitseva, I., Cafiso, D.S., Wang, J., Murray, D., Pentyala, S.N., Smith, S.O., and McLaughlin, S. (2004). Electrostatic sequestration of PIP2 on phospholipid membranes by basic/aromatic regions of proteins. Biophys J *86*, 2188-2207.

Gilfillan, A.M., and Tkaczyk, C. (2006). Integrated signalling pathways for mast-cell activation. Nat Rev Immunol *6*, 218-230.

Graff, J.M., Gordon, J.I., and Blackshear, P.J. (1989a). Myristoylated and nonmyristoylated forms of a protein are phosphorylated by protein kinase C. Science *246*, 503-506.

Graff, J.M., Stumpo, D.J., and Blackshear, P.J. (1989b). Characterization of the phosphorylation sites in the chicken and bovine myristoylated alanine-rich C kinase substrate protein, a prominent cellular substrate for protein kinase C. J Biol Chem *264*, 11912-11919.

Heo, W.D., Inoue, T., Park, W.S., Kim, M.L., Park, B.O., Wandless, T.J., and Meyer, T. (2006). PI(3,4,5)P3 and PI(4,5)P2 lipids target proteins with polybasic clusters to the plasma membrane. Science *314*, 1458-1461.

Lee, H., Park, C., Lee, Y., Suk, H., Clemons, T., and Choi, O. (2005). Antigen-induced Ca mobilization in RBL-2H3 cells: Role of I(1,4,5)P and S1P and necessity of I(1,4,5)P production. Cell Calcium *38*, 581-592.

Li, L., Shin, O.H., Rhee, J.S., Arac, D., Rah, J.C., Rizo, J., Sudhof, T., and Rosenmund, C. (2006). Phosphatidylinositol phosphates as co-activators of Ca2+ binding to C2 domains of synaptotagmin 1. J Biol Chem *281*, 15845-15852.

Ma, H.T., and Beaven, M.A. (2009). Regulation of Ca2+ signaling with particular focus on mast cells. Crit Rev Immunol *29*, 155-186.

Ma, H.T., Peng, Z., Hiragun, T., Iwaki, S., Gilfillan, A.M., and Beaven, M.A. (2008). Canonical transient receptor potential 5 channel in conjunction with Orai1 and STIM1 allows Sr2+ entry, optimal influx of Ca2+, and degranulation in a rat mast cell line. J Immunol *180*, 2233-2239.

McLaughlin, S., and Murray, D. (2005). Plasma membrane phosphoinositide organization by protein electrostatics. Nature *438*, 605-611.

Melicoff, E., Sansores-Garcia, L., Gomez, A., Moreira, D.C., Datta, P., Thakur, P., Petrova, Y., Siddiqi, T., Murthy, J.N., Dickey, B.F., *et al.* (2009). Synaptotagmin-2 controls regulated exocytosis but not other secretory responses of mast cells. J Biol Chem *284*, 19445-19451.

Metzelaar, M.J., Wijngaard, P.L., Peters, P.J., Sixma, J.J., Nieuwenhuis, H.K., and Clevers, H.C. (1991). CD63 antigen. A novel lysosomal membrane glycoprotein, cloned by a screening procedure for intracellular antigens in eukaryotic cells. J Biol Chem *266*, 3239-3245.

Nechushtan, H., Leitges, M., Cohen, C., Kay, G., and Razin, E. (2000). Inhibition of degranulation and interleukin-6 production in mast cells derived from mice deficient in protein kinase Cbeta. Blood *95*, 1752-1757.

Newton, A.C. (2010). Protein kinase C: poised to signal. Am J Physiol Endocrinol Metab *298*, E395-402.

Nishizuka, Y. (1995). Protein kinase C and lipid signaling for sustained cellular responses. FASEB J *9*, 484-496.

Oancea, E., and Meyer, T. (1998). Protein kinase C as a molecular machine for decoding calcium and diacylglycerol signals. Cell *95*, 307-318.

Ozawa, K., Szallasi, Z., Kazanietz, M.G., Blumberg, P.M., Mischak, H., Mushinski, J.F., and Beaven, M.A. (1993a). Ca(2+)-dependent and Ca(2+)-independent isozymes of protein kinase C mediate exocytosis in antigen-stimulated rat basophilic RBL-2H3 cells. Reconstitution of secretory responses with Ca2+ and purified isozymes in washed permeabilized cells. J Biol Chem *268*, 1749-1756.

Ozawa, K., Yamada, K., Kazanietz, M.G., Blumberg, P.M., and Beaven, M.A. (1993b). Different isozymes of protein kinase C mediate feedback inhibition of phospholipase C and stimulatory signals for exocytosis in rat RBL-2H3 cells. J Biol Chem *268*, 2280-2283.

Paddock, B.E., Striegel, A.R., Hui, E., Chapman, E.R., and Reist, N.E. (2008). Ca2+-dependent, phospholipid-binding residues of synaptotagmin are critical for excitation-secretion coupling in vivo. J Neurosci *28*, 7458-7466.

Paumet, F., Le Mao, J., Martin, S., Galli, T., David, B., Blank, U., and Roa, M. (2000). Soluble NSF attachment protein receptors (SNAREs) in RBL-2H3 mast cells: functional role of syntaxin 4 in exocytosis and identification of a vesicle-associated membrane protein 8-containing secretory compartment. J Immunol *164*, 5850-5857.

Peng, Z., and Beaven, M.A. (2005). An Essential Role for Phospholipase D in the Activation of Protein Kinase C and Degranulation in Mast Cells. The Journal of Immunology *174*, 5201-5208.
Posner, R.G., Lee, B., Conrad, D.H., Holowka, D., Baird, B., and Goldstein, B. (1992). Aggregation of IgE-receptor complexes on rat basophilic leukemia cells does not change the intrinsic affinity but can alter the kinetics of the ligand-IgE interaction. Biochemistry *31*, 5350-5356.

Pyenta, P.S., Holowka, D., and Baird, B. (2001). Cross-Correlation Analysis of Inner-Leaflet-Anchored Green Fluorescent Protein Co-Redistributed with IgE Receptors and Outer Leaflet Lipid Raft Components. Biophysical Journal *80*, 2120-2132.

Rhee, S.G., and Choi, K.D. (1992). Regulation of inositol phospholipid-specific phospholipase C isozymes. J Biol Chem *267*, 12393-12396.

Sagi-Eisenberg, R. (2007). The mast cell: where endocytosis and regulated exocytosis meet. Immunol Rev *217*, 292-303.

Sagi-Eisenberg, R., Lieman, H., and Pecht, I. (1985). Protein kinase C regulation of the receptor-coupled calcium signal in histamine-secreting rat basophilic leukaemia cells. Nature *313*, 59-60.

Sander, L.E., Frank, S.P., Bolat, S., Blank, U., Galli, T., Bigalke, H., Bischoff, S.C., and Lorentz, A. (2008). Vesicle associated membrane protein (VAMP)-7 and VAMP-8, but not VAMP-2 or VAMP-3, are required for activation-induced degranulation of mature human mast cells. Eur J Immunol *38*, 855-863.

Schwarz, T.L. (2004). Synaptotagmin promotes both vesicle fusion and recycling. Proc Natl Acad Sci U S A *101*, 16401-16402.

Smith, N.L., Hammond, S., Gadi, D., Wagenknecht-Wiesner, A., Baird, B., and Holowka, D. (2010). Sphingosine derivatives inhibit cell signaling by electrostatically neutralizing polyphosphoinositides at the plasma membrane. Self Nonself *1*, 133-143.

Stauffer, T.P., Ahn, S., and Meyer, T. (1998). Receptor-induced transient reduction in plasma membrane PtdIns(4,5)P2 concentration monitored in living cells. Curr Biol *8*, 343-346.

Stumpo, D.J., Graff, J.M., Albert, K.A., Greengard, P., and Blackshear, P.J. (1989). Molecular cloning, characterization, and expression of a cDNA encoding the "80- to 87-kDa" myristoylated alanine-rich C kinase substrate: a major cellular substrate for protein kinase C. Proc Natl Acad Sci U S A *86*, 4012-4016.

Suzuki, R., Liu, X., Olivera, A., Aguiniga, L., Yamashita, Y., Blank, U., Ambudkar, I., and Rivera, J. (2010). Loss of TRPC1-mediated Ca2+ influx contributes to impaired degranulation in Fyn-deficient mouse bone marrow-derived mast cells. J Leukoc Biol *88*, 863-875.

Trifaro, J.M., Gasman, S., and Gutierrez, L.M. (2008). Cytoskeletal control of vesicle transport and exocytosis in chromaffin cells. Acta Physiol (Oxf) *192*, 165-172.

Varnai, P., and Balla, T. (1998). Visualization of phosphoinositides that bind pleckstrin homology domains: calcium- and agonist-induced dynamic changes and relationship to myo-[3H]inositol-labeled phosphoinositide pools. J Cell Biol *143*, 501-510.

Vasudevan, L., Jeromin, A., Volpicelli-Daley, L., De Camilli, P., Holowka, D., and Baird, B. (2009). The beta- and gamma-isoforms of type I PIP5K regulate distinct stages of Ca2+ signaling in mast cells. J Cell Sci *122*, 2567-2574.

Vig, M., DeHaven, W.I., Bird, G.S., Billingsley, J.M., Wang, H., Rao, P.E., Hutchings, A.B., Jouvin, M.H., Putney, J.W., and Kinet, J.P. (2008). Defective mast cell effector functions in mice lacking the CRACM1 pore subunit of store-operated calcium release-activated calcium channels. Nat Immunol *9*, 89-96.

Wang, J., Arbuzova, A., Hangyas-Mihalyne, G., and McLaughlin, S. (2001). The effector

domain of myristoylated alanine-rich C kinase substrate binds strongly to phosphatidylinositol 4,5-bisphosphate. J Biol Chem *276*, 5012-5019.

Xu, K., Williams, R.M., Holowka, D., and Baird, B. (1998). Stimulated release of fluorescently labeled IgE fragments that efficiently accumulate in secretory granules after endocytosis in RBL-2H3 mast cells. J Cell Sci *111 (Pt 16)*, 2385-2396.

CHAPTER 3

INVESTIGATION OF THE ROLE OF ENDOGENOUS MARCKS PROTEIN IN IgE RECEPTOR SIGNALING IN RBL-2H3 MAST CELLS

3.1 Abstract

MARCKS is a ubiquitous substrate for PKC and is involved in multiple signaling processes such as cell migration and ruffling in various cell types. Due to its reversible sequesteration of phosphoinositides, it is primarily involved in regulating cellular processes that involve PIPs. In this study, we present evidence that endogenous MARCKS in RBL cells is involved in regulating stimulated Ca^{2+} mobilization and granule exocytosis. We find that knockdown of MARCKS results in inhibition of antigen-stimulated Ca^{2+} mobilization. Interestingly, we find that knockdown of MARCKS, specifically inhibits the store-operated Ca^{2+} entry (SOCE) component of antigen-stimulated Ca^{2+} mobilization. We also find that MARCKS positively regulates antigen-stimulated granule exocytosis, likely, due in part to its regulation of Ca^{2+} influx Based on our results, we hypothesize that endogenous MARCKS regulates antigen-stimulated SOCE and granule exocytosis due to its association with Ca^{2+}/calmodulin upon cellular stimulation.

3.2 Introduction

MARCKS, a prominent PKC substrate, is a major regulator of PIP_2 availability in a variety of cell types. MARCKS is an anionic protein (pI = 4.5 - 4.7) due to the presence of a large number of negatively charged amino acids. Its molecular weight is 30 kDa, however, it migrates at 80 kDa in an SDS-PAGE gel due to a high net negative charge (Erusalimsky et al., 1991; Graff et al., 1989a; Harlan et al., 1991; Stumpo et al., 1989).

MARCKS has a very concentrated basic stretch of amino acids (from 151-175 in the full length MARCKS sequence) called the effector domain (ED) with a net positive charge of 13. MARCKS-ED is responsible for most of the known interactions of MARCKS with PIPs, calmodulin and F-actin (Blackshear, 1993; Glaser et al., 1996; Hartwig et al., 1992). Due to the presence of over ten lysine residues in MARCKS-ED, the effector domain associates with the negatively charged PIPs at the plasma membrane due to electrostatic interactions. Apart from the basic amino acids, this effector domain also has four serine residues, three of which get phosphorylated by PKC causing the disruption of MARCKS interaction with PIPs and the dissociation of MARCKS from the plasma membrane.

The translocation of MARCKS into the cytosol can also be caused by Ca^{2+}/calmodulin binding to MARCKS. Calmodulin is a Ca^{2+} binding protein, present in the cytosol, and it is known to bind lysine rich motifs. A rise in intracellular Ca^{2+} leads to calmodulin activation upon Ca^{2+} binding. Ca^{2+}/calmodulin binds to the effector domain of MARCKS leading to the translocation of Ca^{2+}/calmodulin bound MARCKS into the cytosol.

We previously proposed in Chapter 2 that PKC activation regulates accessibility of PIPs under stimulated conditions due to the capacity of PKC to reversibly disrupt the electrostatic interactions between PIPs and MARCKS-ED (McLaughlin and Murray, 2005). In the current study, we have explored the molecular mechanism by which full-length endogenous MARCKS participates in regulating stimulated Ca^{2+} mobilization and granule exocytosis.

The store-operated Ca^{2+} entry (SOCE) component of Ca^{2+} mobilization requires two key proteins: STIM1, an ER transmembrane Ca^{2+} sensor, and Orai1, which is a plasma membrane Ca^{2+} channel subunit. In the current study, we present evidence for a possible regulatory role of MARCKS in antigen-stimulated SOCE and also in granule exocytosis.

3.3 Experimental

Cell culture

RBL cells culture is previously described (Chapter 2).

Immunoprecipitation and Western Blotting

MARCKS was immunoprecipitated using rabbit anti-rat MARCKS polyclonal antibody (Abcam). After harvesting, cells were washed and resuspended in BSS at a concentration of $9x10^6$ / ml. 900 µl of 2X solubilization buffer (20 mM Tris, 100 mM NaCl, 2 mM Na_3VO_4, 60 mM $Na_4P_2O_7$, 0.04 U/ml aprotinin, 0.02% NaN3, 1.0% TritonX-100, 2 mM AEBSF (4-(2-Aminoethyl) benzenesulfonyl fluoride), and a protease inhibitor cocktail) was added to 900 µl cells and incubated on ice for 10 min. Cells were centrifuged at 11000 rpm at 4ºC for 10 min, and the supernatant was incubated with 25 µl of Protein A beads (Pierce) and 5 µg anti-

MARCKS antibody at 4ºC for 2 hrs on a rotator. A control sample was incubated with 5 µg anti-Rab11 antibody. After incubation, beads were pelleted and washed thrice with 1X solubilization buffer (500 µl each) at 2000 rpm for 1 min to remove unbound antibody. The beads were resuspended in 80 µl of 1X SDS sample buffer (50% glycerol, 5% SDS, 0.1% bromophenol blue in 0.25 M Tris) and boiled for 5 min. For reduced samples, 1% β-mercaptoethanol v/v (BME) was also added before boiling.

Immunoprecipitated product samples were electrophoresed on a 10% polyacrylamide gel and run at 25 mA for 1 hr. The electrophoresed proteins were transferred to a polyvinylidene fluoride (PVDF) membrane using a semidry transfer apparatus at 90 mA for 1 hr. The membrane was blocked with 15% BSA (w/v) in Tris-buffered saline with Tween (TBST, 50 mM Tris, pH 7.6, 1 M HCl, 150 mM NaCl and 0.1% Tween 20). To detect MARCKS, the primary antibody was used at 1:10,000 dilution. Biotin SP-goat anti-rabbit IgG (Jackson ImmunoResearch Laboratories) was used at 1:3000 as the secondary antibody, followed by Neutraavidin-conjugated horseradish peroxidase (Pierce) at 1:1000 as the tertiary antibody. Blots were developed using Super Signal West Pico chemiluminescent substrates. Blotting of immunodepleted products was carried out similarly using an aliquot of supernatant of beads after pull-down with antibody.

siRNA design

Two short-interfering RNA (siRNA) nucleotides for gene-silencing of MARCKS were selected from the predicted mRNA sequence of MARCKS (*Rattus Norvegicus*) published in PubMed. siRNA A was selected from a previously published result (Calabrese et. al., Neuron, 2005). siRNA B was selected in close proximity to the mRNA sequence of effector domain of

MARCKS. The siRNAs were purchased from Thermo Scientific Dharmacon.

siRNA A: CUGUACCAGUCAGUAAUUAUU

siRNA B: GGAGAAUGGCCACGUAAAAUU

siRNA knockdown

siRNA-mediated RNA interference was induced in RBL-2H3 cells by electroporation with 1 μM siRNA A, siRNA B, or control siRNA under stringently sterile conditions. Electroporated cells were plated in 25 cm^2 cell culture flasks and 24 hrs later a second knockdown was performed as above in the respective samples and plated in 25 cm^2 cell culture flasks. 48 hrs post-second electroporation, cells were harvested and suspended in BSS and used for functional assays.

Ca^{2+} measurement

Intracellular Ca^{2+} measurement of suspended cells loaded with indo-1 was carried out in a stirred cuvette using steady-state fluorimetry as described in Chapter 2. For quantification of Ca^{2+} response, background fluorescence obtained with EDTA was subtracted from the actual fluorescence value and TritonX-100 treated fluorescence value and their ratio was determined. The normalized Ca^{2+} response was integrated over 300-500 s after stimulation. To determine the percentage inhibition of Ca^{2+} response in MARCKS knockdown cells, the integrated Ca^{2+} response from knockdown cells was subtracted from the integrated Ca^{2+} response from control cells (treated with arbitrary siRNA sequence). The ratio of this difference in the integrated Ca^{2+} response and integrated Ca^{2+} response from control cells was multiplied by 100 to get the percentage inhibition.

Granule exocytosis monitored in suspended cells with FITC-dextran

Cells were loaded with 2 mg/ml FITC-dextran (10,000 MW from Sigma-Aldrich) 24 hrs prior to monitoring granule exocytosis. FITC-dextran loaded cells were washed 3 times with BSS and resuspended at a concentration of $3X10^6$/ml and aliquoted into a cuvette. Time-based acquisition of FITC-dextran release was monitored in an SLM 8100C fluorimeter, and cells were stimulated with 0.2 µg/ml DNP-BSA or 20 ng/ml with 1µg/ml cytochalasin D or 0.5 µM thapsigargin with 50 nM PMA. For quantification of granule exocytosis, baseline fluorescence before stimulation was subtracted from the actual fluorescence value and TritonX-100 treated fluorescence value and their ratio was determined. This normalized granule exocytosis response was integrated over 500-1000 s after stimulation. To determine the percentage inhibition of granule exocytosis in MARCKS knockdown cells, the integrated granule exocytosis response from knockdown cells was subtracted from the integrated granule exocytosis response from control cells (treated with arbitrary siRNA sequence). The ratio of this difference in the integrated response and integrated response from control cells was multiplied by 100 to get the percentage inhibition.

3.4 Results

As previously shown in Chapter 2, the strong temporal synchronization of antigen-stimulated PKCβI and MARCKS-ED oscillations implicates a role for PKC-mediated MARCKS phosphorylation in regulating the interactions between this protein and the plasma membrane. To investigate the role of endogenous MARCKS in mast cell signaling, we knocked down endogenous MARCKS and assessed the effect on signaling processes. We first tried to ascertain the expression level of endogenous MARCKS in RBL-2H3 cells by performing

immunoprecipitation with an anti-MARCKS antibody. We detected a band at 80 kDa by western blotting of the immunoprecipitated product (Figure 3.1). As shown in the literature, MARCKS electrophoreses in the molecular weight range of 80-90 kDa in an SDS-PAGE gel due to its highly anionic net charge. We tested the specificity of this antibody for MARCKS by electrophoresing the immunodepleted samples after MARCKS or Rab11 (control) pull-down and blotting with anti-MARCKS antibody. As shown in Figure 3.2, it appears that the 80 kDa band detected by this antibody is non-specific. We also tried another antibody for MARCKS from GenScript which failed to show any band at 80 kDa (data not shown).

Given the strong electrostatic interactions between MARCKS and phosphoinositides (McLaughlin and Murray, 2005), we were interested in the effects of knockdown of MARCKS on PIP-dependent processes in mast cells. To investigate the possible role of MARCKS in stimulated-Ca^{2+} mobilization in RBL cells, we measured Ca^{2+} levels in suspended siRNA-mediated MARCKS knockdown cells using steady-state fluorimetry. As shown in the representative experiment in Figure 3.3, cells with siRNA A or siRNA B, exhibited 25 $\pm$ 5% (n = 4) inhibition of antigen-stimulated Ca^{2+} mobilization, suggesting that MARCKS plays a positive regulatory role in this process.

To determine if MARCKS regulates the availability of the pool of PIP_2 that is hydrolyzed by PLCγ to produce IP_3, we examined the Ca^{2+} response to antigen in the absence of extracellular Ca^{2+} in siRNA treated cells. As shown in the representative experiment in Figure 3.4, we found that there is no consistent difference in IP_3-dependent Ca^{2+} release from ER stores due to knockdown of MARCKS. However, interestingly, we found that addition of extracellular Ca^{2+} following stimulation results in inhibition of SOCE by 31 $\pm$ 7% (n = 5) in cells which were

Figure 3.1: Western blot of immunoprecipitated product with MARCKS antibody shows up at 80 kDa; immunoprecipitation with Rab11 as a control does not show any band in that molecular weight range. Both MARCKS and Rab 11 immunoprecipitated products were blotted with MARCKS antibody.

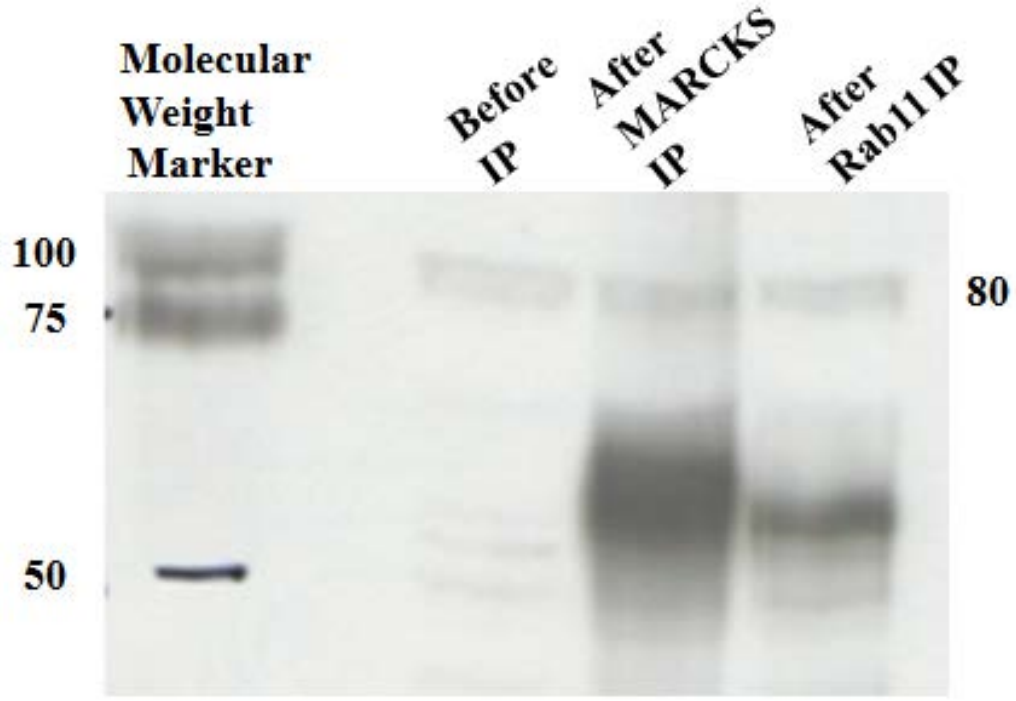

Figure 3.2: Western blot of whole cell lysate of RBL cells (before IP lane) and supernatants after immunoprecipitation with MARCKS and Rab 11 antibody show 80 kDa band. MARCKS antibody was used for blotting.

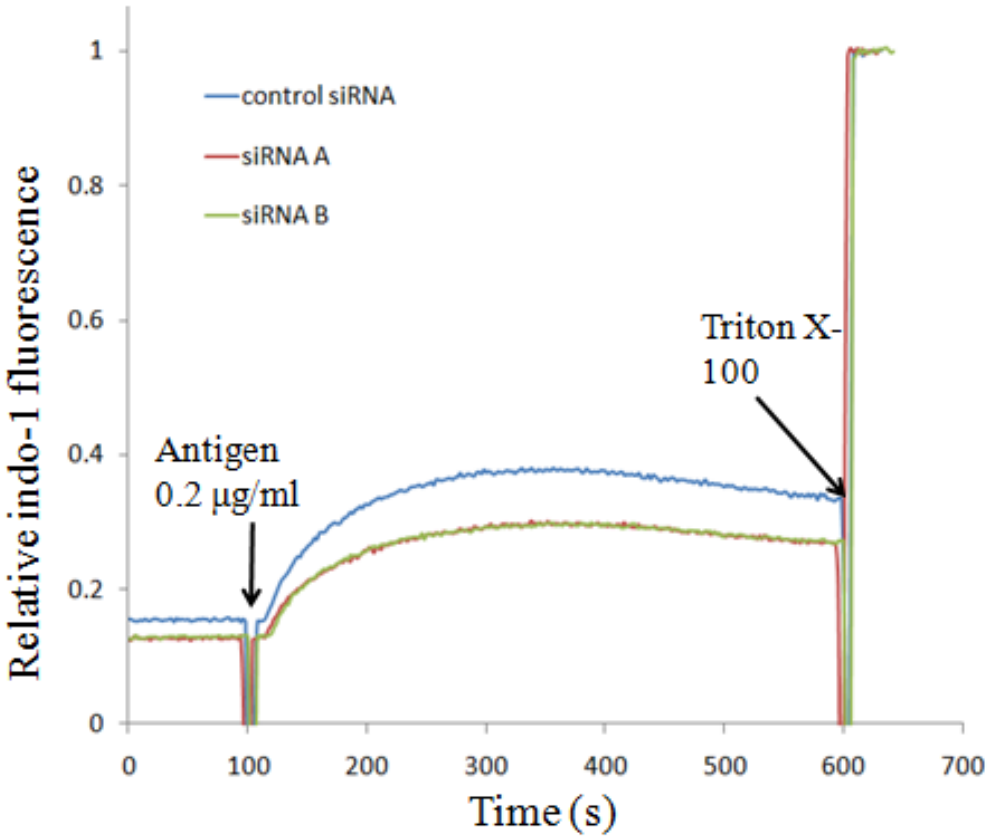

Figure 3.3: Steady-state fluorimetry of Ca^{2+} response to antigen in control RBL cells (blue) and cells with MARCKS knockdown (red for siRNA A treated cells and green for siRNA B treated cells).

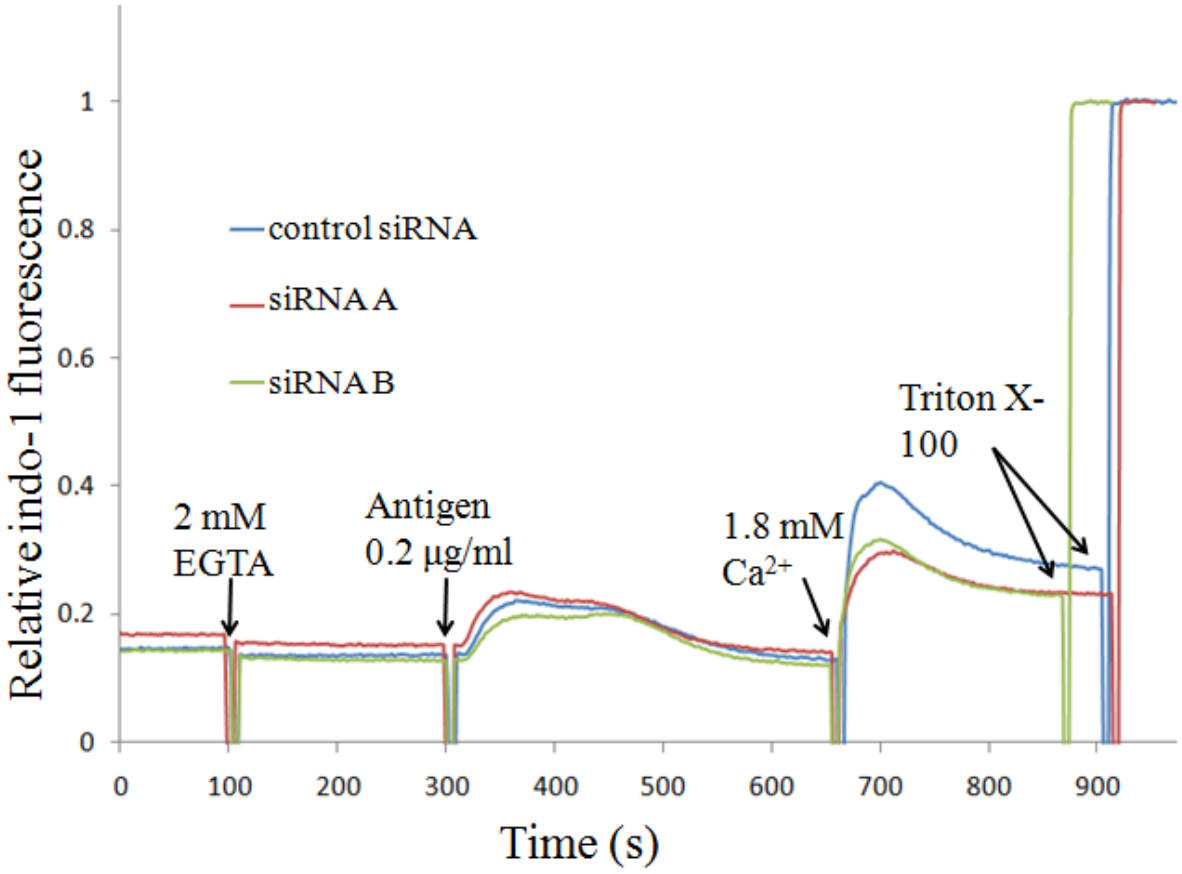

Figure 3.4: Steady-state fluorimetry shows antigen-stimulated Ca^{2+} response to antigen in the absence of extracellular Ca^{2+} followed by antigen-stimulated SOCE due to addition of extracellular Ca^{2+}. Control cells (blue), siRNA A treated cells (red) and siRNA B treated cells (green). Buffer had 1.8 mM Ca^{2+} and it was chelated with 2 mM EGTA before antigen stimulation to monitor the response in the absence of extracellular Ca^{2+}.

treated with MARCKS siRNA, with similar inhibition levels for both siRNA A and siRNA B. This suggests that MARCKS is strongly modulating antigen-stimulated SOCE. We also determined the effect of MARCKS RNAi on SOCE stimulated by thapsigargin as shown in Figure 3.5, and found small amount of inhibition with limited data (10%; n = 2).

Results in Chapter 2 supported the role of PIP_2 in mediating granule exocytosis in mast cells, and our data suggested that this is regulated by PKC-dependent phosphorylation of MARCKS-ED. We investigated whether knockdown of endogenous MARCKS has an effect on granule exocytosis stimulated by antigen or thapsigargin. We performed steady-state fluorimetry of FITC-dextran-loaded cells in a stirred cuvette to monitor granule exocytosis. As represented in Figure 3.6, we observed 42 $\pm$ 6% (n = 4) inhibition of antigen-stimulated degranulation in MARCKS knockdown cells as determined by the integrated FITC fluorescence response over 15 minutes after stimulation. This observation suggests that endogenous MARCKS positively regulates granule exocytosis through some other pathway also that may or may not involve PIPs. Since granule exocytosis in suspended cells is a kinetically slower process, we enhanced it by pre-treating the cells with cytochalasin D and then stimulated with antigen. As shown in Figure 3.7, we observed a higher rate of granule exocytosis under these conditions for both control and siRNA-knockdown cells, and the inhibitory effect of MARCKS-knockdown on degranulation was somewhat lower (30 $\pm$ 3%, n = 2) as compared to the effect observed without cytochalasin D.

We also investigated the effect of endogenous MARCKS on thapsigargin-stimulated degranulation in the presence of PMA to achieve a detectable response. We found no difference in the degranulation response of control cells and siRNA-treated cells as shown in Figure 3.8. It

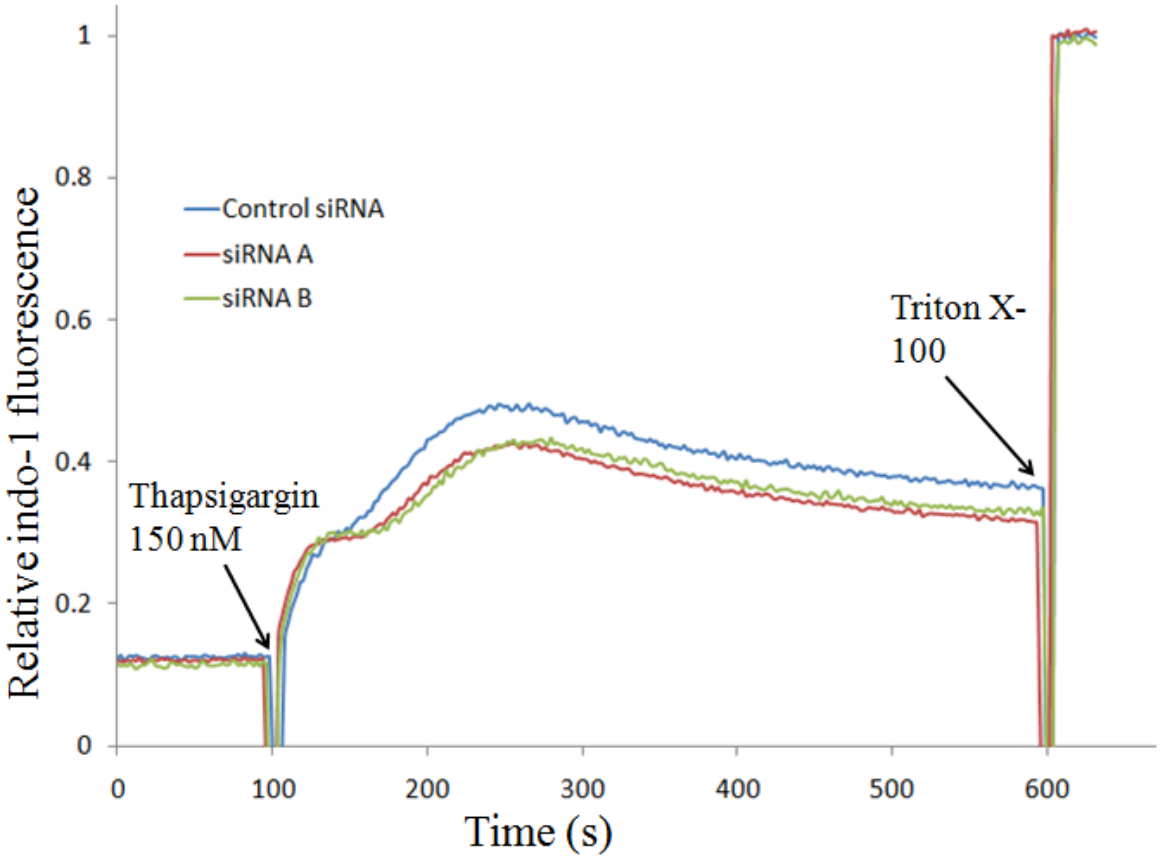

Figure 3.5: Ca^{2+} mobilization in response to thapsigargin in control RBL cells (blue), siRNA A treated cells (red) and siRNA B treated cells (green).

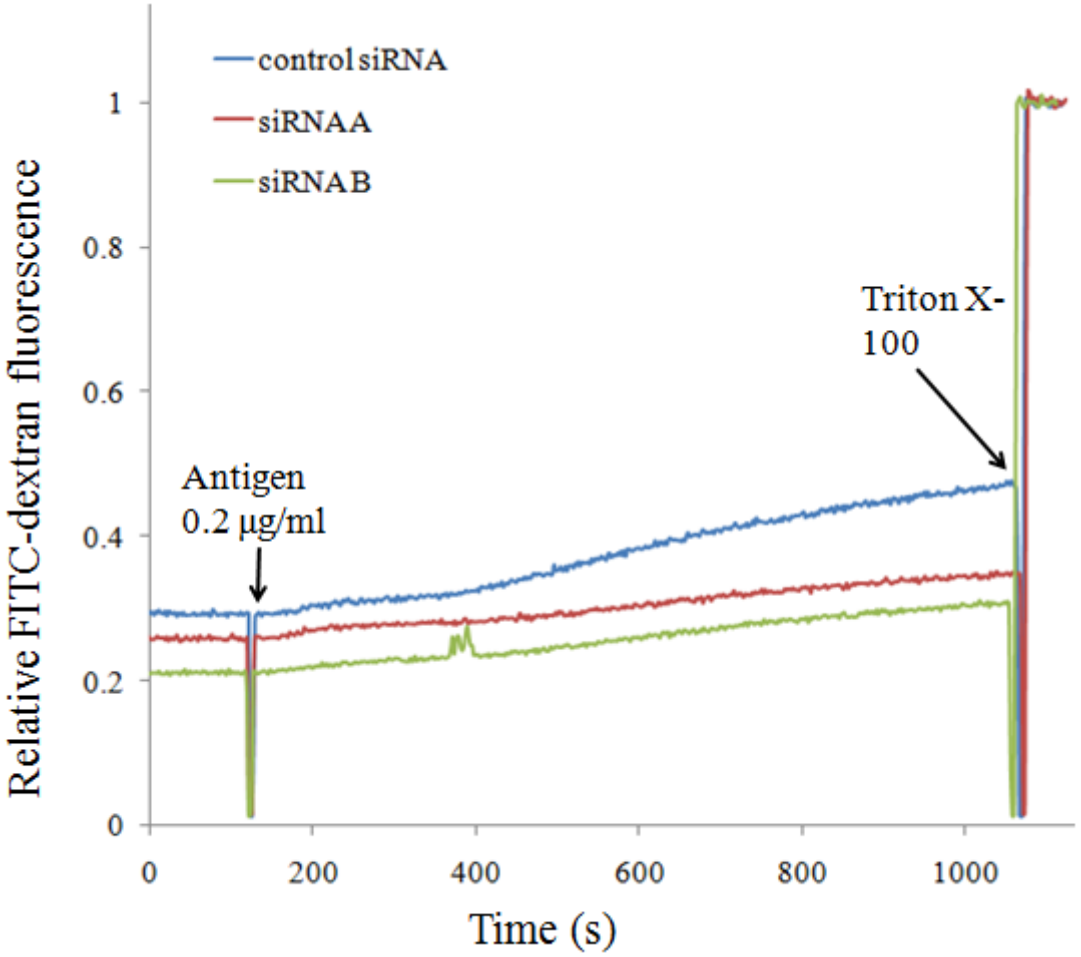

Figure 3.6: Steady-state fluorimetry to monitor degranulation as FITC-dextran release from antigen-stimulated control RBL cells (blue), siRNA A treated cells (red) and siRNA B treated cells (green).

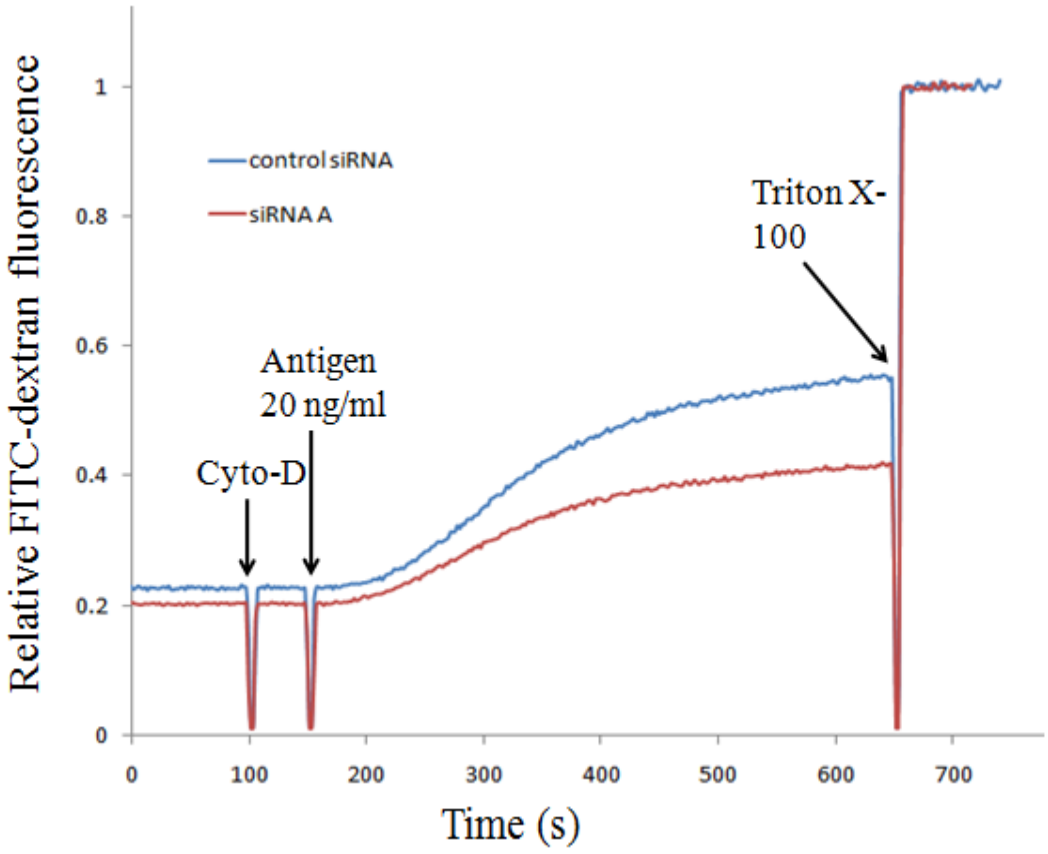

Figure 3.7: Steady-state fluorimetry to monitor antigen-stimulated degranulation after pre-treatment with cytochalasin D. FITC-dextran release from antigen-stimulated control RBL cells (blue) and siRNA A treated cells (red).

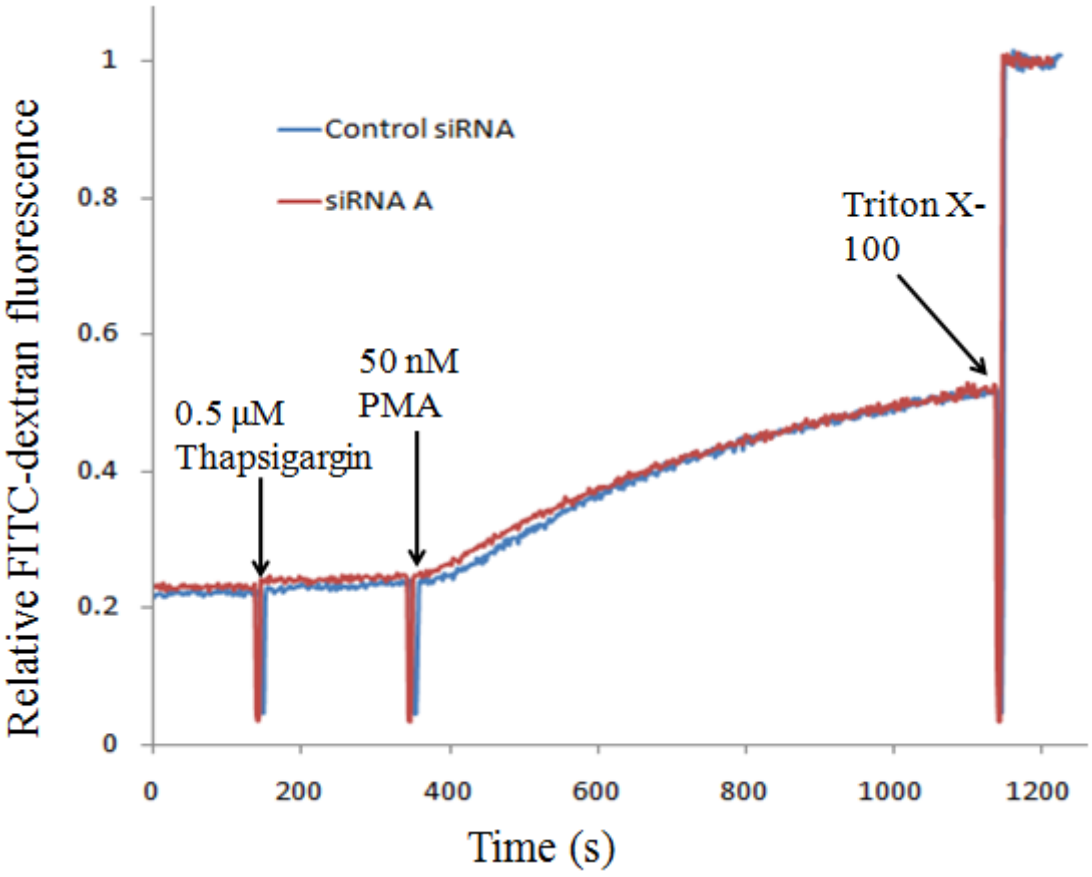

Figure 3.8: Steady-state fluorimetry to monitor degranulation as FITC-dextran release from thapsigargin and PMA-stimulated control RBL cells (blue) and siRNA A treated cells (red).

is possible that addition of PMA might have compensated for any inhibitory effect that might occur for thapsigargin stimulation in the absence of PMA, but this response was insufficient to permit evaluation.

Thus, our results provide evidence for modulation of antigen-stimulated SOCE by endogenous MARCKS in RBL cells. We also observe positive regulation of antigen-stimulated granule exocytosis by MARCKS, likely, due in part to its role in SOCE.

3.5 Discussion

Our data provides substantial evidence that endogenous MARCKS participates in regulating antigen-stimulated SOCE and granule exocytosis in RBL cells. To account for our findings, we hypothesize that MARCKS regulation of SOCE is due to its interaction with other binding proteins, most likely, calmodulin. It has been speculated that PKC-dependent phosphorylation of MARCKS prevents binding of MARCKS to Ca^{2+}/calmodulin (Graff et al., 1989b), indicating that PKC phosphorylating MARCKS and Ca^{2+}/calmodulin binding to MARCKS are competing processes. There is also evidence in the literature showing that MARCKS dissociates from MARCKS-Ca^{2+}/calmodulin complex upon PKC phosphorylation, and this causes activation of other calmodulin-dependent pathways (McIlroy et al., 1991). McIlroy and colleagues also show in this study that binding of MARCKS-ED to calmodulin inhibits the interaction of calmodulin with its other binding partners, most notably myosin light chain kinase, indicating that MARCKS can control the availability of calmodulin for its interaction with its partner proteins. Recently, it was demonstrated by Mullins and colleagues (Mullins et al., 2009) that binding of calmodulin with STIM1 causes inhibition of SOCE. Based

on the above findings and our data with knockdown of MARCKS, we hypothesize that association of MARCKS with Ca^{2+}/calmodulin is the key to regulating calmodulin-STIM1 interaction, thereby regulating STIM1-mediated inactivation of SOCE. As depicted in Figure 3.9, a rise in intracellular Ca^{2+} causes Ca^{2+}/calmodulin binding to MARCKS, however, calmodulin can also bind to STIM1 if calmodulin is not bound to MARCKS. In MARCKS knockdown cells, we observe reduced antigen-stimulated SOCE (Figure 3.4), most likely because calmodulin cannot be sequestered by MARCKS due to its low expression. Therefore, calmodulin is available to bind to STIM1, causing STIM1-mediated inactivation of SOCE. We thus speculate that the role of MARCKS in mast cell signaling is to inhibit the STIM1-mediated inactivation of SOCE and hence it is positively regulating SOCE.

We also provide evidence for the participation of endogenous MARCKS in positively regulating antigen-stimulated granule exocytosis in mast cells. It is well established that SOCE is important for stimulated degranulation in mast cells, so inhibition of SOCE in MARCKS knockdown cells would cause significant inhibition of stimulated granule exocytosis. Additionally, previous studies have suggested that PKC-dependent phosphorylation of MARCKS causes F-actin disassembly which facilitates granule exocytosis in platelets and chromaffin cells (Trifaro et al., 2008). It is possible that in MARCKS RNAi cells, there is inhibition of F-actin disassembly (which in control cells is regulated by PKC-mediated MARCKS phosphorylation), and this enhances inhibition of stimulated granule exocytosis in these cells as compared to control cells.

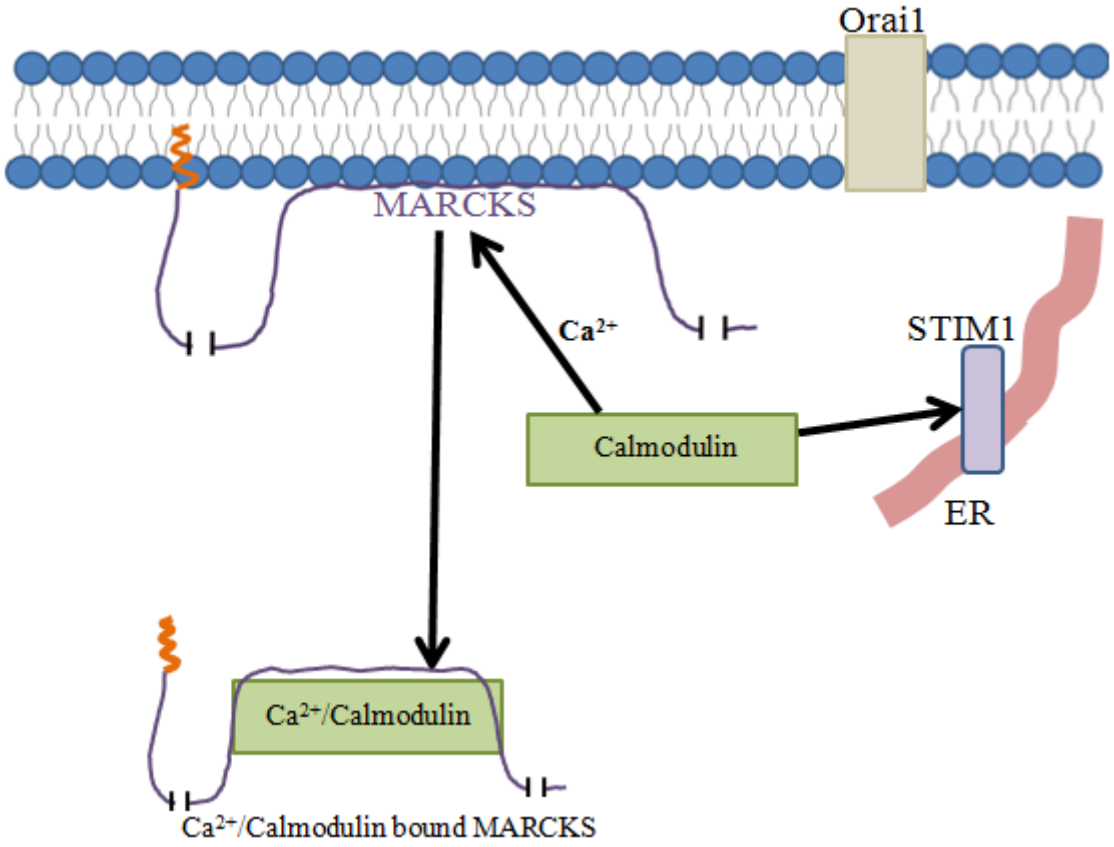

Figure 3.9: Schematic diagram showing Ca^{2+}/calmodulin binding to MARCKS causing a translocation of Ca^{2+}/calmodulin bound MARCKS into the cytosol. The diagram also shows another binding partner for calmodulin – STIM1.

REFERENCES

Blackshear, P.J. (1993). The MARCKS family of cellular protein kinase C substrates. J Biol Chem *268*, 1501-1504.

Erusalimsky, J.D., Brooks, S.F., Herget, T., Morris, C., and Rozengurt, E. (1991). Molecular cloning and characterization of the acidic 80-kDa protein kinase C substrate from rat brain. Identification as a glycoprotein. J Biol Chem *266*, 7073-7080.

Glaser, M., Wanaski, S., Buser, C.A., Boguslavsky, V., Rashidzada, W., Morris, A., Rebecchi, M., Scarlata, S.F., Runnels, L.W., Prestwich, G.D., *et al.* (1996). Myristoylated alanine-rich C kinase substrate (MARCKS) produces reversible inhibition of phospholipase C by sequestering phosphatidylinositol 4,5-bisphosphate in lateral domains. J Biol Chem *271*, 26187-26193.

Graff, J.M., Stumpo, D.J., and Blackshear, P.J. (1989a). Molecular cloning, sequence, and expression of a cDNA encoding the chicken myristoylated alanine-rich C kinase substrate (MARCKS). Mol Endocrinol *3*, 1903-1906.

Graff, J.M., Young, T.N., Johnson, J.D., and Blackshear, P.J. (1989b). Phosphorylation-regulated calmodulin binding to a prominent cellular substrate for protein kinase C. J Biol Chem *264*, 21818-21823.

Harlan, D.M., Graff, J.M., Stumpo, D.J., Eddy, R.L., Jr., Shows, T.B., Boyle, J.M., and Blackshear, P.J. (1991). The human myristoylated alanine-rich C kinase substrate (MARCKS) gene (MACS). Analysis of its gene product, promoter, and chromosomal localization. J Biol Chem *266*, 14399-14405.

Hartwig, J.H., Thelen, M., Rosen, A., Janmey, P.A., Nairn, A.C., and Aderem, A. (1992). MARCKS is an actin filament crosslinking protein regulated by protein kinase C and calcium-calmodulin. Nature *356*, 618-622.

McIlroy, B.K., Walters, J.D., Blackshear, P.J., and Johnson, J.D. (1991). Phosphorylation-dependent binding of a synthetic MARCKS peptide to calmodulin. J Biol Chem *266*, 4959-4964.

McLaughlin, S., and Murray, D. (2005). Plasma membrane phosphoinositide organization by protein electrostatics. Nature *438*, 605-611.

Mullins, F.M., Park, C.Y., Dolmetsch, R.E., and Lewis, R.S. (2009). STIM1 and calmodulin interact with Orai1 to induce Ca2+-dependent inactivation of CRAC channels. Proc Natl Acad Sci U S A *106*, 15495-15500.

Stumpo, D.J., Graff, J.M., Albert, K.A., Greengard, P., and Blackshear, P.J. (1989). Molecular cloning, characterization, and expression of a cDNA encoding the "80- to 87-kDa" myristoylated alanine-rich C kinase substrate: a major cellular substrate for protein kinase C. Proc Natl Acad

Sci U S A *86*, 4012-4016.

Trifaro, J.M., Gasman, S., and Gutierrez, L.M. (2008). Cytoskeletal control of vesicle transport and exocytosis in chromaffin cells. Acta Physiol (Oxf) *192*, 165-172.

CHAPTER 4

SUMMARY AND FUTURE DIRECTIONS

This dissertation illuminates the role of PKCβI, MARCKS-ED and PIP_2 in regulation of granule exocytosis in RBL mast cells. We utilize mutated MARCKS-ED (MARCKS-ED SA4) as a tool to investigate PKC-dependent exposure of PIP_2 in perturbing cellular signaling. We further probe the role of endogenous MARCKS by knocking down its expression to get a more detailed view of MARCKS in mast cell signaling. Drawing from our combined results from expression of mutated MARCKS-ED and knockdown of endogenous MARCKS, we propose that MARCKS exerts both positive and negative regulation on stimulated granule exocytosis. This is finely tuned by two parallel pathways dependent on MARCKS translocation into the cytosol.

It is well established in the literature that PKCβI plays an important role in granule exocytosis of mast cells, but the mechanism remains poorly understood. In chapter 2, we investigated the spatial and temporal changes of PKCβI-EGFP using real-time fluorescence imaging, and we conclude that PKCβI oscillations follow the time course of Ca^{2+} oscillations as shown in figure 2.3. To monitor the activity of PKCβI at the plasma membrane, we co-expressed PKCβI substrate mRFP-MARCKS-ED and demonstrated that its displacement from the plasma membrane is synchronized with the oscillatory recruitment of PKCβI to the plasma membrane as illustrated in figure 2.5. Hence, we demonstrated that PKC and MARCKS-ED show oscillatory association with the plasma membrane due to changes in intracellular Ca^{2+} levels.

MARCKS is well known for its association with phosphoinositides at the plasma membrane. We evaluated the capacity of PKC-mediated phosphorylation of MARCKS-ED in

regulating PIP_2 availability at the plasma membrane and its possible role in stimulated granule exocytosis. For this purpose, we created MARCKS-ED which lacks the capacity to be phosphorylated by PKC because we mutated serine residues to alanines. We showed in figures 2.6 and 2.7 that antigen-stimulated Ca^{2+} mobilization in RBL cells expressing MARCKS-ED SA4 is delayed possibly due to inhibition of PIP_2 hydrolysis by PLCγ, consistent with limited availability of PIP_2 in this case. Under similar conditions, we observed that SOCE stimulated by antigen and thapsigargin is not inhibited as observed in figures 2.10 and 2.11. These results indicate that only the release from stores component of Ca^{2+} mobilization that is affected by MARCKS-ED SA4 expression.

There is growing evidence in the literature to suggest that PIP_2 plays an important role in vesicle fusion. High concentration of PIP_2 has been observed at the sites of vesicle docking in PC12 membrane sheets (James et al., 2008). It has also been speculated that the presence of PIP_2 in membrane enhances the affinity of Ca^{2+} towards synaptotagmin and facilitates the insertion of Ca^{2+}/synaptotagmin complex into the membrane, thereby, triggering vesicle fusion (Bai et al., 2004). We investigated the effect of sequestration of PIP_2 on granule exocytosis using MARCKS-ED SA4 as a probe to perturb PIP_2 availability at the plasma membrane. With both antigen and thapsigargin stimulation we observed reduced granule exocytosis, thereby supporting the model of PIP_2 availability being an important factor in the downstream events leading to granule exocytosis. Delayed Ca^{2+} release from stores upon antigen stimulation may contribute to reduced granule exocytosis. However, using thapsigargin as a stimulus and bypassing IP_3-mediated Ca^{2+} mobilization, we still observe similar inhibitory level of granule exocytosis as observed with antigen stimulation. As described previously for thapsigargin stimulation, we did not observe inhibition of Ca^{2+} mobilization upon expression of MARCK-ED

SA4. Thus, our studies in chapter 2 lead us to conclude that expression of MARCK-ED SA4 results in a direct inhibition of granule exocytosis, most likely due reduced availability of PIP_2 to interact with its binding partners like synaptotagmin, an interaction which is critical for granule exocytosis. We also showed that over-expression of the wild type sequence of MARCKS-ED does not cause inhibition of granule exocytosis, in contrast to the non-phosphorylatable MARCKS-ED SA4 mutant expression, thus indicating that PKC activity at the plasma membrane controls the availability of PIP_2 to participate in granule exocytosis.

Furthermore, to understand the role of endogenous MARCKS in mast cell signaling, we performed RNA interference in RBL cells to knock down this protein. We observed that reduced levels of endogenous MARCKS results in perturbation of stimulated mast cell signaling. Interestingly, we observed that knockdown of MARCKS causes a significant reduction in SOCE stimulated by antigen, but it does not have an effect on Ca^{2+} release from stores. Not surprisingly, we also observed reduced antigen-stimulated granule exocytosis due to MARCKS siRNA, indicating that under physiological conditions, MARCKS positively regulates antigen-stimulated SOCE and granule exocytosis. This was contradictory to our hypothesis in chapter 2, in which we proposed that MARCKS negatively regulates granule exocytosis because it reversibly binds to PIP_2 at the plasma membrane, thereby, limiting the availability of PIP_2 to participate in granule exocytosis events. We were aware of our preliminary results in chapter 3 and hence we were very careful in stating our hypothesis in chapter 2. We used MARCKS-ED SA4 as a tool to perturb PIP-dependent signaling in stimulated RBL cells in chapter 2, but these results cannot be used to conclusively state the role of endogenous full length MARCKS in signaling. A survey of the literature reveals that in addition to being a target for phosphorylation by PKC, MARCKS also interacts with Ca^{2+} bound calmodulin (Arbuzova et al., 2002).

Ca^{2+}/calmodulin binds to lysine rich protein motifs. The effector domain of MARCKS which contains the serine residues that get phosohorylated by PKC, also has the lysine rich amino acid sequence which is a target for Ca^{2+}/calmodulin. A rise in intracellular Ca^{2+} causes calmodulin activation leading to Ca^{2+}/calmodulin binding to MARCKS, and this results in translocation of Ca^{2+}/calmodulin-bound MARCKS to the cytosol. An interesting finding in the literature points towards the role of Ca^{2+}/calmodulin in negatively regulating SOCE. Mullins et al. provide evidence for a mechanism suggesting that Ca^{2+}/calmodulin binds to STIM1 leading to inhibition of SOCE (Mullins et al., 2009).

Our data in chapter 3 show reduced antigen-stimulated SOCE and granule exocytosis by knocking down MARCKS, and from the literature we surmise that MARCKS interacts with Ca^{2+}/calmodulin and Ca^{2+}/calmodulin binds to STIM1 leading to decreased SOCE. Based on this information, a plausible explanation for our results is that low expression level of MARCKS causes a higher free concentration of Ca^{2+}/calmodulin as it is not fully sequestered by endogenous MARCKS upon stimulation. A higher free concentration of Ca^{2+}/calmodulin would imply that more Ca^{2+}/calmodulin is available to bind to STIM1, thereby, leading to higher STIM1-mediated inactivation of SOCE as compared to control cells which were treated with an arbitrary siRNA sequence. We thus hypothesize in chapter 3 that association of MARCKS with Ca^{2+}/calmodulin under stimulated conditions inhibits the interaction of Ca^{2+}/calmodulin with STIM1, hence positively regulating SOCE and granule exocytosis.

In summary, we have developed a very useful tool - MARCKS-ED SA4, to sequester PIPs at the plasma membrane and we demonstrated with multiple investigations, its capacity to perturb PIP_2-dependent signaling. Due to the lack of PIP5K inhibitors which synthesize PIP_2,

MARCKS-ED SA4 can be a very attractive probe to investigate the role of PIP_2 in various signaling cascades in which PIP_2 plays a key role, but the mechanism of its participation is not well understood. Also, our results combined from chapter 2 and 3, reveal that endogenous MARCKS has both positive and negative regulatory roles in signaling. As shown by our experimental data with MARCKS-ED SA4, we hypothesize that endogenous MARCKS reversibly sequesters PIPs until they are dissociated by PKC phosphorylation, thereby, exerting a negative regulatory role on granule exocytosis prior to cell activation. However, in parallel, endogenous MARCKS also interacts with Ca^{2+}-bound calmodulin after a rise in intracellular Ca^{2+} upon cell stimulation. Binding of MARCKS to Ca^{2+}/calmodulin results in sequestration of calmodulin, thereby limiting the interaction of calmodulin with STIM1, thus, enhancing SOCE, and this leads to increased granule exocytosis. Hence, MARCKS regulates granule exocytosis in a finely tuned manner due to its participation in two independent pathways as depicted in figure 4.1, both of which ultimately lead to granule exocytosis. As shown in chapter 2, one pathway illuminates the negative regulation of granule exocytosis due to PKC-mediated MARCKS phosphorylation leading to availability of PIP_2 to participate in stimulated granule exocytosis. As illustrated in chapter 3, the other pathway reveals the positive regulation of SOCE by MARCKS, which is critical for stimulated granule exocytosis, thereby enhancing it.

We can test our hypothesis of MARCKS involvement in two pathways leading to degranulation with a calmodulin inhibitor that inhibits the interaction of Ca^{2+}/calmodulin with STIM1. RBL cells expressing normal levels of endogenous MARCKS, treated with a calmodulin inhibitor, are expected to show higher antigen-stimulated SOCE as compared to cells not treated with the inhibitor under similar conditions. If our hypothesis is correct then there would be no inhibition of antigen-stimulated SOCE in MARCKS knockdown cells treated with calmodulin

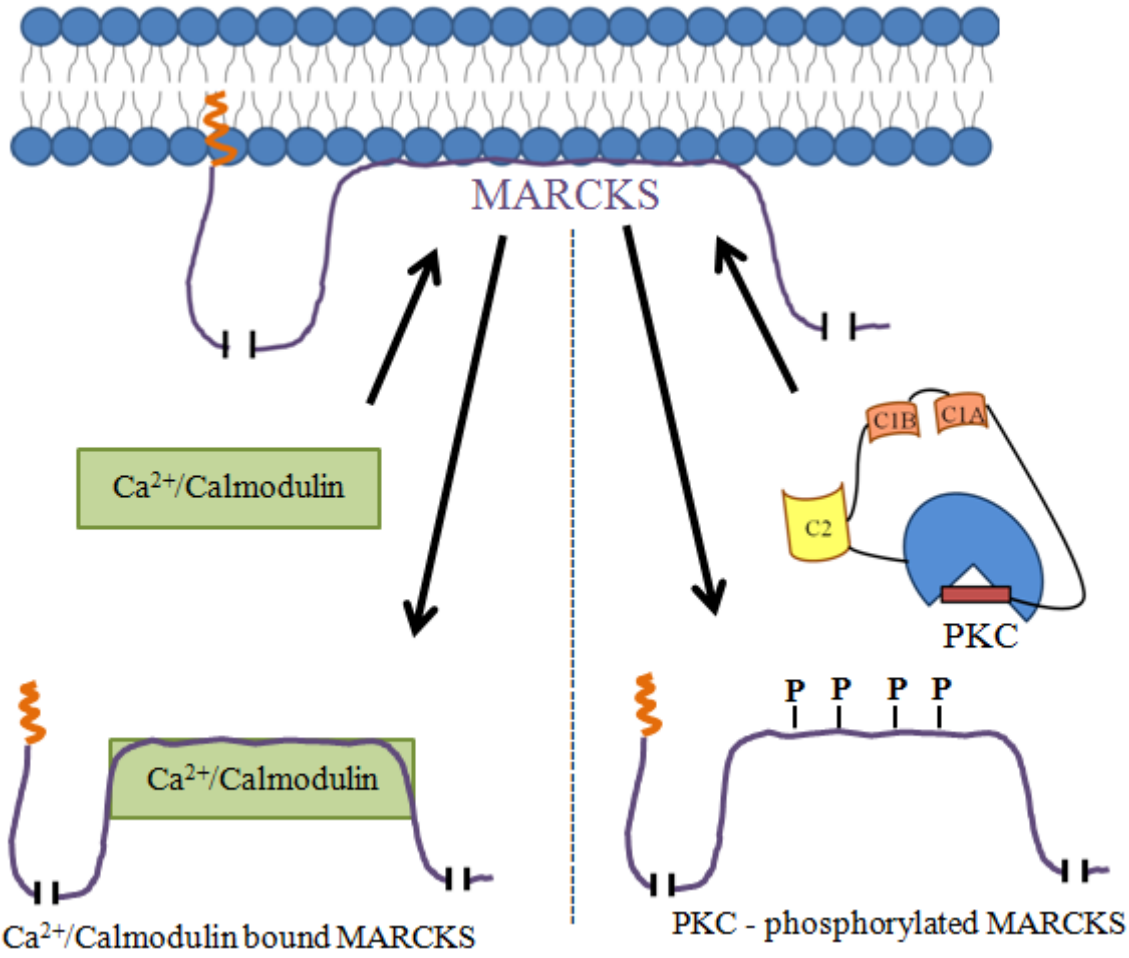

Figure 4.1: MARCKS participation in two independent pathways. Left side shows Ca^{2+}/calmodulin binding to MARCKS leading to translocation of Ca^{2+}/calmodulin bound MARCKS into the cytosol. Right side represents phosphorylation of MARCKS by PKC resulting in translocation of phosphorylated MARCKS into the cytosol.

inhibitor as compared to control cells not treated with MARCKS siRNA and calmodulin inhibitor. Conversely, if cells expressing MARCKS-ED SA4, are treated with calmodulin inhibitor, then they would be expected to show enhanced antigen-stimulated SOCE as compared to MARCKS-ED SA4 expressing cells not treated with calmodulin inhibitor. However, antigen-stimulated granule exocytosis in cells expressing MARCKS-ED SA4 and in the presence of calmodulin inhibitor will be inhibited but to a lesser extent compared to the percentage inhibition observed due to expression of MARCKS-ED SA4 alone. We expect reduced inhibition of antigen-stimulated granule exocytosis in cells which express MARCKS-ED SA4 and have been treated with calmodulin inhibitor as compared to cells expressing MARCKS-ED SA4 but not treated with calmodulin inhibitor due to the predicted higher SOCE in the former case but not in the latter. We expect that higher SOCE will counteract the inhibitory effect of MARCKS-ED SA4 in stimulated granule exocytosis in cells treated with calmodulin inhibitor. This would help support our hypothesis.

We expressed full-length wild type MARCKS tagged with mRFP in RBL cells and upon antigen stimulation observed periodic dissociation and association with the plasma membrane as seen with mRFP-MARCKS-ED (data not shown). In the future, we would also like to confirm our results shown with MARCKS-ED SA4 with full-length MARCKS SA4. We would expect that full-length MARCKS with the SA4 mutation will show inhibitory effect on stimulated granule exocytosis similar to those we observed with MARCKS-ED SA4. Full-length MARCKS SA4 retains myristoylation at its N-terminus. It would be interesting to determine if this mutant exhibits a preference for ordered lipid pool of PIP_2 at the plasma membrane and compare it with MARCKS-ED association with PIP_2 at the plasma membrane. There is growing evidence in the literature for different pools of PIP_2 regulating different set of pathways. It would be of interest

to create a mutant MARCKS probe that can differentially associate with PIP_2 in ordered lipid pool vs. disordered lipid pool. This would help us gain mechanistic insights to see if there is a specific pool of PIP_2 that regulates stimulated granule exocytosis.

Another approach to show that expression of MARCKS-ED SA4 delays antigen-stimulated Ca^{2+} from stores due to delayed hydrolysis of PIP_2, is to determine the rate of IP_3 production under these conditions. We would expect delayed IP_3 production in MARCKS-ED SA4 expressing cells stimulated by antigen as compared to cells expressing wild type MARCKS-ED. It would be of interest to correlate the time of delay in IP_3 production to the time of delay in Ca^{2+} release.

Having shown that MARCKS-ED SA4 inhibits stimulated granule exocytosis, we would like to take our experiments one step further down the signaling cascade to see if expression of this mutant has an effect on cytokine production. The rapid release of pre-formed chemical mediators from mast cells is followed by de novo synthesis and secretion of various cytokines over the course of hours (Qiao et al., 2006). An effect on cytokine production or secretion due to expression of MARCKS-ED SA4 can throw light on the involvement of PIP_2 in this process if there is any.

A major limitation to interpreting our results has been our inability to correlate the level of MARCKS knockdown to its effect on inhibiting SOCE and granule exocytosis. We have thus far been unable to determine the percentage of reduced protein expression in MARCKS knockdown cells due to the lack of a rat specific MARCKS antibody. We suggest the use of reverse transcription polymerase chain reaction (RT-PCR) to determine the level of endogenous

MARCKS, which would be based on the mRNA sequence determined from the cDNA library generated for RBL cells. If we can show that as the percentage of MARCKS expression decreases we observe similar percentage reduction in antigen-stimulated SOCE and granule exocytosis, then it would support our results suggesting that MARCKS has a direct positive regulatory effect on stimulated signaling.

It would be of interest to see whether a phosphomimetic mutant of MARCKS, in which serine residues are mutated to glutamate, to mimic the phosphorylated state of MARCKS would have an effect on mast cell signaling. We would expect that expression of phosphomimetic MARCKS (cytosol localized) will not have any effect on antigen-stimulated release of Ca^{2+} from stores, SOCE or stimulated granule exocytosis as it would not interact either with PIP_2 or with Ca^{2+}/calmodulin with or without stimulation.

REFERENCES

Arbuzova, A., Schmitz, A.A., and Vergeres, G. (2002). Cross-talk unfolded: MARCKS proteins. Biochem J *362*, 1-12.

Bai, J., Tucker, W.C., and Chapman, E.R. (2004). PIP2 increases the speed of response of synaptotagmin and steers its membrane-penetration activity toward the plasma membrane. Nat Struct Mol Biol *11*, 36-44.

James, D.J., Khodthong, C., Kowalchyk, J.A., and Martin, T.F. (2008). Phosphatidylinositol 4,5-bisphosphate regulates SNARE-dependent membrane fusion. J Cell Biol *182*, 355-366.

Mullins, F.M., Park, C.Y., Dolmetsch, R.E., and Lewis, R.S. (2009). STIM1 and calmodulin interact with Orai1 to induce Ca2+-dependent inactivation of CRAC channels. Proc Natl Acad Sci U S A *106*, 15495-15500.

Qiao, H., Andrade, M.V., Lisboa, F.A., Morgan, K., and Beaven, M.A. (2006). FcepsilonR1 and toll-like receptors mediate synergistic signals to markedly augment production of inflammatory cytokines in murine mast cells. Blood *107*, 610-618.

APPENDIX 1

DNP-FUNCTIONALIZED POLYMERS TO ENGAGE RECEPTORS AND CONTROL CELLULAR RESPONSES IN MAST CELLS

A.1 Abstract

Functionalized polymers α,ω-bi[2,4-dinitrophenyl][poly(ethylene oxide)- poly(2-methoxystyrene)- poly(ethylene oxide)] (DNP-PEO-P2MS-P2MS(-SO_3Na)-PEO-DNP) and biodegradable polylactide polymers α,ω-bi[2,4-dinitrophenyl(DNP)] [Poly(lactide)-β-Poly(ethylene glycol)-β-Poly(lactide)] with variable molecular weights and structures were synthesized. Incorporation of PEO and sulfonation enhance their solubility. We demonstrate here that they bind specifically to anti-DNP IgE in solution and to IgE-receptor complexes on RBL-2H3 cells. Although these DNP-functionalized ligands do not stimulate the granule exocytosis response, they have the potential to inhibit the robust response stimulated by other multivalent DNP ligands. Binding and degranulation studies carried out with these polymers are useful for learning how specific ligands that crosslink IgE-receptors control the cellular response. Further, this type of characterization provides useful information for the development of better inhibitors of potent allergens. In separate studies, we show the potential of these functionalized polymers to be utilized in biosensors due to their specificity for IgE binding, after the polymers are electrospun with carbon nanotubes on silicon substrates.

A.2 Introduction

Allergic reactions mediated by the IgE antibody require clustering of IgE-FcεRI on mast cell surface by bivalent or multivalent ligands, and this is a key step for initiating signal transduction resulting in granule exocytosis. IgE antibody has two Fab segments, each of which binds an antigenic group. Crosslinking of anti-DNP IgE-FcεRI complexes can be controlled by the orientation and flexibility of DNP ligands with varying lengths, composition, and DNP valency. Previous studies demonstrated that monovalent ligands do not stimulate mast cells due to lack of crosslinking, whereas multivalent ligands can successfully cause cell activation. Bivalent ligands can act as either triggers or inhibitors of granule exocytosis depending on whether they bind intermolecularly (activation) or intramolecularly (inhibition) (Baird et al., 2003; Kane et al., 1988).

Multivalent DNP_{16}-BSA (DNP conjugated to bovine serum albumin) is commonly used to trigger activation of RBL-2H3 cells, but it cannot be used to decipher structural requirements due to its heterogeneity. Also, DNP tends to be sequestered within BSA and thereby not readily accessible to IgE (Xu et al., 1998). Previously our lab synthesized structurally well-defined rigid DNA ligands functionalized with DNP to gain mechanistic insights into the IgE-FcεRI cross-linking requirement of mast cell signaling (Sil et al., 2007).

In the present study, we investigated a series of DNP-functionalized poly(2-methoxystyrene) polymers (P2MS) synthesized by researchers at Clark Atlanta University (CAU) (Figure A.1). We tested these polymers for their capacity to bind to anti-DNP IgE and their potential to stimulate or inhibit degranulation. Aqueous solubility of these polymers was

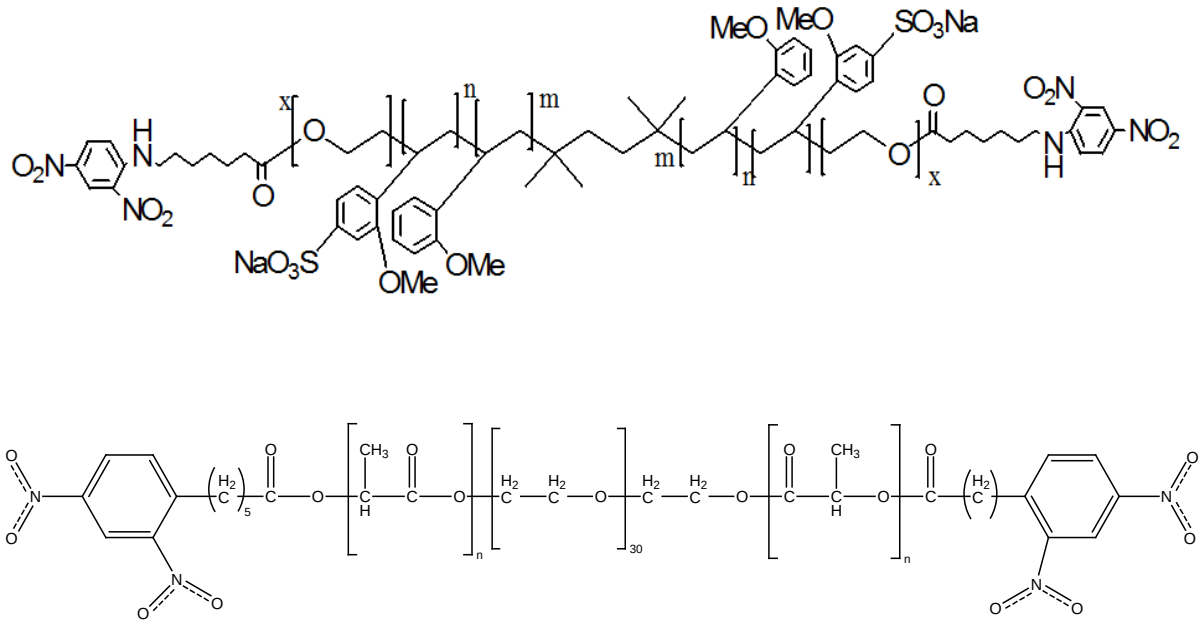

Figure A.1: Polystyrene polymer structure corresponding to DNP-$(PEO)_x$-$(P2MS)_m$-P2MS(-$SO_3Na)_n$-(PEO)-DNP above. Biodegradable polylactide structure below: α,ω-bi[2,4-dinitrophenyl(DNP)] [Poly(lactide)-β-Poly(ethylene glycol)-β-Poly(lactide)].

enhanced by incorporation of PEO and sulfonation.

We also characterized a polylactide polymer (structure shown in figure A.1) synthesized at CAU. Polylactides can be degraded by hydrolysis of the ester linkage, resulting in non-toxic, biologically inert byproducts. Polylactide polymers are being widely used for therapeutic applications due to their biocompatibility and biodegradation properties. The characterization of P2MS-57 polymer and polylactide polymers was performed by an undergraduate student, Olga Morozova, under my supervision.

A.3 Experimental

Cell Culture

RBL cells culture is previously described (Chapter 2).

DNP-Polystyrene Synthesis and Characterization (Performed at CAU)

Figure A.1 shows the generic structure of these polymers. They were synthesized using alpha-methyl styrene and 2-methoxystyrene as the base monomers and functionalized with DNP groups on both ends (Sannigrahi et al., 2008). DNP functionalized poly(2-methoxystyrene) was sulfonated in 1,2-dichloroethane at -10º C with acetyl sulfate, which was produced in situ by the reaction of acetic anhydride and sulfuric acid. Acetyl sulfate solution was prepared by mixing fixed amount of 1,2-dichloroethane with 1 ml (10.5 mmol) acetic anhydride. The solution was cooled to 0^0 C and 0.3 ml (5 mmol) 98% sulfuric acid was carefully added. During the preparation, an excess of acetic anhydride was used to remove any traces of water and the reaction mixture was stirred until a homogeneous and clear solution was obtained. The

sulfonation reaction was carried out by progressive addition of acetyl sulfate solution to 0.5 g (a 5% w/w solution) poly (2-methoxystyrene) in 10 ml 1,2-dichloroethane at -10º C. The reaction continued until all the polymer was separated from solution and was terminated by adding few drops of 2-propanol. The insoluble polymer was washed thoroughly with 1,2-dichloroethane several times to remove access acetyl sulfate. Finally, polymer was dissolved in de-ionized water and titrated with 0.01 M NaOH solution to prepare Na-salt of sulfonated polymer. The titrated solution was washed with diethyl ether to remove phenolphthalein indicator and other small molecules. P2MS-xSO_3Na-PEO was isolated by evaporating water under rotatory evaporator and azeotropic drying with toluene. The extent of sulfonation levels was also determined from the titration. The degree of sulfonation (x) expressed as mole percent of the sulfonated 2-methoxystyrene repeating units, P2MS-xSO_3Na-PEO was 67%.

For characterization of these DNP-functionalized, sulfonated polymers, ^{1}H NMR spectra were obtained using a Bruker ARX 400 NMR spectrometer in D_2O, and trimethylsiloxane was used as internal standard. Spectra showed characteristic proton absorption of DNP at 8 ppm. By carrying out quantitative analysis of the NMR peaks, the degree of functionality was determined. Fourier transform infrared spectroscopy (FTIR) was also performed on the polymer samples and asymmetric and symmetric stretching for NO_2 observed at 1536 cm^{-1} and 1351 cm^{-1}, respectively. FTIR spectra were recorded on a Nicolet 510P FT-IR spectrometer with an accuracy band of ± 2 cm^{-1}. P2MS-SO_3Na samples were measured as KBr pellets.

For determination of molecular weights, size exclusion chromatography (SEC) was performed using a Perkin Elmer Binary LC pump 250, a 2792 injector and Perkin Elmer LC-30

RI detector. Three columns, HR3, HR 4E and HR 5E were used in conjunction with 2-μm pre-column filter. The columns were housed in an oven maintained at 30ºC. Tetrahydrofuran was used as the eluent at a flow rate of 1 ml/ min. Molecular weights were calculated relative to polystyrene molecular weight standards (Aldrich).

Differential scanning calorimetry measurements were performed on a Seiko DSC220 at a heating rate of 5˚C per minute, and the reported values were obtained from the second heating after quench-cooling the sample. The glass transition temperatures (T_g) were taken at the midpoints of the heat capacity changes, the melting temperatures (T_m) were taken at the maximum of the enthalpy endothermic peaks.

Binding study of polymers with anti-DNP FITC-IgE

To determine the binding affinity of these polymers with IgE antibody, fluorescence measurements were made using FITC-IgE as previously established (Erickson et al., 1986) in an SLM 8000 fluorimeter. The equilibrium binding equation to determine the fraction of bound sites is as follows:

L = Free ligand concentration

R = Free IgE binding sites

R_{tot} = Total IgE binding sites (bound to ligand + free)

K_a = Apparent association constant

f = fraction of IgE binding sites occupied by the ligand at equilibrium

$$L + R \leftrightarrow LR$$

$$K_a = \frac{k_{on}}{k_{off}} = \frac{[LR]}{[L][R]} = \frac{1}{K_d}$$

$$R_{tot} = [R] + [LR]$$

$$f = \frac{[LR]}{[R] + [LR]}$$

$$f = \frac{K_a[L]}{1 + K_a[L]}$$

The fluorescence values obtained after addition of small aliquots of ligand were plotted against the ligand concentration after volume correction. The fraction of bound sites at varying ligand concentration was determined from these corrected fluorescence values (Erickson et al., 1986). The values obtained were fitted in the above hyperbolic equation using Sigma software to generate apparent association constant values (K_a). The inverse of K_a is defined as the apparent dissociation constant K_d.

Granule exocytosis assay

For measuring the granule exocytosis response triggered by multivalent DNP-BSA or DNP-functionalized polymers, RBL cells were sensitized with 1 μg/ml anti-DNP IgE and plated overnight at a density of 2.5 x 10^5 cells in a 96-well plate under sterile conditions. These cells were incubated with DNP liganads for 1 h at 37ºC, and the exocytotic release of the granule marker β-hexosaminidase was used to quantify the extent of degranulation as previously described (Naal et al., 2004).

To determine inhibition of degranulation, IgE-sensitized RBL cells were pre-incubated with varying concentrations of DNP-polymer for 30 minutes at 37˚C, followed by stimulation

with 2 ng/ml DNP-BSA for 30 minutes, also at 37˚C, and then β-hexosaminidase release was measured.

Ca^{2+} measurement

Intracellular Ca^{2+} changes were measured in suspended cells loaded with indo-1 in a stirred cuvette using steady-state fluorimetry as described in Chapter 2. Cells were stimulated with 1 μM P2MS-57 followed by 0.2 μg/ml DNP-BSA.

Microscopy visualized PKCβI-EGFP recruitment and IgE clustering

PKCβI-EGFP transfected cells, sensitized with IgE, were stimulated with 50 nM or 1 μM P2MS-57 for 5 minutes at 25˚C as described in Chapter 2 for DNP-BSA stimulation.

IgE-FcεRI Clustering

RBL-2H3 cells plated in MatTek dishes were sensitized with Alexa488-conjugated IgE at a concentration of 3 μg/ml for 1 h at 37˚C. Labeled cells were incubated for 15 minutes at 37˚C with 50 nM or 1 μM P2MS-57 polymer in phosphate buffered saline with 1 mg/ml BSA (PBS-BSA) and then fixed with 4% paraformaldehyde and 0.01% glutaraldehyde for 15 minutes at room temperature. Fixed cells were imaged with Leica TCS SP2 confocal microscope.

Binding with electrospun polymers

BS 5-20 polymer [Table A.1] was electrospun in chlorobenzene with 1% single walled

Polymer Name	Structure	Molecular weight kDa	DNP functionalit-zation (%)	Dissociation constants (K_d) with cells nM
BS 5-25	DNP-PEO_{47}-P2MS$_{23}$-P2MS(-$SO_3Na)_{46}$-PEO_{47}-DNP	16.1	47	240.7 ± 12.4
BS 9-3	DNP-PEO_{143}-P2MS$_{32}$-P2MS(-$SO_3Na)_{48}$-PEO_{143}-DNP	26.6	63	410.9 ± 43.8
BS 5-14	DNP-PEO_{240}-P2MS$_{24}$-P2MS(-$SO_3Na)_{36}$-PEO_{240}-DNP	32.6	69	200.4 ± 15.7
BS 5-20	DNP-PEO_{331}-P2MS$_{65}$-P2MS(-$SO_3Na)_{90}$-PEO_{331}-DNP	59.5	28	260.0 ± 8.7
P2MS-10	DNP-PEO_4-P2MS$_{26}$-P2MS(-$SO_3Na)_{52}$-PEO_4-DNP	15.8	>92	49.5 ± 10.3
P2MS-57	DNP-PEO_4-P2MS$_{32}$-P2MS(-$SO_3Na)_{67}$-PEO_4-DNP	20.1	>92	54.3 ± 5.9

Table A.1: Series of polystyrene polymers with varying molecular weights, % DNP functionality and apparent dissociation constants with RBL cells. Standard deviation for dissociation constants is from n = 2-3 for each polymer. DNP functionalization was determined from quantitative analysis of NMR spectra by CAU researchers. % DNP functionality is % of ideal two DNP groups per polymer.

carbon nanotubes on silicon wafer by researchers at CAU. We tested the specificity of these electrospun polymers towards IgE antibody by labeling the samples with FITC-IgE or FITC-IgG (for control) at a concentration of 3 μg/ml in PBS-BSA for 1 h at 37˚C. Samples were washed with PBS to remove unbound antibody and then imaged using confocal microcopy.

A.4 Results

We have characterized a variety of polystyrene DNP-functionalized polymers (Figure A.1) for specific binding with anti-DNP IgE. We further evaluated their potential to stimulate or inhibit signaling events in mast cells. Researchers at CAU synthesized these DNP-functionalized polymers and determined their molecular weights and DNP percentage via spectroscopy, chromatography and calorimetry studies as described in the experimental section. These polymers vary in their molecular weight and DNP functionalization as summarized in Table A.1.

To test the specific binding of these polymers with anti-DNP IgE, we performed equilibrium titrations with RBL cells sensitized with FITC-IgE as previously described (Erickson et al., 1986). We determined the apparent dissociation binding constants (K_d) from these equilibrium binding studies by fitting the data to a simple binding equation described in the experimental section. As demonstrated in the representative binding curve in Figure A.2, the fraction of IgE-binding sites in solution vs. P2MS-57 polymer concentration resulted in a hyperbolic curve from which K_d was determined to be 178.3 $\pm$ 97 nM (n = 4). We also determined the apparent dissociation constants for P2MS-57 polymer binding to IgE-FcεRI on cells as shown in Figure A.3. After this initial assessment of binding data, we focused our efforts on studying P2MS-57 polymer more extensively due to its high DNP functionality and its

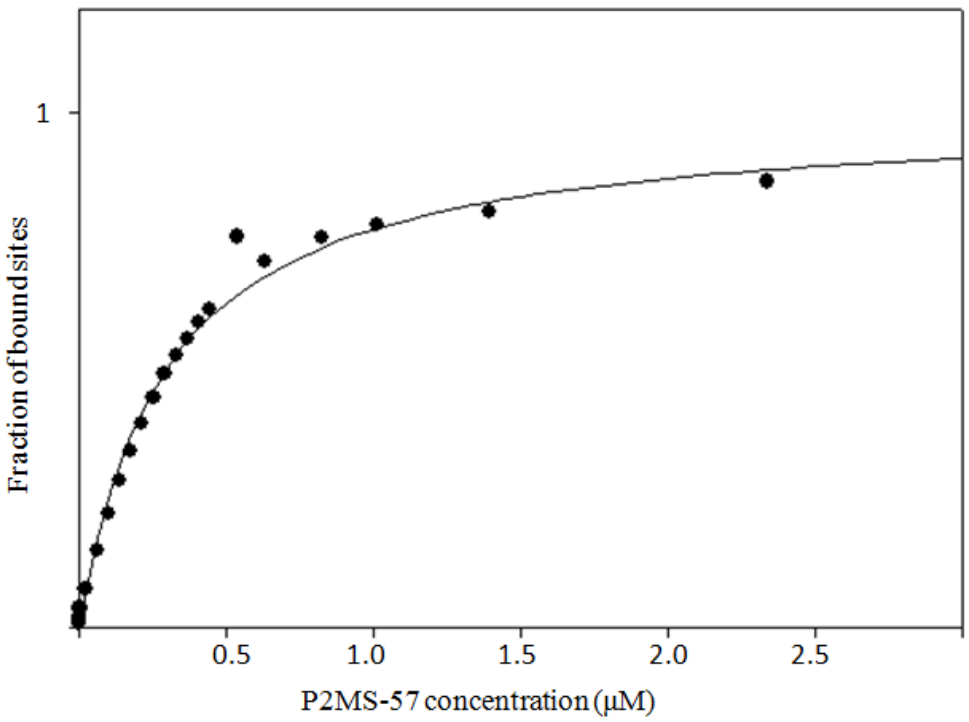

Figure A.2: Representative binding curve for P2MS-57 polymer binding to soluble FITC-IgE from fluorescence quenching assay.

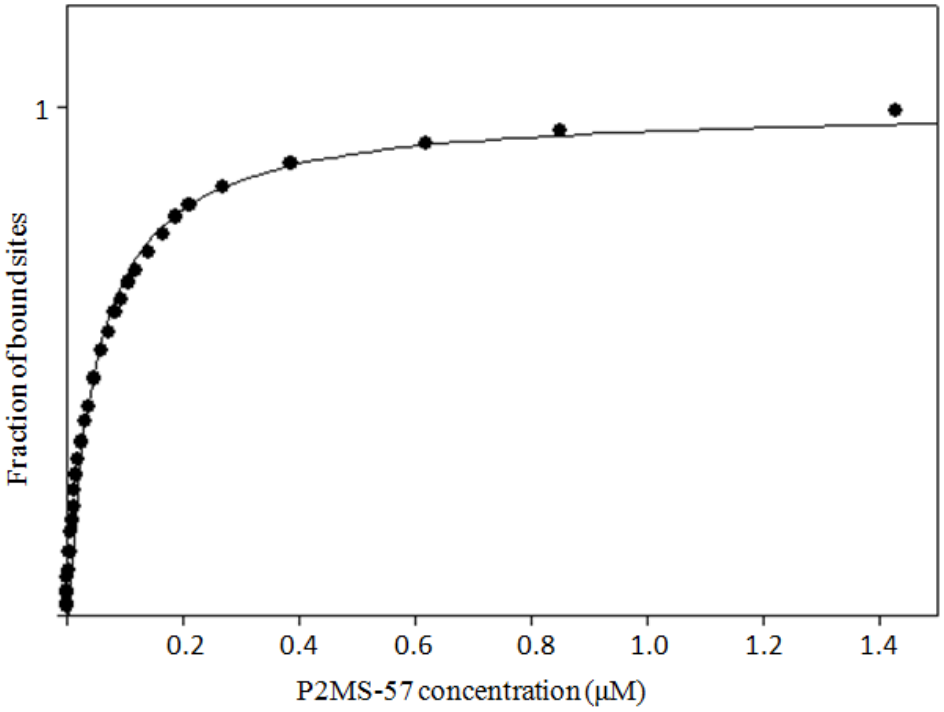

Figure A.3: Representative binding curve for P2MS-57 polymer binding to FITC-IgE bound to RBL-2H3 cells.

relatively tight binding affinity (K_d = 54.3 $\pm$ 5.9 nM; n = 3). Dissociation constants for polymer binding to IgE on RBL cells summarized in Table A.1.

We also assessed the bivalent binding of these polymers by first determining the total available IgE binding sites with a monovalent ligand, DNP-aminocaproyl-L-tyrosine (DCT). As shown in Figure A.4, the initial data points were extrapolated to determine the total number of binding sites from DCT binding curve. We performed the binding experiment with the same sample of FITC-IgE sensitized cells with P2MS-57 polymer and found that the ratio of polymer per binding site is higher than 1, suggesting that these polymers are not binding bivalently and have some other complex binding mechanism. It is also possible that the binding conditions are not appropriate for determining available sites.

We examined the capacity of these DNP-functionalized polymers to trigger granule exocytosis in RBL cells. As shown in a single representative experiment in Figure A.5, we observed less than 1% granule exocytosis response as measured by β-hexosaminidase release from cells incubated with P2MS-57 polymer at varying concentrations, under similar conditions, multivalent DNP-BSA shows a granule exocytosis response of ~55%. P2MS-57 polymer was further tested for its capacity to inhibit granule exocytosis stimulated by multivalent antigen DNP-BSA. For investigating the inhibitory capacity of the polymer, we pre-incubated it with IgE-sensitized cells and then incubated with a sensitive concentration of DNP-BSA which was determined to be 2 ng/ml from Figure A.5. We found that the IC_{50} inhibitory concentration (i.e. 50% inhibitory concentration of ligand) of P2MS-57 polymer is 4.5 $\pm$ 2.1 μM (n = 4) as shown in Figure A.6. We tried to optimize the assay for determining the IC_{50} concentration by lowering the concentration of DNP-BSA used to 1 ng/ml and the time of incubation to 10 minutes. As

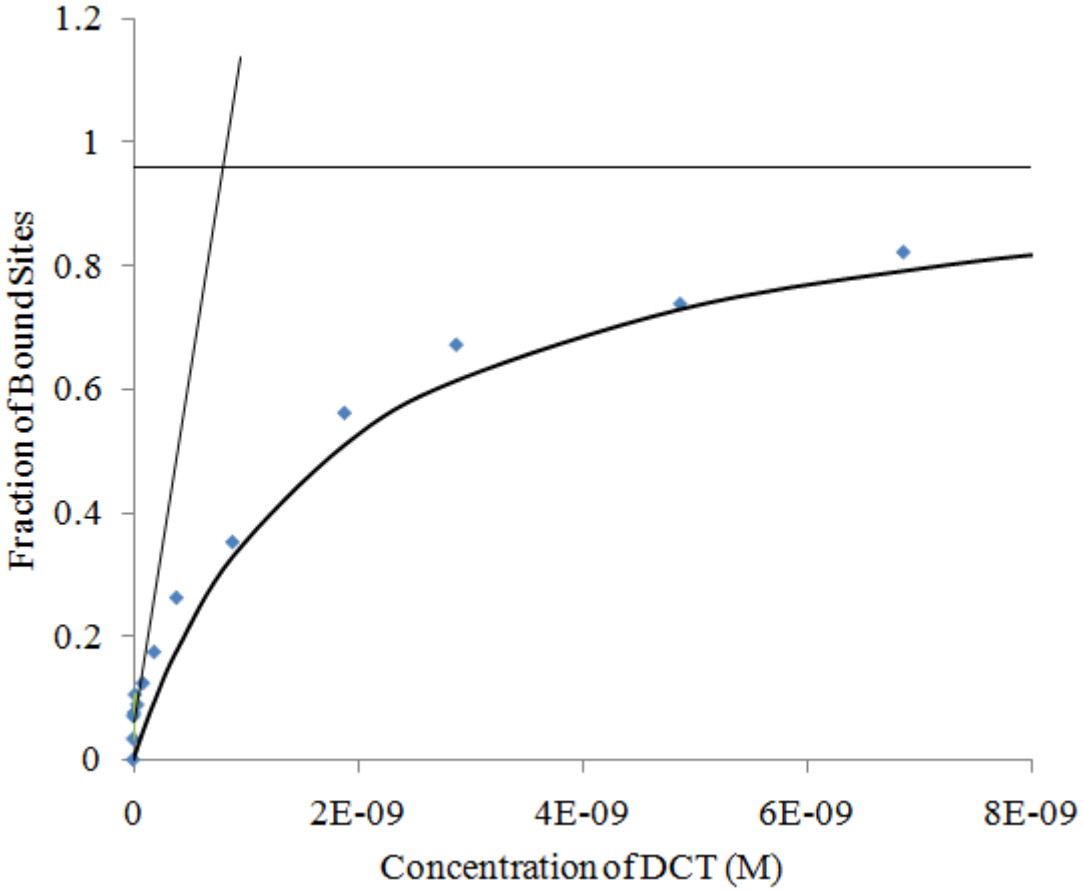

Figure A.4: Representative binding curve with DCT monovalent ligand binding to FITC-IgE bound to RBL-2H3 cells

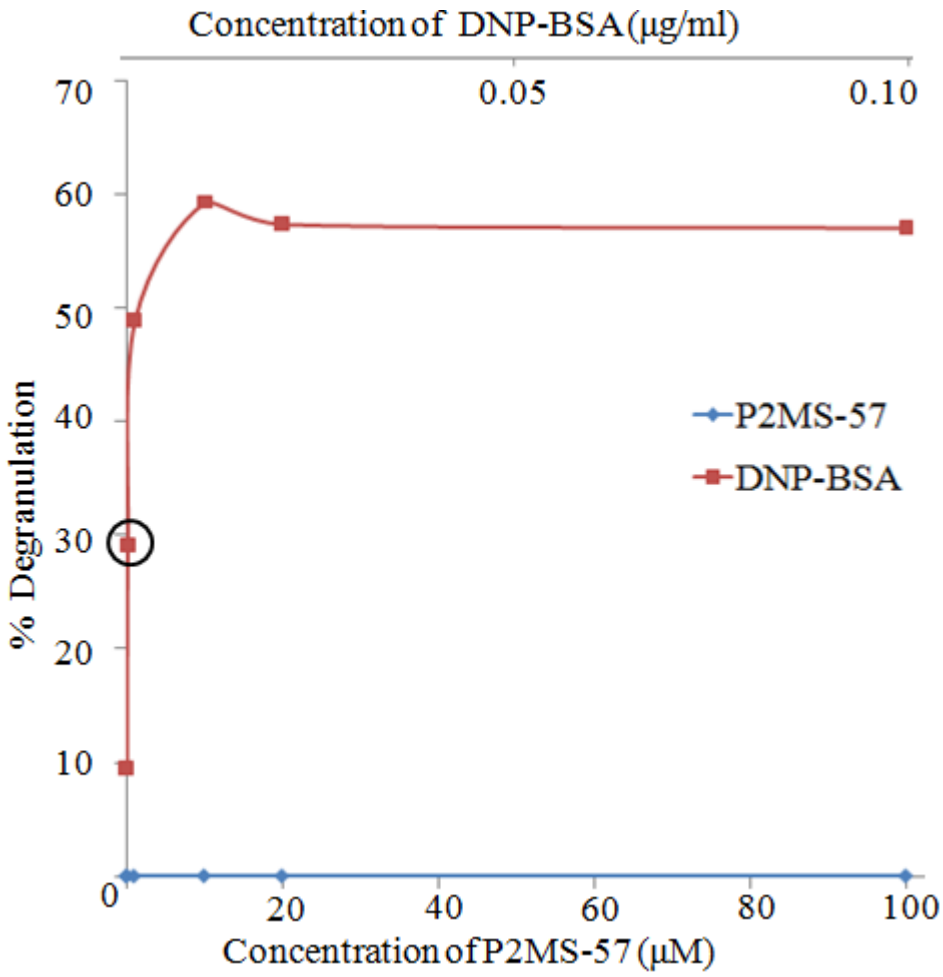

Figure A.5: β-hexosaminidase release for monitoring granule exocytosis response in RBL cells upon incubation with P2MS-57 polymer with varying concentrations (blue). Dose-response degranulation data with DNP-BSA to determine a sensitive concentration range for inhibition studies with polymers (red). Sensitive concentration (= 2 ng/ml) is circled in black.

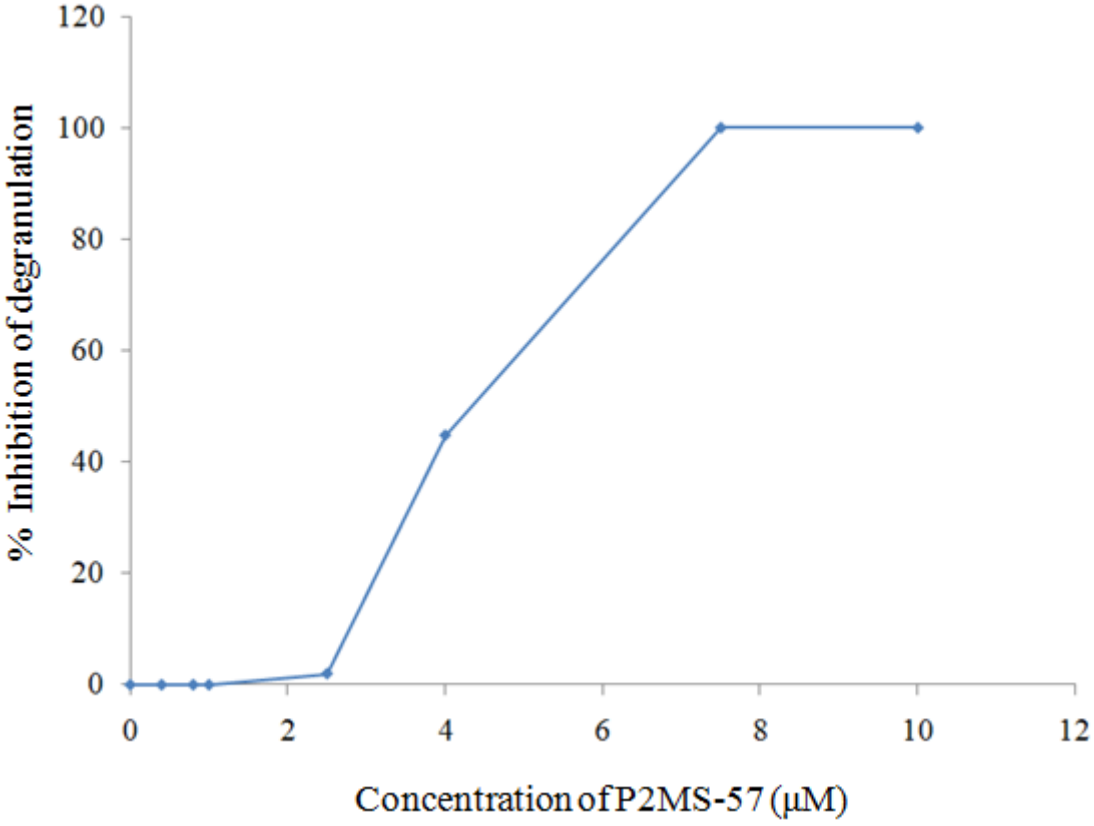

Figure A.6: Inhibition of degranulation stimulated with 2 ng/ml DNP-BSA with P2MS-57 polymer. β-hexosaminidase release in the absence of inhibition was 60%.

shown in Figure A.7, we observed an IC_{50} concentration of 2 μM for P2MS-57 polymer as compared to 4.5 μM obtained previously.

Since granule exocytosis requires Ca^{2+} mobilization and PKC activation, we evaluated the effect of P2MS-57 polymer in stimulating Ca^{2+} mobilization and PKC activation. As shown in Figure A.8, blue trace represents a standard antigen-stimulated Ca^{2+} response in RBL cells. We observed no Ca^{2+} mobilization in indo-1 loaded cells when an aliquot of 1 μM P2MS-57 (final concentration in cell solution = 0.25 μM) was added to them (red trace) in Figure A.8. Addition of multivalent DNP-BSA to the same sample of cells gave a robust Ca^{2+} response, although the rate was delayed compared to the sample that contained no inhibitor. Also, we did not observe recruitment of PKCβI-EGFP to the plasma membrane as examined by confocal microscopy in Figure A.9. Our results, thus, strongly suggest that P2MS-57 do not stimulate normal signaling events in the mast cell signaling cascade at the concentrations that we evaluated.

We investigated whether P2MS-57 causes clustering of FcεRI-IgE on RBL cells, and observed no detectable patching of Alexa488-IgE upon incubation with P2MS-57 polymer as determined by confocal microscopy (Figure A.10), consistent with other results indicating that this polymer is not cross linking IgE-FcεRI at detectable levels at the concentrations we evaluated, and they did not trigger a detectable response in RBL cells.

We also characterized the binding and stimulated granule exocytosis capacity of a biodegradable polylactide polymer: polylactide 3 (Figure A.1) (molecular weight – 10.5 kDa; DNP functionality – 70%). Unlike the sulfonated polystyrene polymers (Figure A.1), polylactide

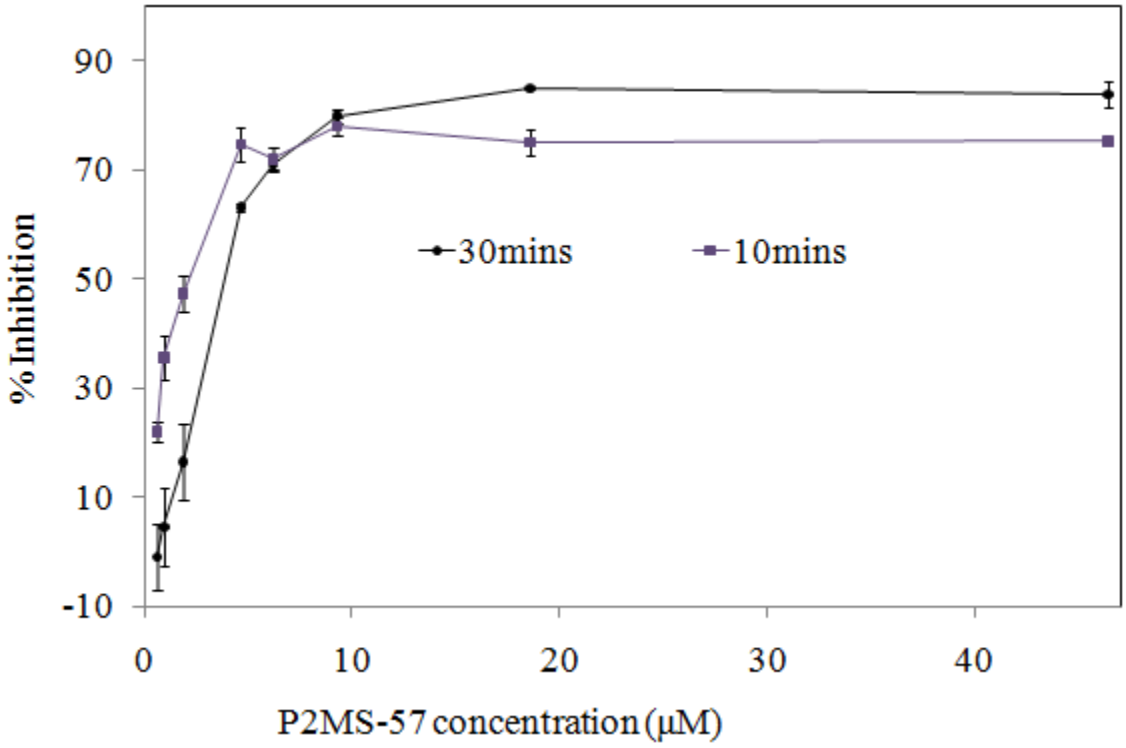

Figure A.7: Inhibition of degranulation with P2MS-57 polymer stimulated with 1 ng/ml DNP-BSA and incubated for 10 minutes (squares) or 30 minutes (circles) with DNP-BSA.

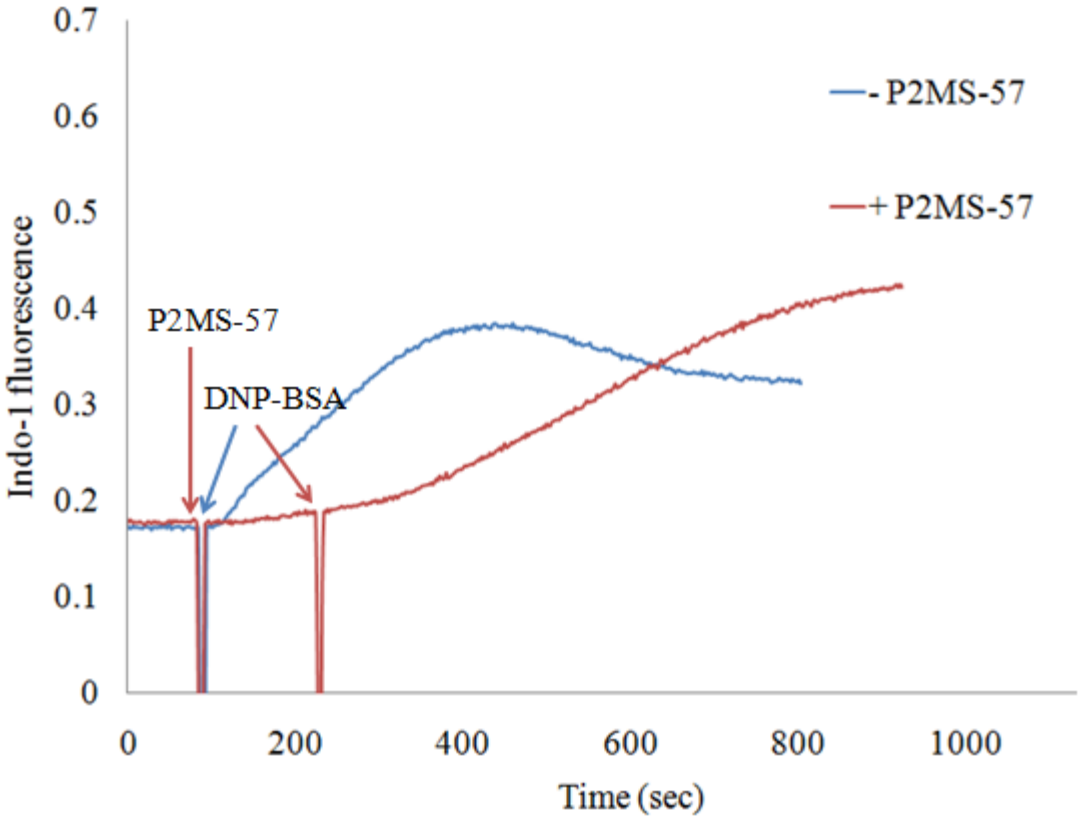

Figure A.8: Ca^{2+} mobilization in response to DNP-BSA in RBL cells (blue). 1 μM P2MS-57 addition showed no Ca^{2+} mobilization in cells (red), this was followed by 0.2 μg/ml DNP-BSA addition to get a robust response.

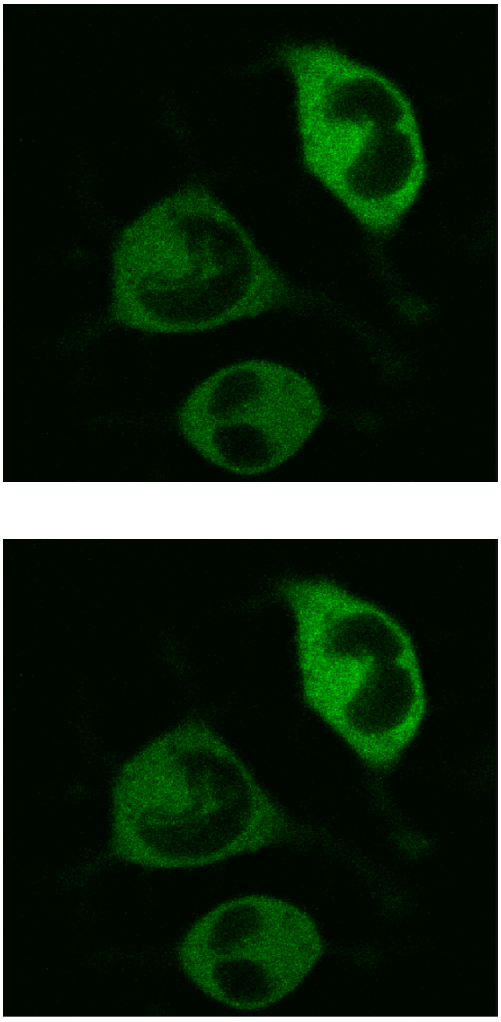

Figure A.9: Confocal images of PKCβI-EGFP transfected cells showing pre-stimulation (above) and post-stimulation (below) with P2MS-57 polymer (50 nM) after 5 minutes.

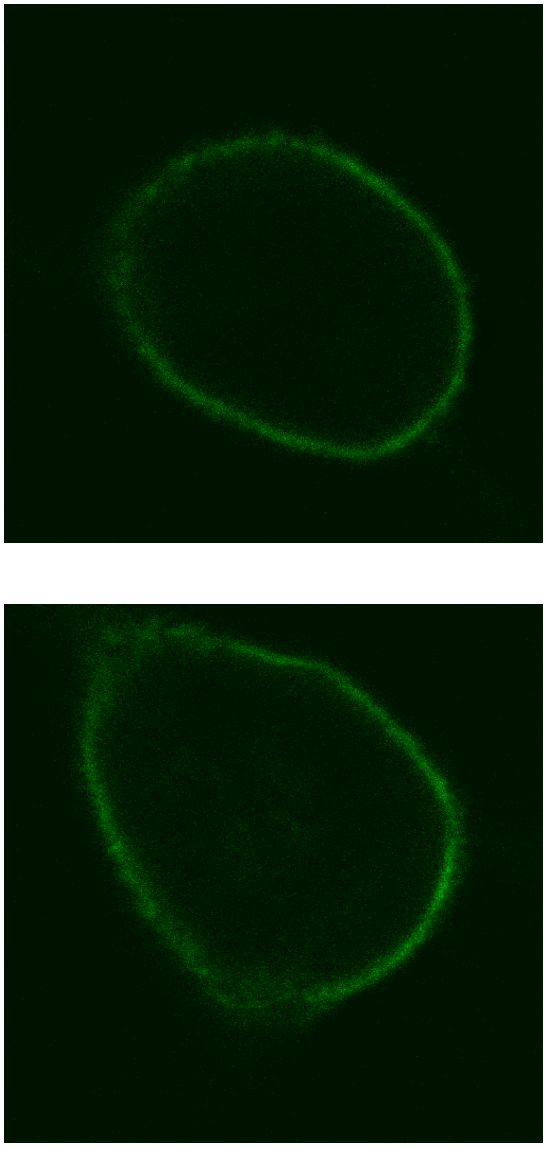

Figure A.10: Confocal image of equatorial sections of Alexa-488 IgE sensitized RBL cells without (above) and with (below) P2MS-57 polymer (50 nM) showing uniform distribution of IgE. Labeled cells were incubated for 15 minutes at 37˚C with 50 nM P2MS-57.

3 is insoluble in aqueous solution at 1 μM and hence we dissolved it in DMSO and used a final concentration of 2% DMSO v/v in the cell solution. Similar to the fluorescence quenching assay used for polystyrene polymers, we determined the K_d for polylactide 3 binding to IgE-FcεRI on cells to be 2.8 $\pm$ 1.1 nM (n = 5) as shown in a representative binding curve in Figure A.11. Dissociation constant for polylactide 3 binding to IgE in solution was determined to be 4.2 $\pm$ 1.8 nM (n = 4). When compared to the dissociation constants for P2MS-57 polymer (54.3nM with IgE on cells and 178.3 nM with IgE in solution), we observe more than tenfold decrease in the K_d of polylactide 3 with IgE in solution as well as with IgE-FcεRI on cells, indicating that polylactide 3 binds much more tightly to IgE, most likely due to its smaller molecular weight and architecture. Under similar conditions, we also determined K_d with DCT ligand and found it to be 1.5 $\pm$ 0.7 nM with IgE on cells and 4.6 $\pm$ 1.0 nM with IgE in solution.

We found that polylactide 3 also did not trigger granule exocytosis in IgE-sensitized RBL cells similar to the polystyrene polymers under similar conditions. We were interested to assess the capacity of polylactide 3 to inhibit DNP-BSA stimulated granule exocytosis and determine its IC_{50} concentration. We tried multiple conditions by varying time of incubation with 1 ng/ml DNP-BSA (Figure A.12) and also variable concentrations of DNP-BSA (Figure A.13) to achieve the lowest IC_{50} concentration which was determined to be 50 nM with 1 ng/ml DNP-BSA stimulation for 10 minutes and 45 nM with 0.2 ng/ml DNP-BSA stimulation for 30 minutes. We also determined IC_{50} concentration for DCT under similar variable conditions of time of incubation with DNP-BSA and varying concentration of DNP-BSA (Figure A.14 and Figure A.15 respectively). We determined the lowest IC_{50} concentration with DCT to be 23 nM with 1 ng/ml DNP-BSA stimulation for 10 minutes and 7 nM with 0.2 ng/ml DNP-BSA stimulation for 30 minutes, indicating that DCT is still more potent in inhibiting degranulation as compared to

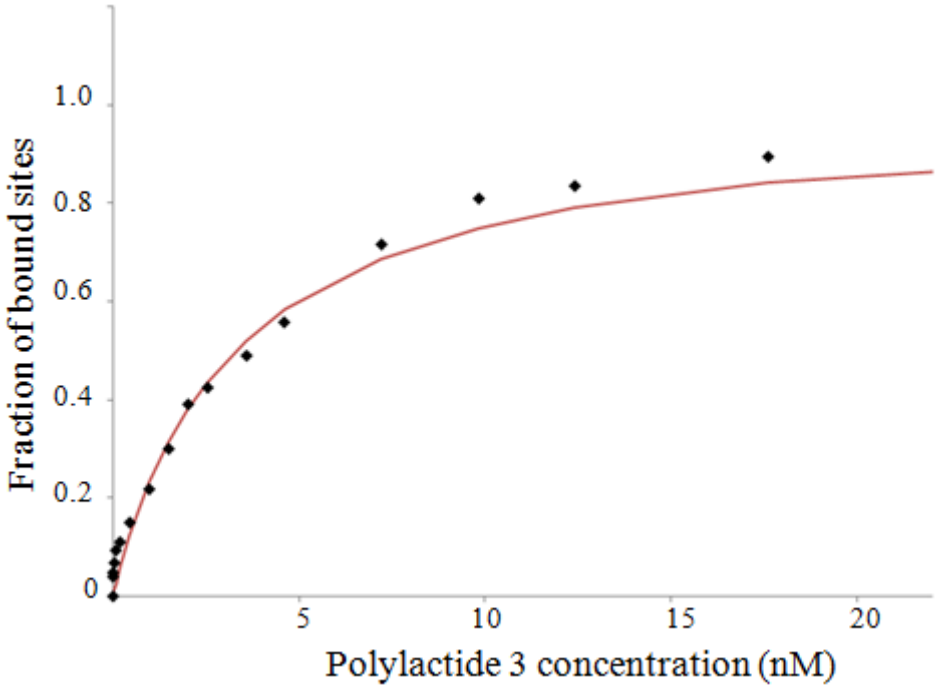

Figure A.11: Representative binding curve for polylactide 3 polymer binding to FITC-IgE bound to RBL-2H3 cells.

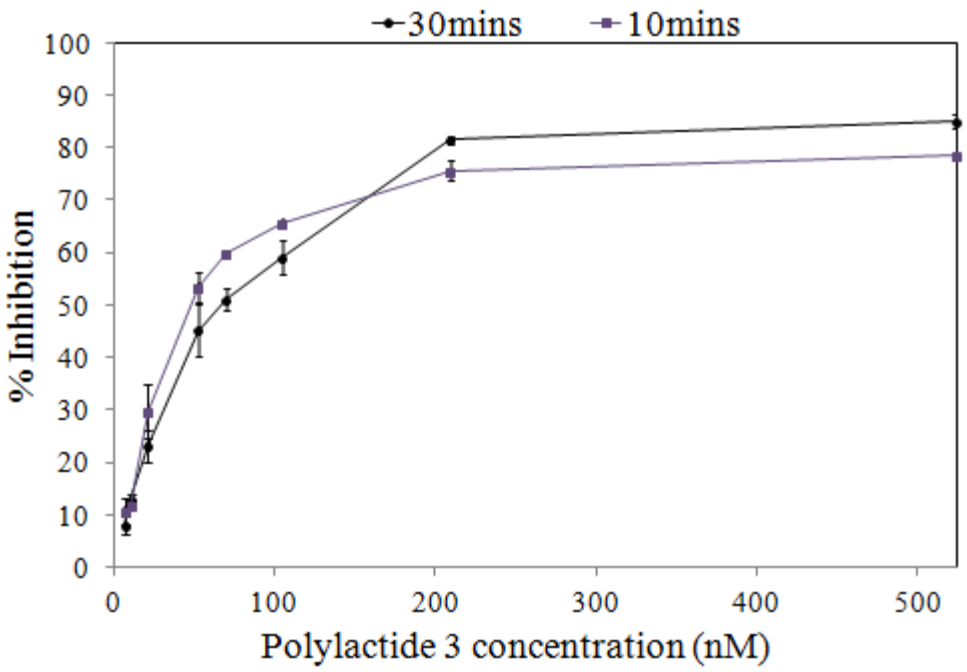

Figure A.12: Inhibition of degranulation with polylactide 3 polymer stimulated with 1 ng/ml DNP-BSA and incubated for 10 minutes (squares) or 30 minutes (circles) with DNP-BSA gave IC_{50} values of 50 nM and 69 nM respectively.

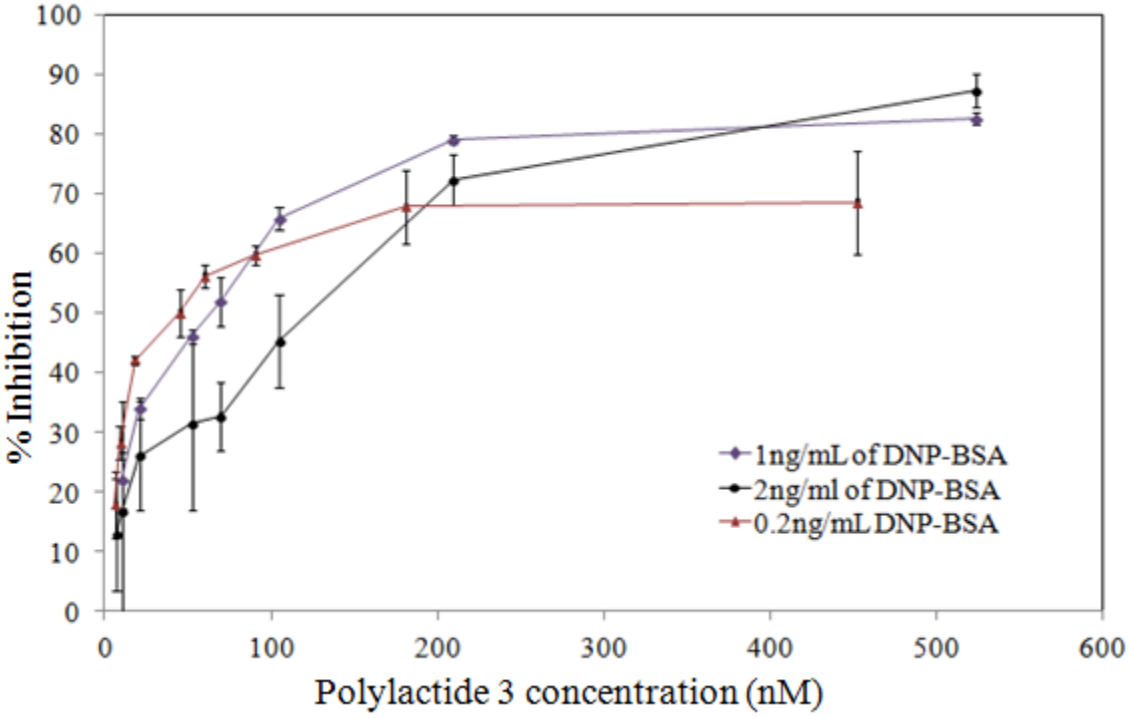

Figure A.13: Inhibition of degranulation with polylactide 3 polymer stimulated with 0.2 ng/ml, 1 ng/ml or 2 ng/ml for 30 minutes gave IC50 values of 45 nM, 70 nM and 130 nM respectively.

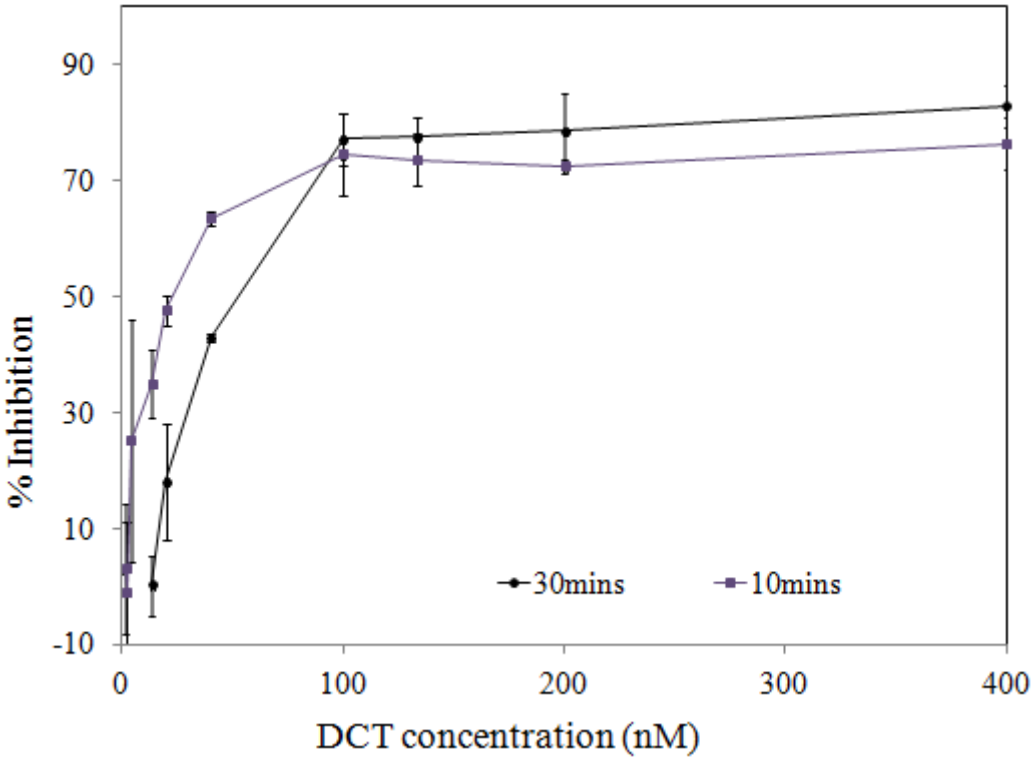

Figure A.14: Inhibition of degranulation with DCT stimulated with 1 ng/ml DNP-BSA and incubated for 10 minutes (squares) or 30 minutes (circles) with DNP-BSA gave IC_{50} values of 23 nM and 52 nM respectively.

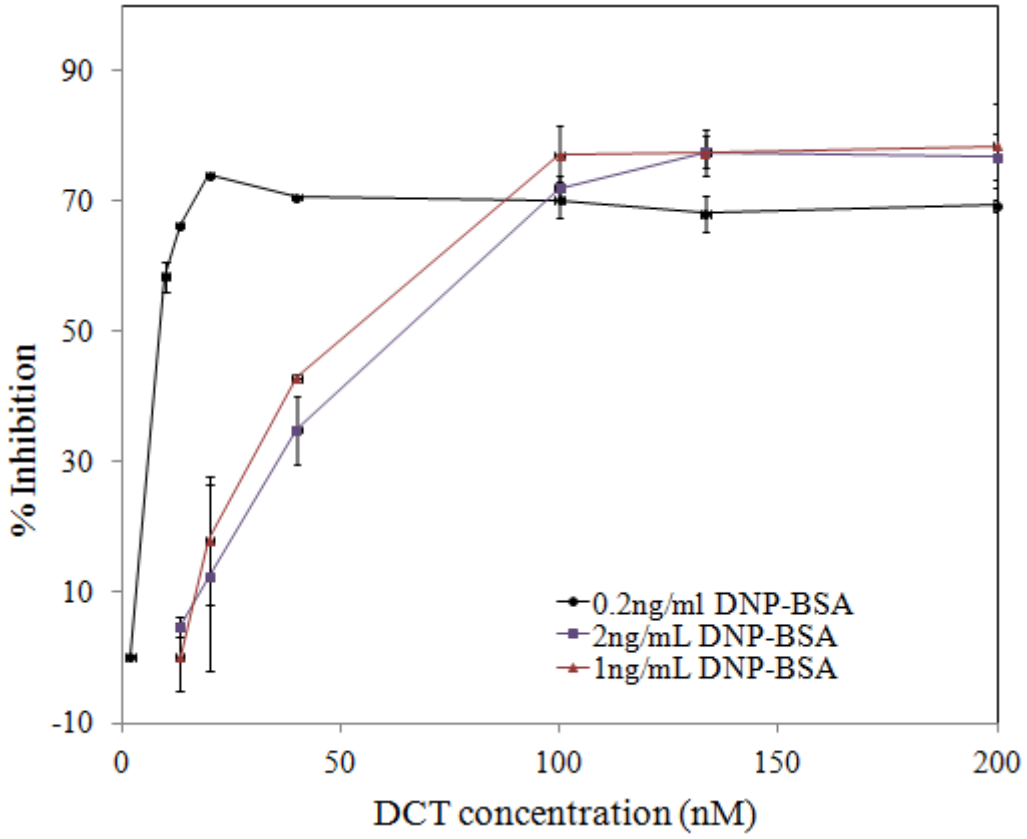

Figure A.15: Inhibition of degranulation with DCT polymer stimulated with 0.2 ng/ml, 1 ng/ml or 2 ng/ml DNP-BSA for 30 minutes gave IC_{50} values of 7 nM, 53 nM and 70 nM respectively.

polylactide 3 polymer. The low aqueous solubility of polylactide 3 and 70% DNP content can account for the slightly higher IC_{50} of polylactide 3 as compared to DCT. It is also possible that polylactide 3 was degraded over time; the rate of degradation of this biodegradable polymer needs to be established to rule out this possibility.

Another area of considerable interest is to utilize these polymers for biosensors by electrospinning them on single walled carbon nanotubes. These electrospun fibers have been found to be stable in aqueous solution, and it has been previously established that films of single walled carbon nanotubes mixed with CDNP-PEO-P2MS-PEO-CDNP are conductive as demonstrated by electrical conductivity measurements (data not published). We performed some preliminary experiments and found that BS 5-20 polymer electrospun on to silicon wafers could bind to anti-DNP FITC-IgE binding as shown in Figure A.16.

A.5 Discussion

Polystyrene polymers functionalized by DNP and with enhanced solubility in water by incorporation of PEO and sulfonation (Figure A.1) were investigated for their binding properties and capacity to trigger or inhibit cellular signaling in mast cells. A biodegradable polylactide polymer, polylactide 3 (Figure A.1), was also characterized. We found that these polymers bind specifically to anti-DNP IgE immobilized on RBL cells; however, they did not elicit detectable signaling responses as determined by the lack of stimulated Ca^{2+} mobilization, PKC activation or granule exocytosis.

Since these polymers did not detectably crosslink IgE-FcεRI to initiate signaling even

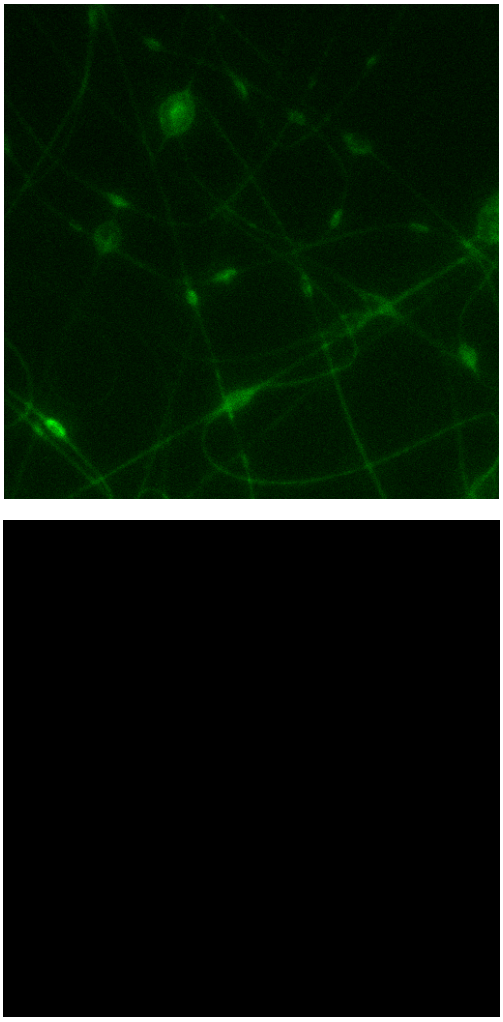

Figure A.16: Specificity of anti-DNP FITC-IgE binding with BS 5-20 polymer electrospun on silicon wafers with 1% single walled carbon nanotubes (above). No binding was observed with nonspecific FITC-IgG (below).

though they demonstrated tight binding to IgE-FcεRI, this indicates that they are either binding bivalently intramolecularly or they are simply binding as monovalent ligands. To address the question regarding the bivalent binding of these polymers, we performed our binding studies in parallel with a monovalent ligand, DCT. With DCT binding studies, we had an approximate estimate of the IgE binding sites available and we then compared our polymer binding data with it to assess if these polymers are binding bivalently. Our data indicate that these polymers are not binding bivalently as determined by the ratio of polymer/binding site. However, the DNP functionality was not taken into account for determining the apparent dissociation constants or bivalency.

In the current study, we also found that both polystyrene and polylactide polymers can inhibit the granule exocytosis response stimulated by multivalent DNP-BSA. We observed an IC_{50} value of ~ 5 μM with P2MS-57 polymer in the presence of 2 ng/ml DNP-BSA. We were able to lower the IC_{50} value to 2 μM for this polymer by reducing the DNP-BSA concentration to 1 ng/ml instead of 2 ng/ml and the time of incubation to 10 minutes instead of 30 minutes (Figure A.7). We were also able to lower the IC_{50} concentration of polylactide 3 to 45 - 50 nM after optimization of inhibition conditions as shown in Figure A.12 and A.13. However, under similar conditions, we found that the monovalent ligand DCT still has lower IC_{50} value indicating that it is still more potent in inhibiting granule exocytosis than these synthetic ligands.

In summary, we have established very good optimization conditions for characterizing the binding and inhibition capacity of DNP-functionalized polymers. Our data will provide good guidelines for assay of future DNP ligands to determine their potential in allergy therapeutics. Also, our preliminary data showing specificity of IgE towards these polystyrene polymers mixed

with single walled carbon nanotubes and electrospun on silicon substrate shows potential for their use in electrical and conductivity measurements for use in biosensors for detecting sensitive levels of IgE.

However, some key questions still need to be addressed to better understand the binding mechanism of these polymers with IgE in solution and IgE bound to RBL cells. Determining the length of each of these polymers by light scattering or by using a random walk model would help us correlate the dissociation constants with the size of each of these polymers. The distance between two IgE binding sites is about 10 nm (Baird et al., 1993). Polymers with an end to end distance close to 10 nm are expected to show intramolecular binding predominantly, and therefore have a higher potential for utility in allergy inhibition. For developing polymers in the future, it may be useful to synthesize lower molecular weight polymers with smaller size to achieve lower IC_{50} concentration. Enhancement of aqueous solubility of polylactide series of polymers and an evaluation their rate of degradation as a solid and in aqueous and organic solvents would also be helpful in obtaining a more accurate binding constant and inhibitory concentration. It would also be on great interest to visualize whether IgE-FcεRI is intermolecularly or intramolecularly crosslinked by these polymers by using super resolution microscopy techniques like STORM. To gain more insights in the inhibitory mechanism of granule exocytosis, we can test for upstream signaling steps like Lyn phosphorylation which can be tested by Western Blotting. Quantifying the percent inhibition of Ca^{2+} mobilization by DNP-BSA in the presence of each of these polymers and correlating it with the percent inhibition in stimulated granule exocytosis would also help in further dissecting the mode of inhibition.

Electrospun fibers mixed with single walled carbon nanotubes need to be evaluated for

their capacity to show change in conductance before and after IgE binding before they can used for fabrication of an electro-conductive biosensor. Optimization of electrochemical measurements with these polymer fibers electrospun on silicon substrate is currently in progress by CAU researchers.

REFERENCES

Baird, B., Zheng, Y., and Holowka, D. (1993). Structural mapping of IgE-FcεRI, an immuno-receptor complex. Accts. Chem. Res. *26*, 428-434.

Baird, E.J., Holowka, D., Coates, G.W., and Baird, B. (2003). Highly effective poly(ethylene glycol) architectures for specific inhibition of immune receptor activation. Biochemistry *42*, 12739-12748.

Erickson, J., Kane, P., Goldstein, B., Holowka, D., and Baird, B. (1986). Cross-linking of IgE-receptor complexes at the cell surface: a fluorescence method for studying the binding of monovalent and bivalent haptens to IgE. Mol Immunol *23*, 769-781.

Kane, P.M., Holowka, D., and Baird, B. (1988). Cross-linking of IgE-receptor complexes by rigid bivalent antigens greater than 200 A in length triggers cellular degranulation. J Cell Biol *107*, 969-980.

Naal, R.M., Tabb, J., Holowka, D., and Baird, B. (2004). In situ measurement of degranulation as a biosensor based on RBL-2H3 mast cells. Biosens Bioelectron *20*, 791-796.

Sannigrahi, B., Sil, D., Baird, B., Wang, X.-Q., and Khan, I. (2008). Synthesis and Characterization of α,ω-bi[2,4-dinitrophenyl (DNP)] poly(2-methoxystyrene) Functional Polymers. Initial Evaluation of the Interaction of the Functional Polymers with RBL Mast Cells. Journal of Macromolecular Science, Part A *45*, 664-671.

Sil, D., Lee, J.B., Luo, D., Holowka, D., and Baird, B. (2007). Trivalent ligands with rigid DNA spacers reveal structural requirements for IgE receptor signaling in RBL mast cells. ACS Chem Biol *2*, 674-684.

Xu, K., Goldstein, B., Holowka, D., and Baird, B. (1998). Kinetics of multivalent antigen DNP-BSA binding to IgE-Fc epsilon RI in relationship to the stimulated tyrosine phosphorylation of Fc epsilon RI. J Immunol *160*, 3225-3235.